



IPP Summer University for Plasma Physics and Fusion Research

Greifswald, Sept. 2016

Wendelstein project W7-X

DIAGNOSTICS FOR FUSION PLASMAS

with contributions from many colleagues
and some textbooks (see reference list at the end)



Outline of this talk:

- 1) Basics, measured quantities, principles and some physics
(here we stick to the magnetic field, electrons and protons)
- 2) Techniques, practical considerations and some results



Challenges in a fusion relevant plasma:

- It is extremely hot
- Impurities can pollute it
(anything heavier than H,D,T)
- ➔ Nothing made of material
can touch it
- Radiation and fast particles
- Intense EM background
- Wide range of timescales:
Several seconds τ_Z , L/R , ...
↔ GHz-range: fast MHD, ...

$T > 10^8$ K
(about 10 keV)

Only H^+ , D^+ , e^-
(ideally); reactor: T^+

In reality: also
traces (!!) of
C, Fe,



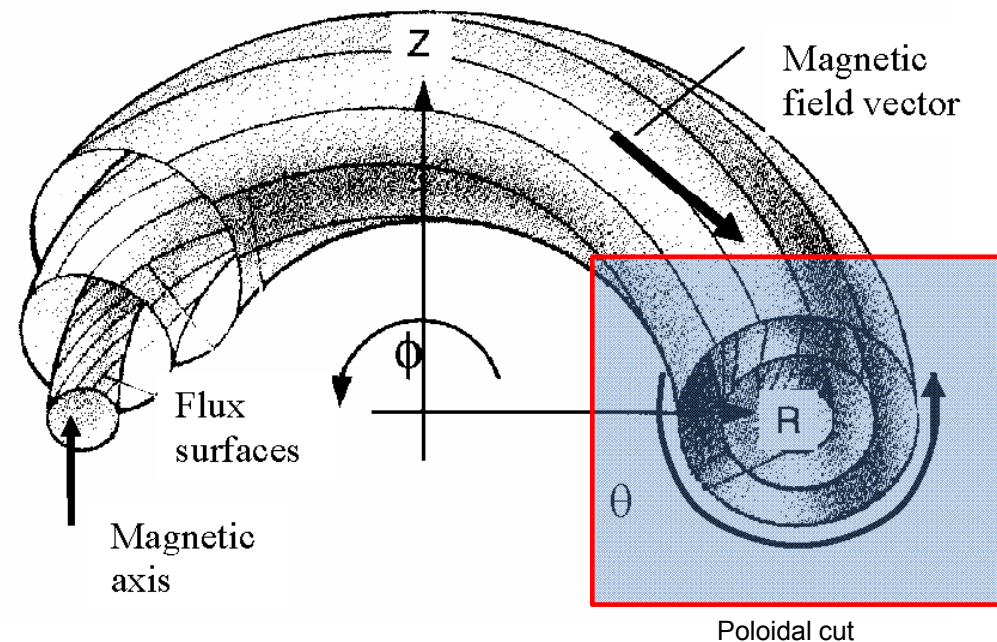
The most important ingredient for plasma fusion: the magnetic field

The concept of nested magnetic flux surfaces:

Almost all quantities are constant on one and the same flux surface

Problem: how can we map from magnetic coordinates $\{Z, \theta, \phi\}$ to „real-space“ coordinates $[x, y, z]$?

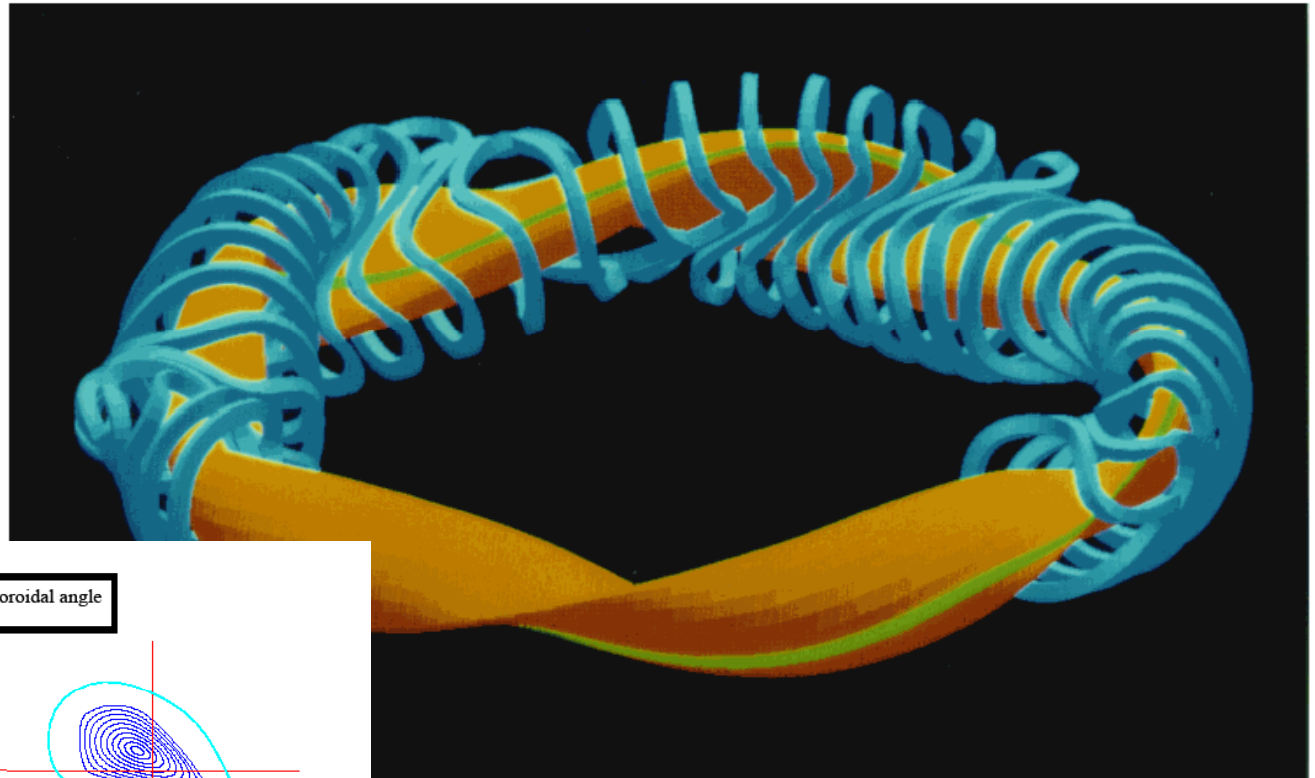
The situation is relatively „simple“
in a tokamak:
there we have axisymmetry !



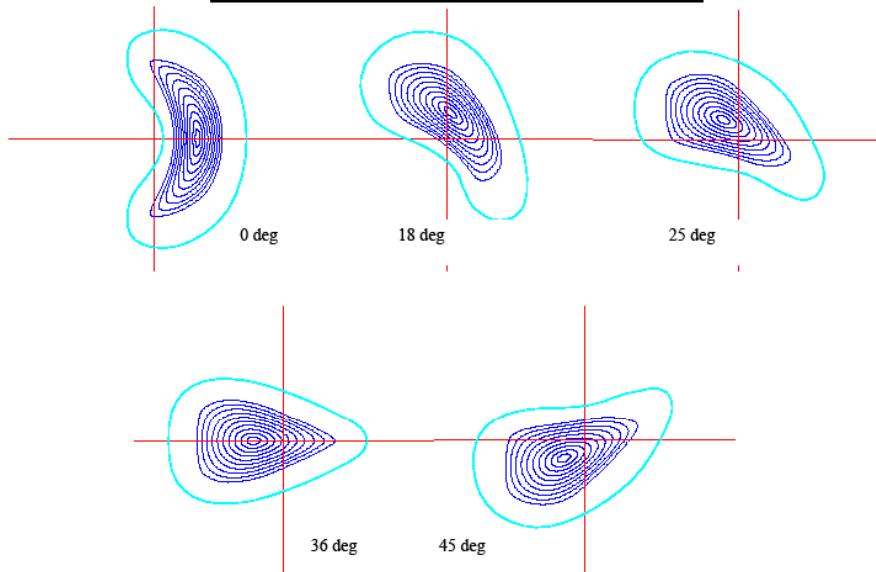


The situation is more complex
in a stellarator: full 3-D !

W7-X: an artist's view



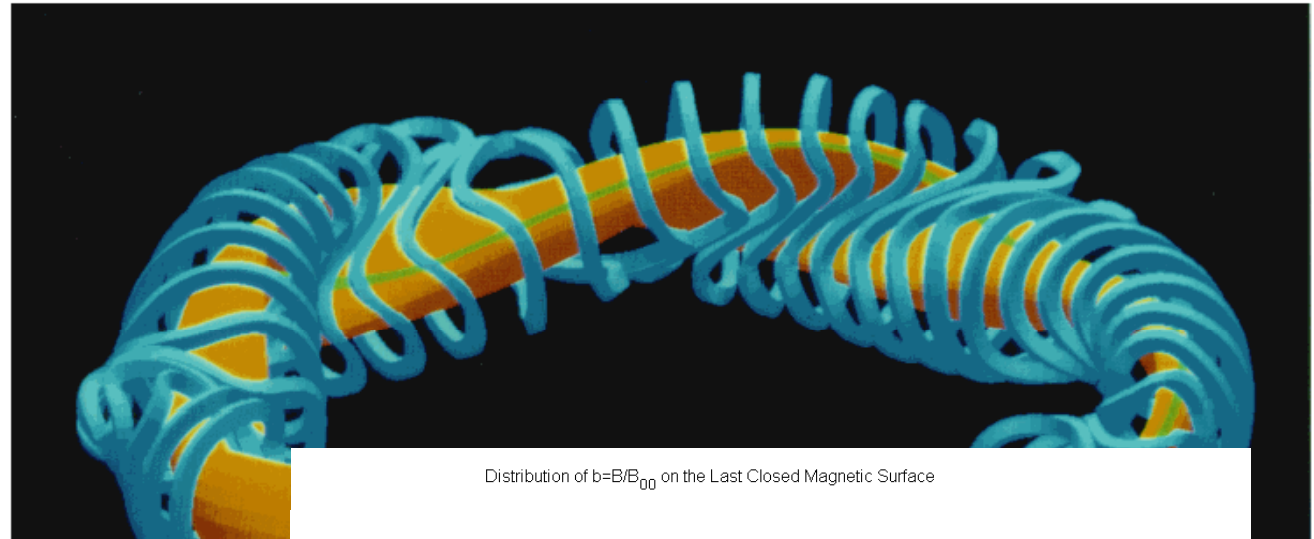
W7-X: Change of the plasma shape with the toroidal angle





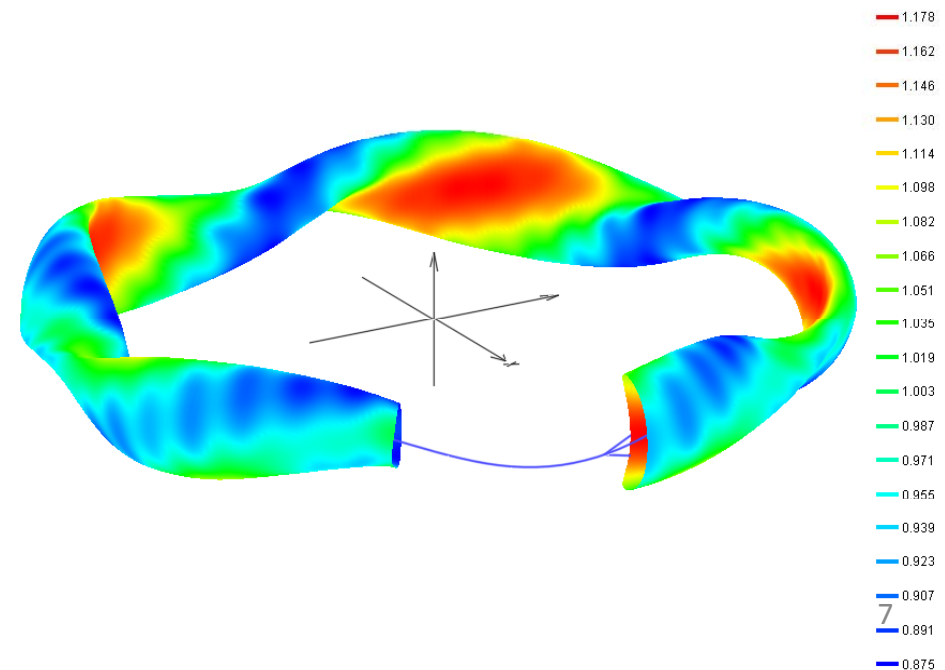
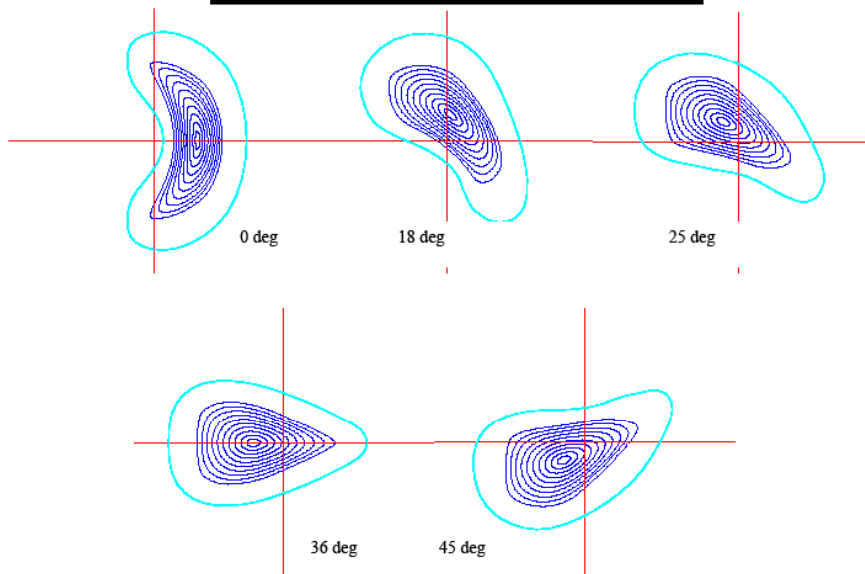
The situation is more complex
in a stellarator: full 3-D !

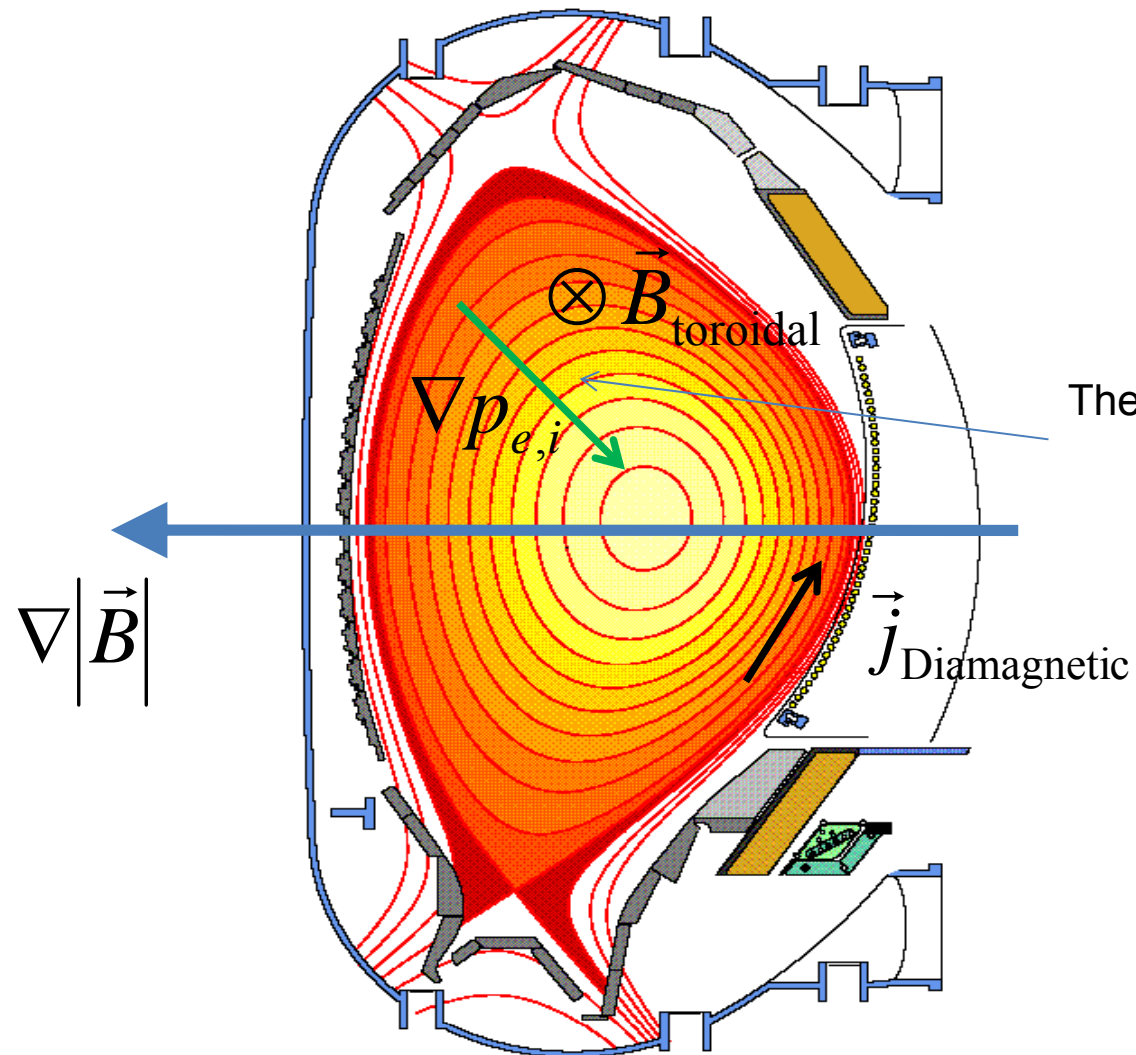
W7-X: an artist's view



Distribution of $b=B/B_{00}$ on the Last Closed Magnetic Surface

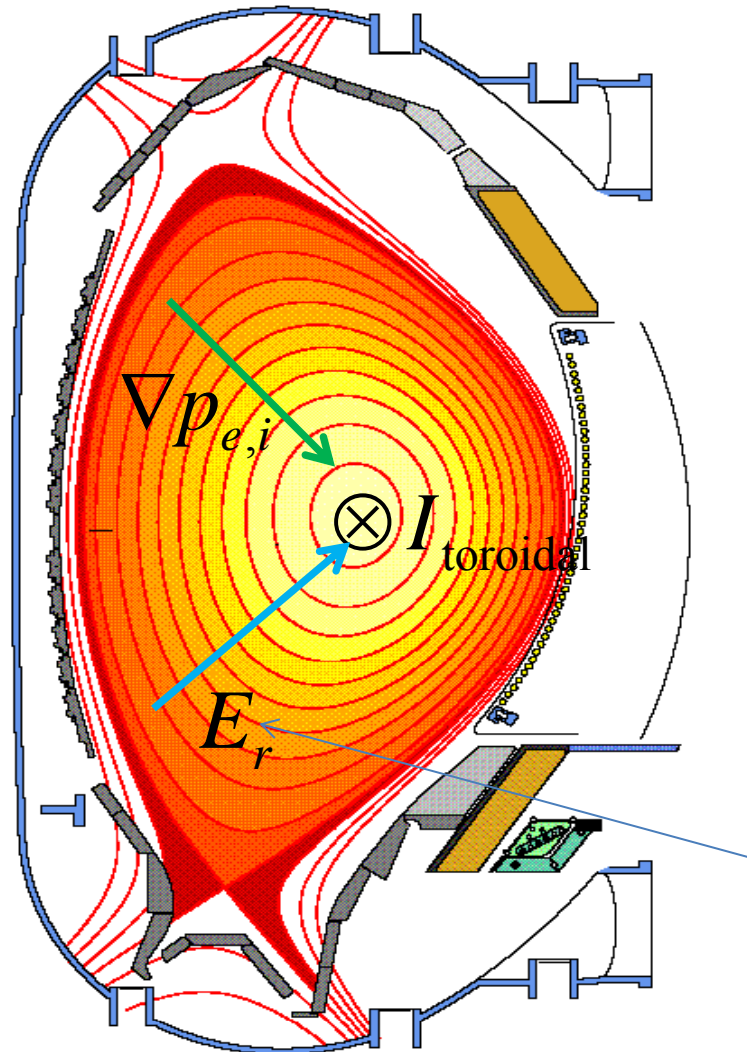
W7-X: Change of the plasma shape with the toroidal angle





The famous pressure equilibrium:

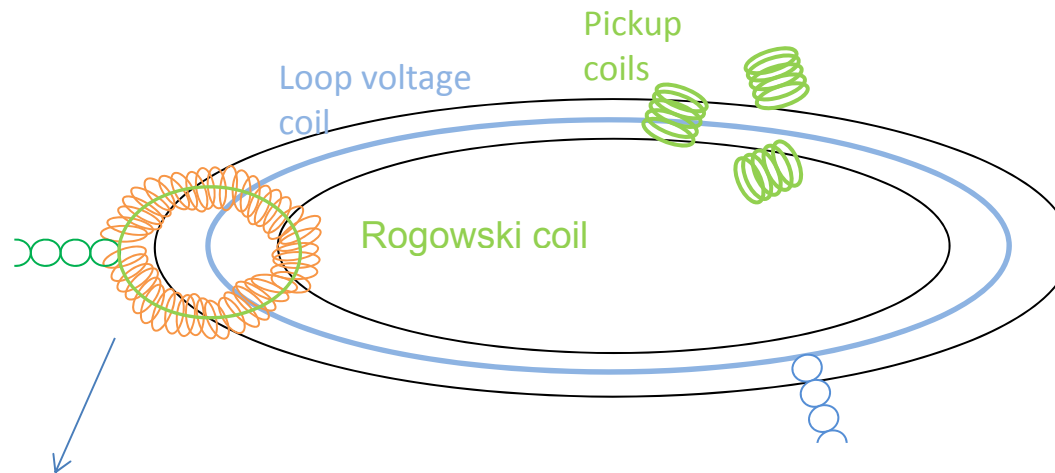
$$\nabla p = \vec{j} \times \vec{B}$$



The famous pressure equilibrium:

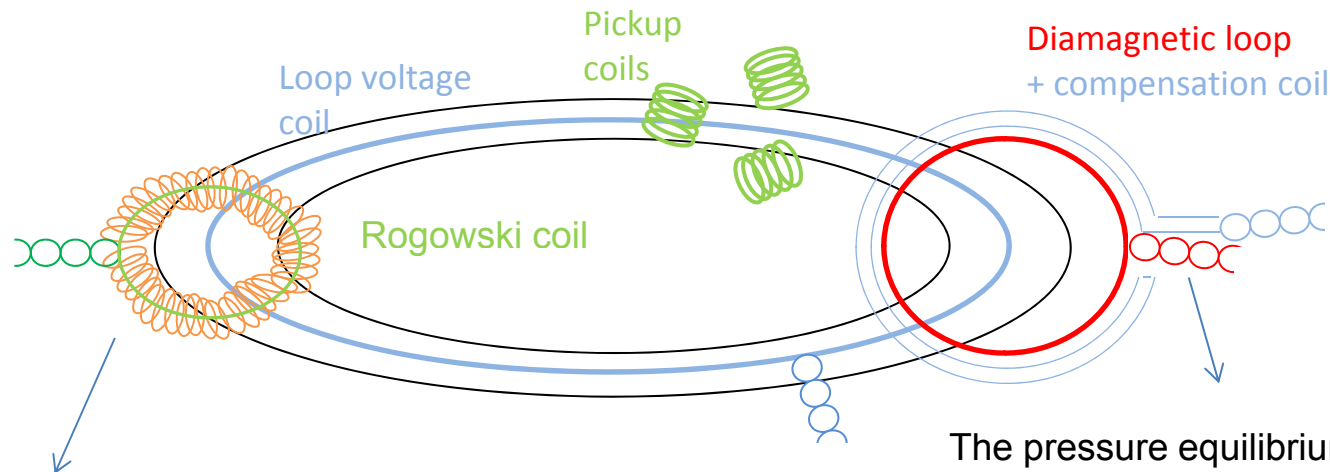
$$\nabla p = \vec{j} \times \vec{B}$$

Typically, the radial ion transport
is not exactly equal to the
electron transport
→ a radial electric field E_r builds up
until an equilibrium is maintained



Ampère's law provides the toroidal
plasma current

$$I = \int \vec{j} \cdot d\vec{A} = \frac{1}{\mu_0} \oint B_\theta dl$$
$$\Rightarrow I_{\text{plasma}} = \frac{2\pi a}{NA\mu_0} \int U dt$$



Ampère's law provides the toroidal
plasma current

$$I = \int \vec{j} \cdot d\vec{A} = \frac{1}{\mu_0} \oint B_\theta dl$$

$$\Rightarrow I_{\text{plasma}} = \frac{2\pi a}{NA\mu_0} \int U dt$$

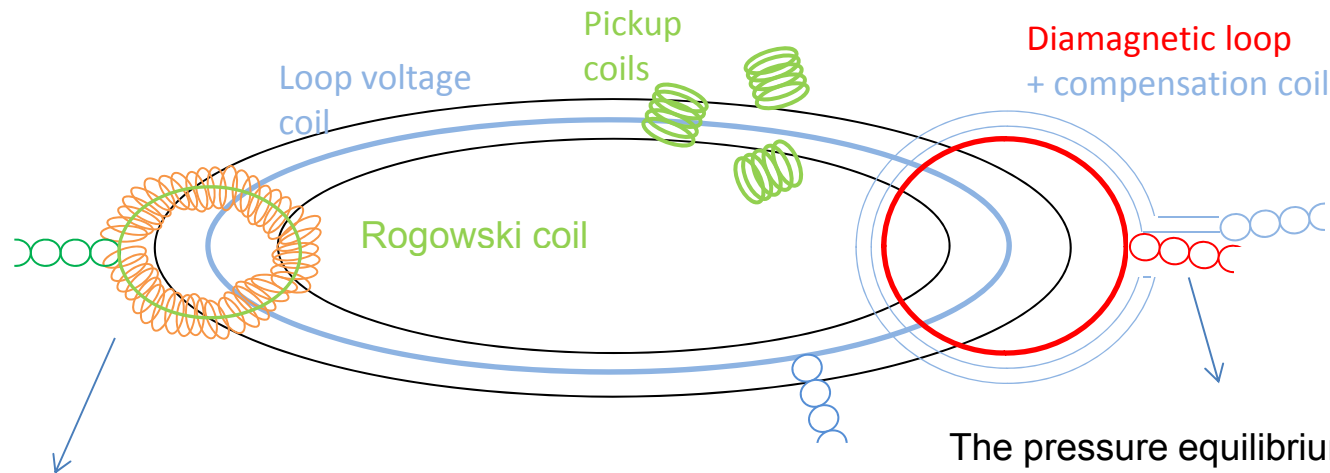
The pressure equilibrium provides in
simplified cylindrical geometry:

$$\nabla p = \vec{j} \times \vec{B}$$

$$\mu_0 \frac{dp}{dr} + \frac{d}{dr} \left(\frac{B_\phi^2}{2} \right) + \frac{B_\theta}{r} \frac{d}{dr} (rB_\theta) = 0$$

$$\Phi = -\frac{2\pi\mu_0}{B_0} \int_0^a p r dr + \frac{\mu_0^2 I_z^2(a)}{8\pi B_0} + \frac{\pi\mu_0}{B_0} \int_0^a j_z B_\phi r^2 dr$$

$$= -\frac{\mu_0 W}{3\pi R B_0} + \frac{\mu_0^2 I_{\text{plasma}}^2}{8\pi B_0} + \frac{\pi\mu_0 l_{\text{vac}}}{R} \int_0^a j_z r^3 dr$$



Ampères law provides the toroidal
plasma current

$$I = \int \vec{j} \cdot d\vec{A} = \frac{1}{\mu_0} \oint B_\theta dl$$

$$\Rightarrow I_{\text{plasma}} = \frac{2\pi a}{NA\mu_0} \int U dt$$

The pressure equilibrium provides in
simplified cylindrical geometry:

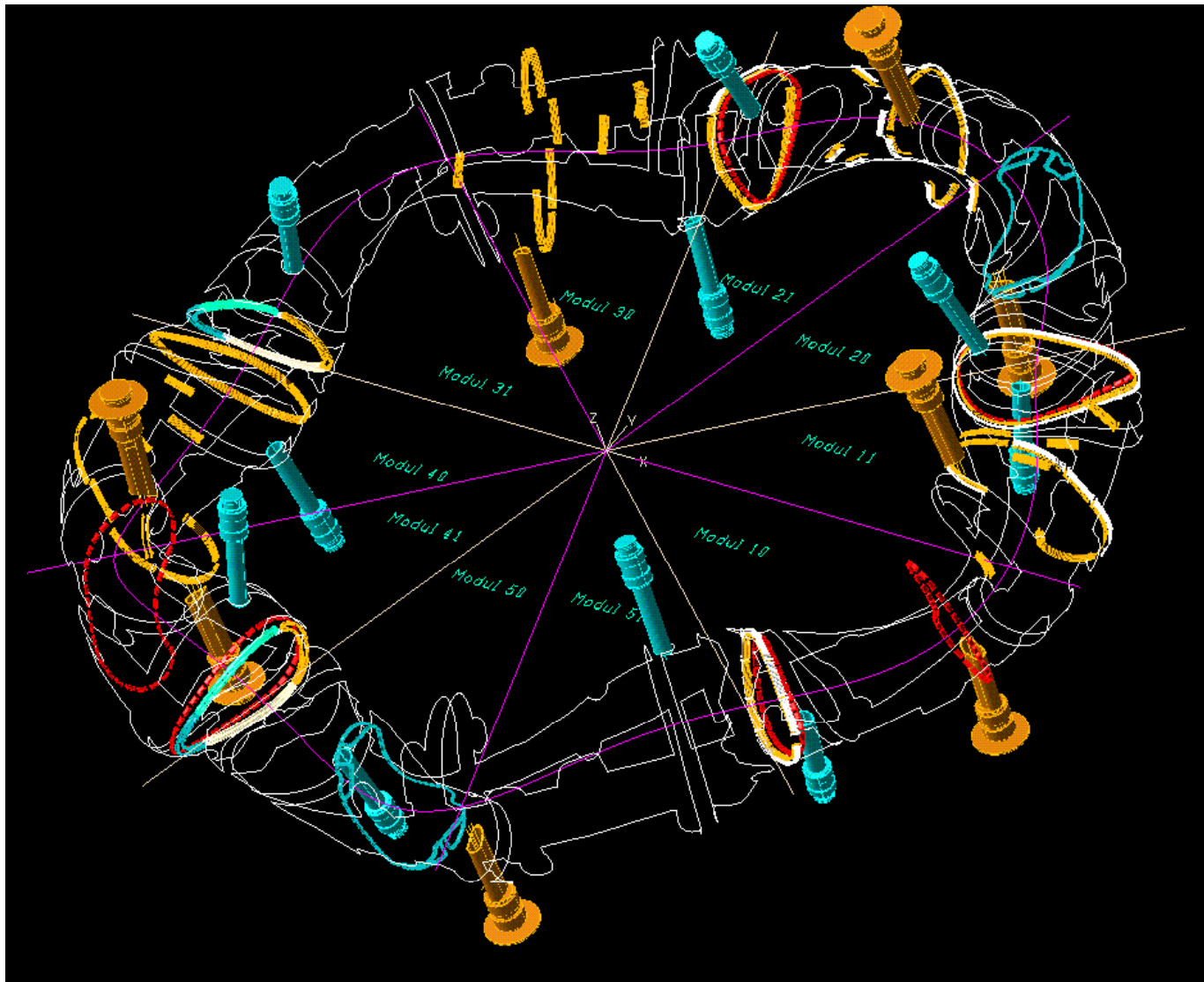
$$\nabla p = \vec{j} \times \vec{B}$$

$$\mu_0 \frac{dp}{dr} + \frac{d}{dr} \left(\frac{B_\phi^2}{2} \right) + \frac{B_\theta}{r} \frac{d}{dr} (r B_\theta) = 0$$

$$\Phi = -\frac{2\pi\mu_0}{B_0} \int_0^a p r dr + \frac{\mu_0^2 I_z^2(a)}{8\pi B_0} + \frac{\pi\mu_0}{B_0} \int_0^a j_z B_\phi r^2 dr$$

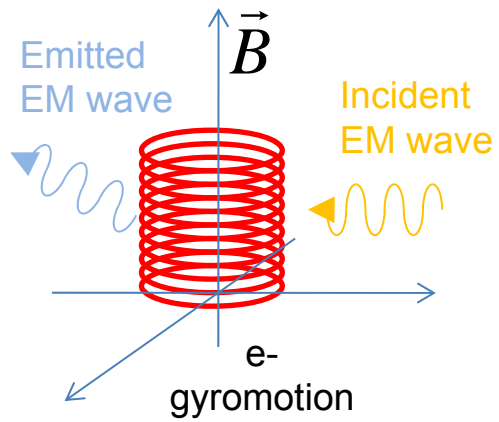
$$= -\frac{\mu_0 W}{3\pi R B_0} + \frac{\mu_0^2 I_{\text{plasma}}^2}{8\pi B_0} + \frac{\pi\mu_0 l_{\text{vac}}}{R} \int_0^a j_z r^3 dr$$

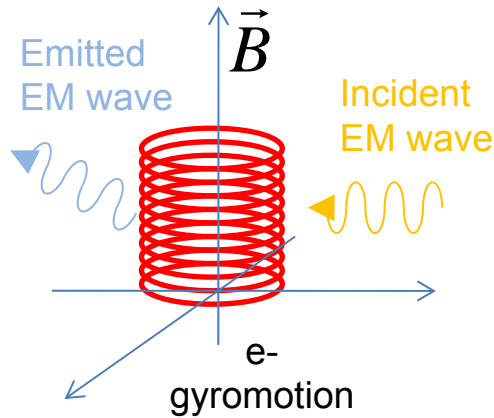
$$p_{\text{plasma}} = k (n_e T_e + n_i T_i) \Rightarrow W_{\text{kinetic}} = \int k (n_e T_e(\vec{r}) + n_i T_i(\vec{r})) d^3 r$$





.....then we continue with the magnetic field and the electrons.....





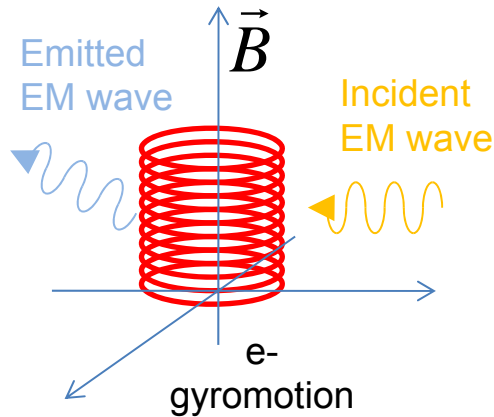
Frequency of the emitted wave $\omega = l \cdot \omega_{cyclotron} = l \cdot \frac{eB}{m_e}$

Emission parallel to B \rightarrow no harmonics ($l = 1$)

Emission perpendicular to B: \rightarrow polarization perpendicular to B: X-mode

\rightarrow polarization parallel to B: O-mode

$$\frac{d^2 P}{d\omega d\Omega} = const \cdot \omega^2 \sum_{l=1}^{\infty} \left\{ \frac{V_{\parallel}^2}{c^2} J_l \left(\frac{\omega V_{\parallel}}{\omega_c c} \right) + \frac{V_{\perp}^2}{c^2} J_l \left(\frac{\omega V_{\perp}}{\omega_c c} \right) \right\} \cdot \delta(\omega - l\omega_c)$$



Frequency of the emitted wave $\omega = l \cdot \omega_{\text{cyclotron}} = l \cdot \frac{eB}{m_e}$

Emission parallel to B \rightarrow no harmonics ($l = 1$)

Emission perpendicular to B: \rightarrow polarization perpendicular to B: X-mode

\rightarrow polarization parallel to B: O-mode

$$\frac{d^2 P}{d\omega d\Omega} = \text{const} \cdot \omega^2 \sum_{l=1}^{\infty} \left\{ \frac{V_{\parallel}^2}{c^2} J_l^2 \left(\frac{\omega V_{\parallel}}{\omega_c c} \right) + \frac{V_{\perp}^2}{c^2} J_l^2 \left(\frac{\omega V_{\perp}}{\omega_c c} \right) \right\} \cdot \delta(\omega - l\omega_c)$$

The EM-waves experience a refractive index N for $\omega > \omega_{\text{cyclotron}}$

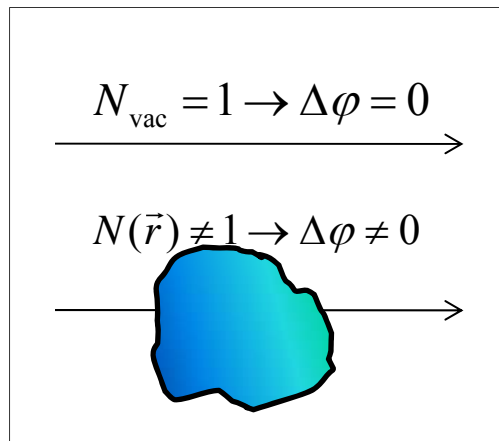
$$N^2 \approx 1 - \frac{\omega_p^2}{\omega^2}; \quad \omega_p = \sqrt{\frac{n_e e^2}{\epsilon_0 m_e}}$$

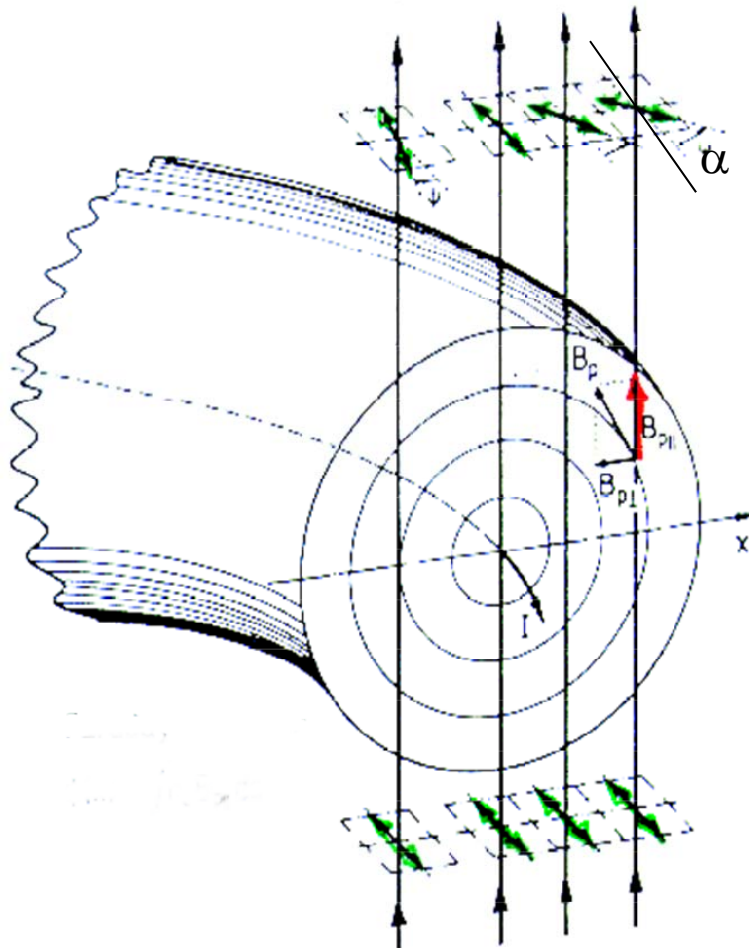
Below the (electron) plasma frequency the plasma becomes conductive

\rightarrow EM-waves are absorbed (reflected) \rightarrow cut-off density (for X-mode !)

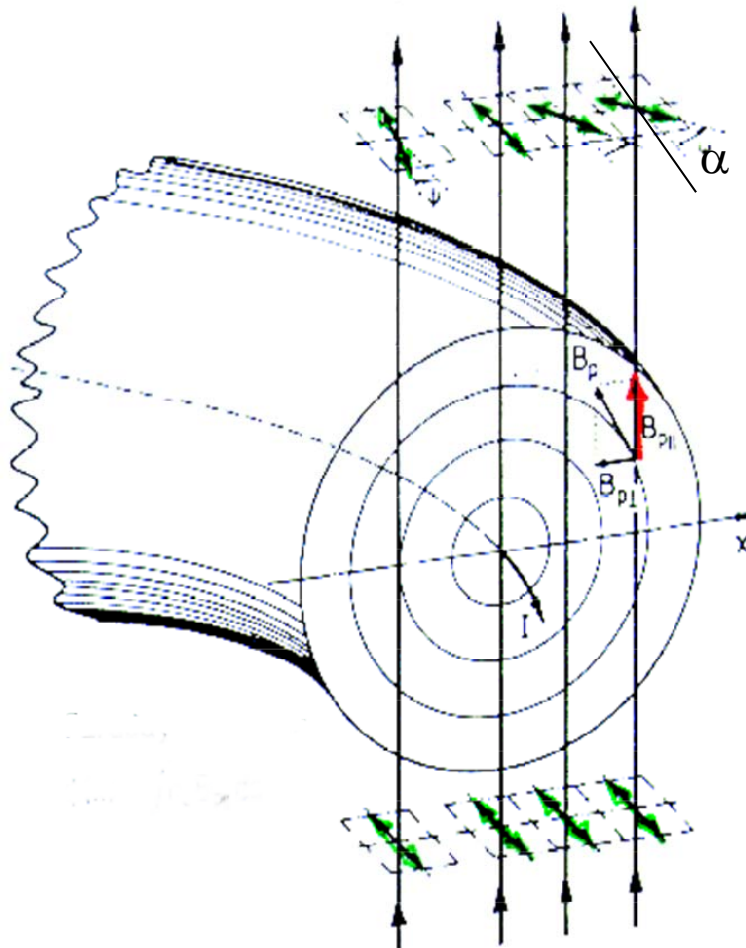
\rightarrow N approaches 0 \rightarrow waves are reflected

\rightarrow higher EM-frequencies can travel freely but experience a phase shift





Array of microwave senders on the bottom
and receivers / polarizers / interferometers
on the top



Array of microwave senders on the bottom
and receivers / polarizers / interferometers
on the top

Interferometry: measure the phase shift

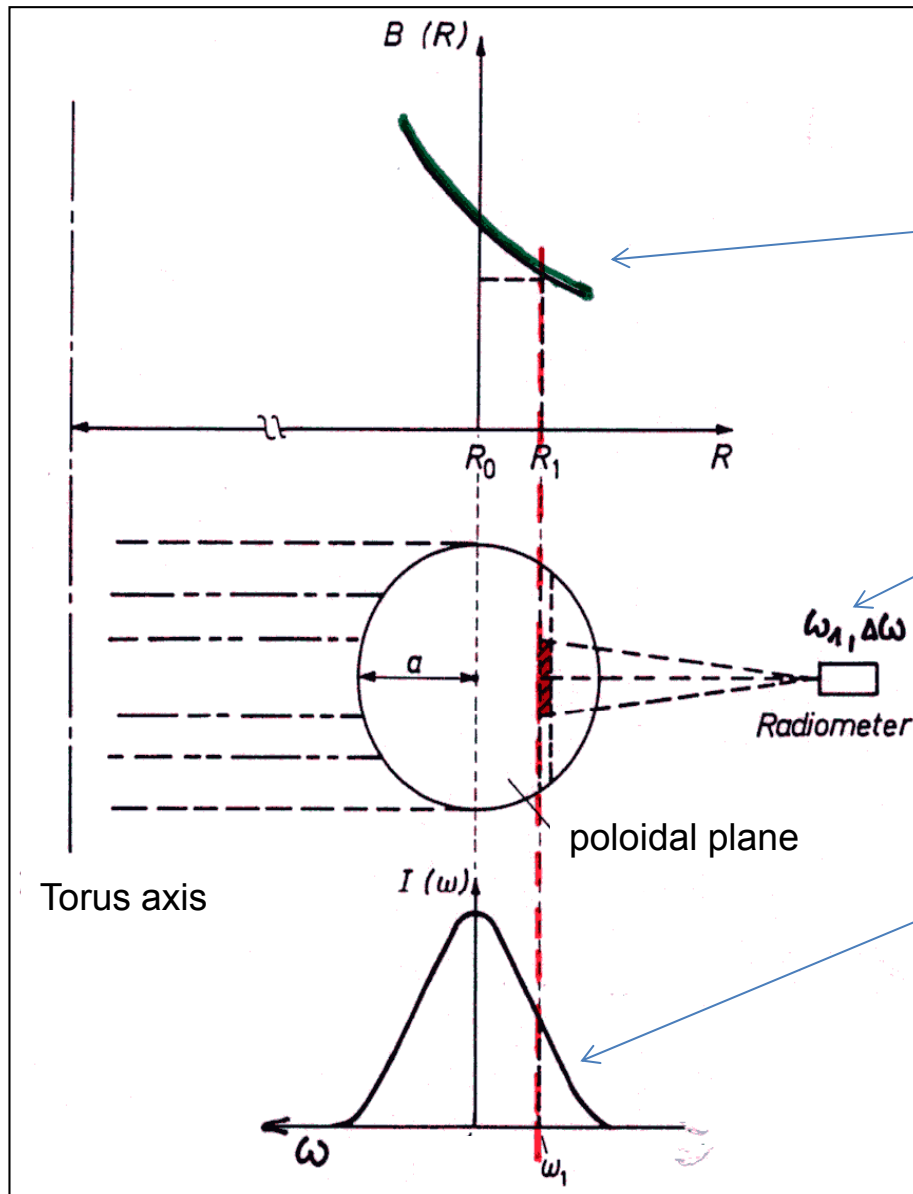
$$\Delta\varphi \propto \lambda \int_{l1}^{l2} n_e dl$$

Faraday rotation: measure the polarization angle

$$\alpha \propto \lambda^2 \int_{l1}^{l2} B_{\parallel} n_e dl$$

The Cotton-Mouton-effect: see Faraday-rotation

$$\alpha \propto \lambda^3 \int_{l1}^{l2} B_{\perp} n_e dl$$



In a toroidal fusion experiment holds roughly:

$$B(R) \propto 1/R$$

The emitted frequency ω from gyrating electrons is localized:

$$I(\omega) = \frac{\omega^2}{8\pi^3 c^2} \cdot T_e \cdot (1 - e^{-\tau})$$

With the optical thickness τ for (ideal) blackbody radiation ($\tau \rightarrow \infty$ at cut-off n_e) it follows:

$$I(\omega) \propto T_e(R)$$

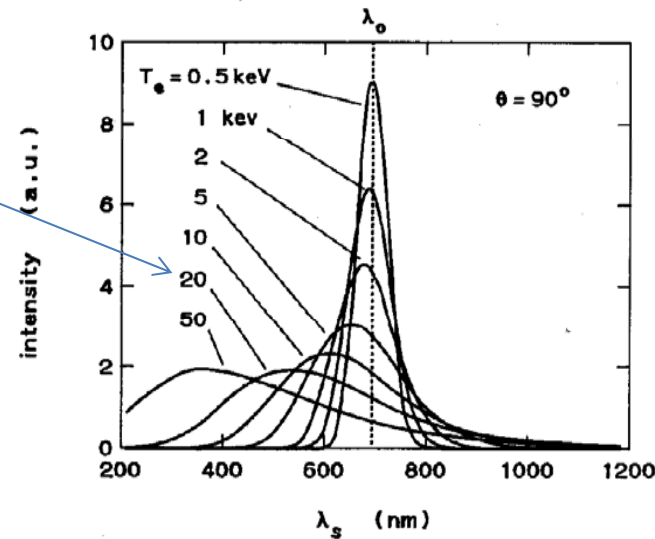
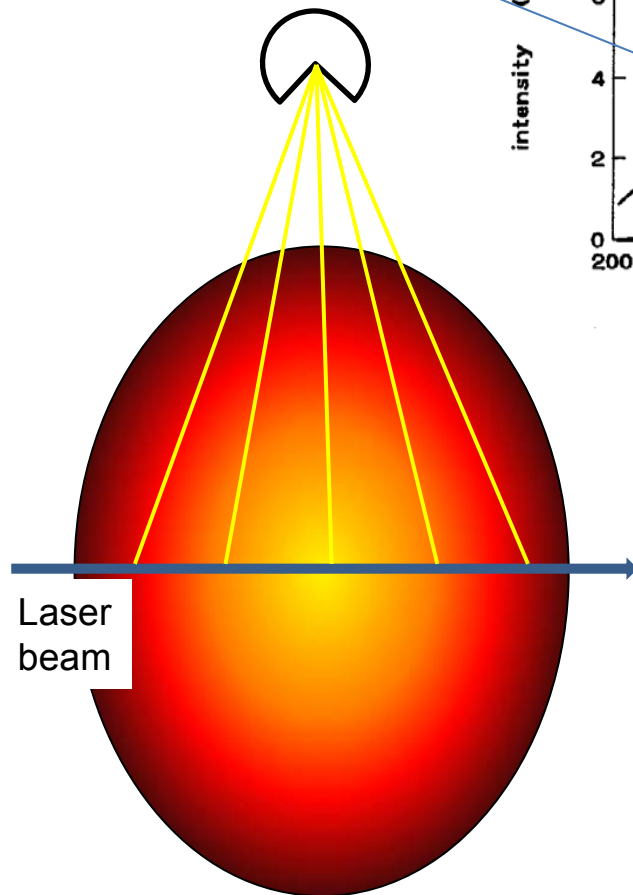
At the cutoff-layer the blackbody-limit is reached, here the plasma is optically thick



.....and some (beam assisted) active diagnostics.

Hutchinson: Principles of
plasma diagnostics

Spectroscopic observation



The moving electrons scatter
the laser light. Their thermal
velocity produces a Doppler
shift (line broadening).

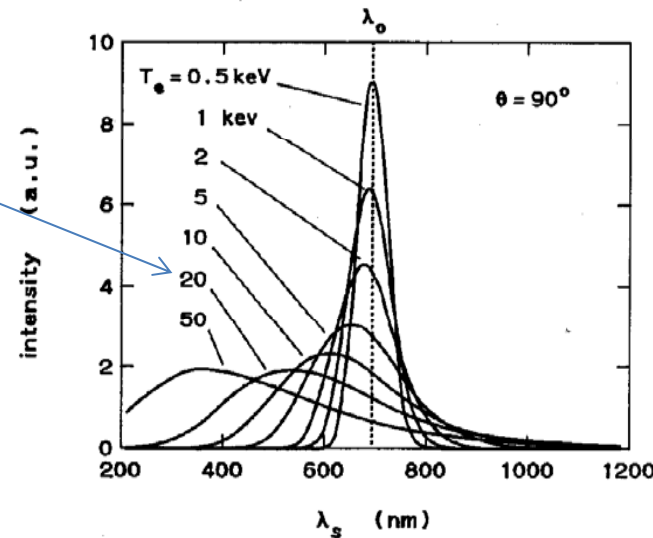
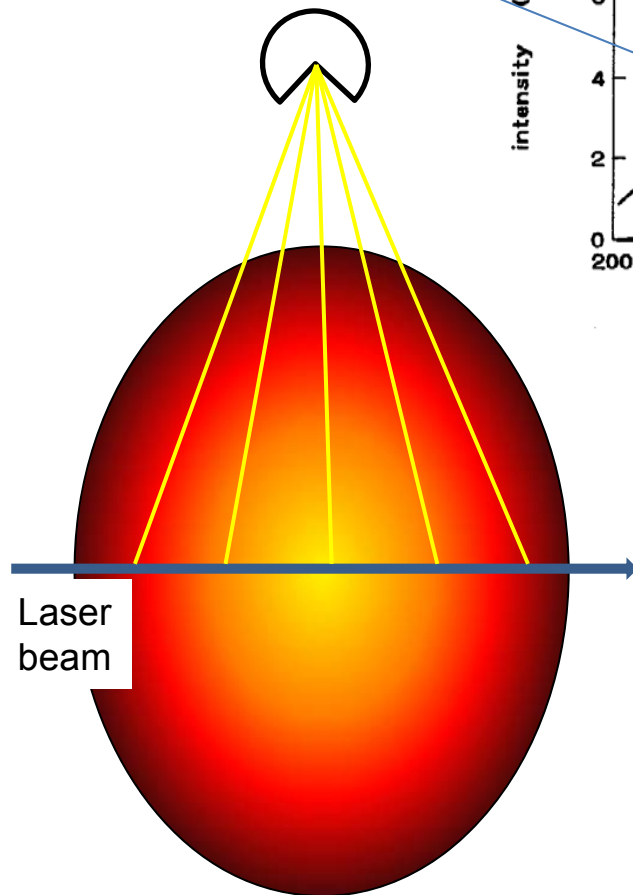
At higher temperatures a
relativistic blue shift occurs.

The Thomson cross section:

$$\sigma_{\text{Thomson}} = \frac{8\pi}{3} \left(\frac{e^2}{4\pi\epsilon_0 m_e c^2} \right)^2$$

Hutchinson: Principles of
plasma diagnostics

Spectroscopic observation



The moving electrons scatter
the laser light. Their thermal
velocity produces a Doppler
shift (line broadening).

At higher temperatures a
relativistic blue shift occurs.

The Thomson cross section:

$$\sigma_{\text{Thomson}} = \frac{8\pi}{3} \left(\frac{e^2}{4\pi\epsilon_0 m_e c^2} \right)^2$$

The scattered light intensity is proportional to n_e :

$$dI_z(\lambda) \propto n_e(r) \sqrt{\frac{m_e}{2\pi k T_e}} \cdot \exp\left\{-\frac{m_e V_z^2}{2k T_e}\right\} dV_z \quad z - \text{line of sight}$$

according to a Maxwellian distribution with a mean velocity

$$|\hat{V}_z^e| = \sqrt{\frac{8kT_e}{\pi m_e}} \Rightarrow \Delta\lambda_{\text{Broad}} = \lambda_{\text{Laser}} \cdot \frac{|\hat{V}_z^e|}{c} = f(T_e)$$

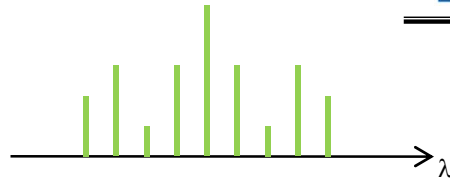


The motional Stark effect: Beam Emission Spectroscopy

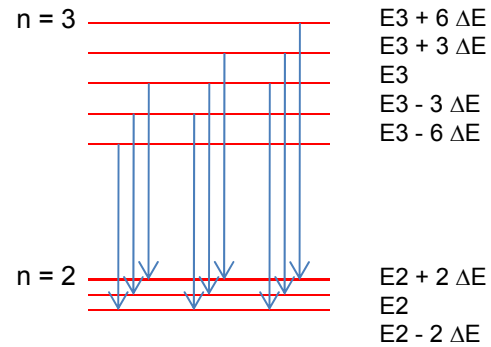
Max-Planck-Institut
für Plasmaphysik
EURATOM Assoc.



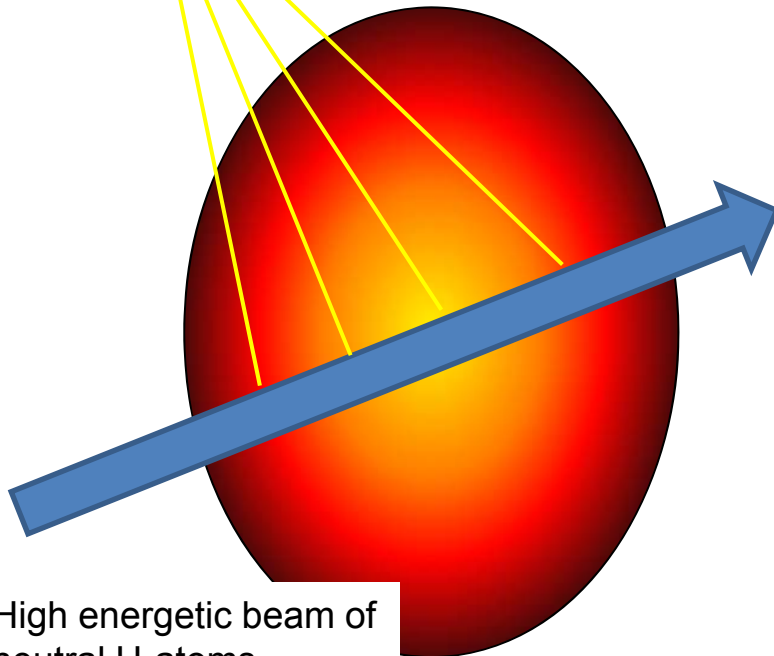
$\pi \pi \pi \sigma \sigma \sigma \pi \pi \pi$



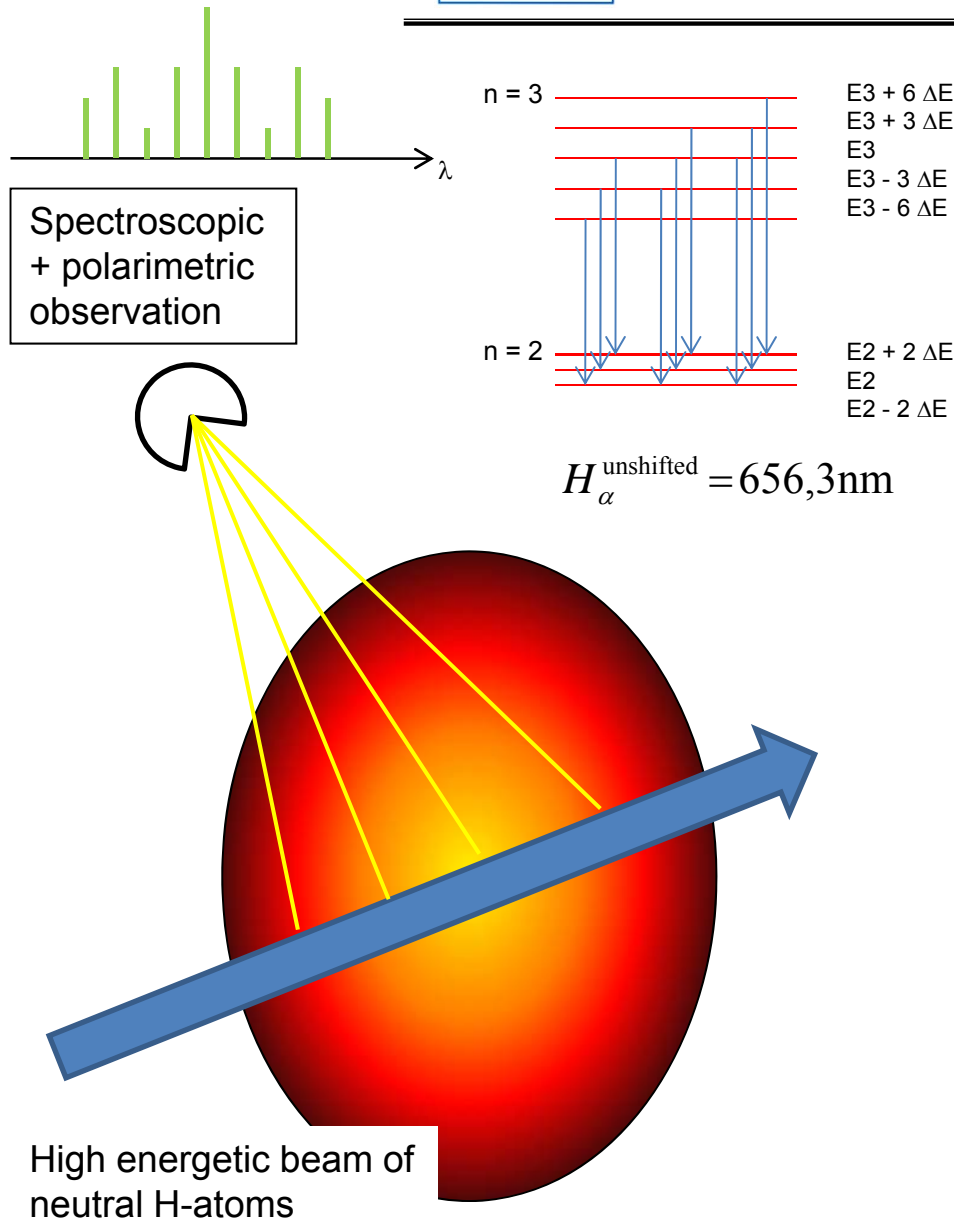
Spectroscopic
+ polarimetric
observation



$$H_{\alpha}^{\text{unshifted}} = 656,3\text{nm}$$



High energetic beam of
neutral H-atoms



The neutrals experience a relativistically transformed E-field from B by:

$$\vec{E}_{\text{motional}} = \vec{V} \times \vec{B} \quad (= V_{\text{beam}} \cdot B_{\perp})$$

leading to a Stark line splitting of the H_{α} line

$$\Delta\lambda_s = \frac{3a_0 e \lambda_a V_{\text{beam}}}{2hc} \sqrt{B_{\phi}^2 \sin^2 \Omega + B_{\theta}^2}$$

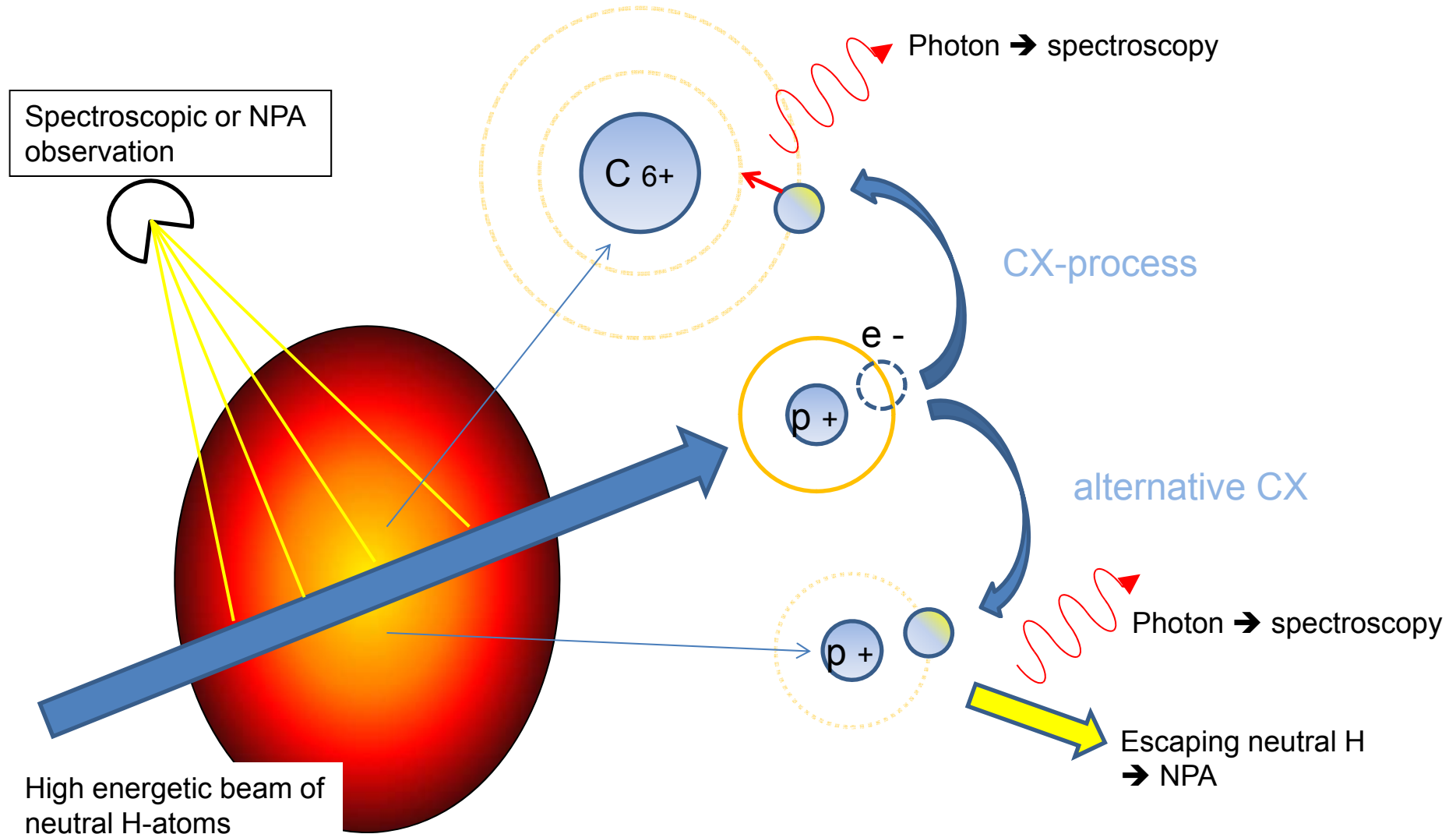
with the σ to π line intensities I and the definition equations:

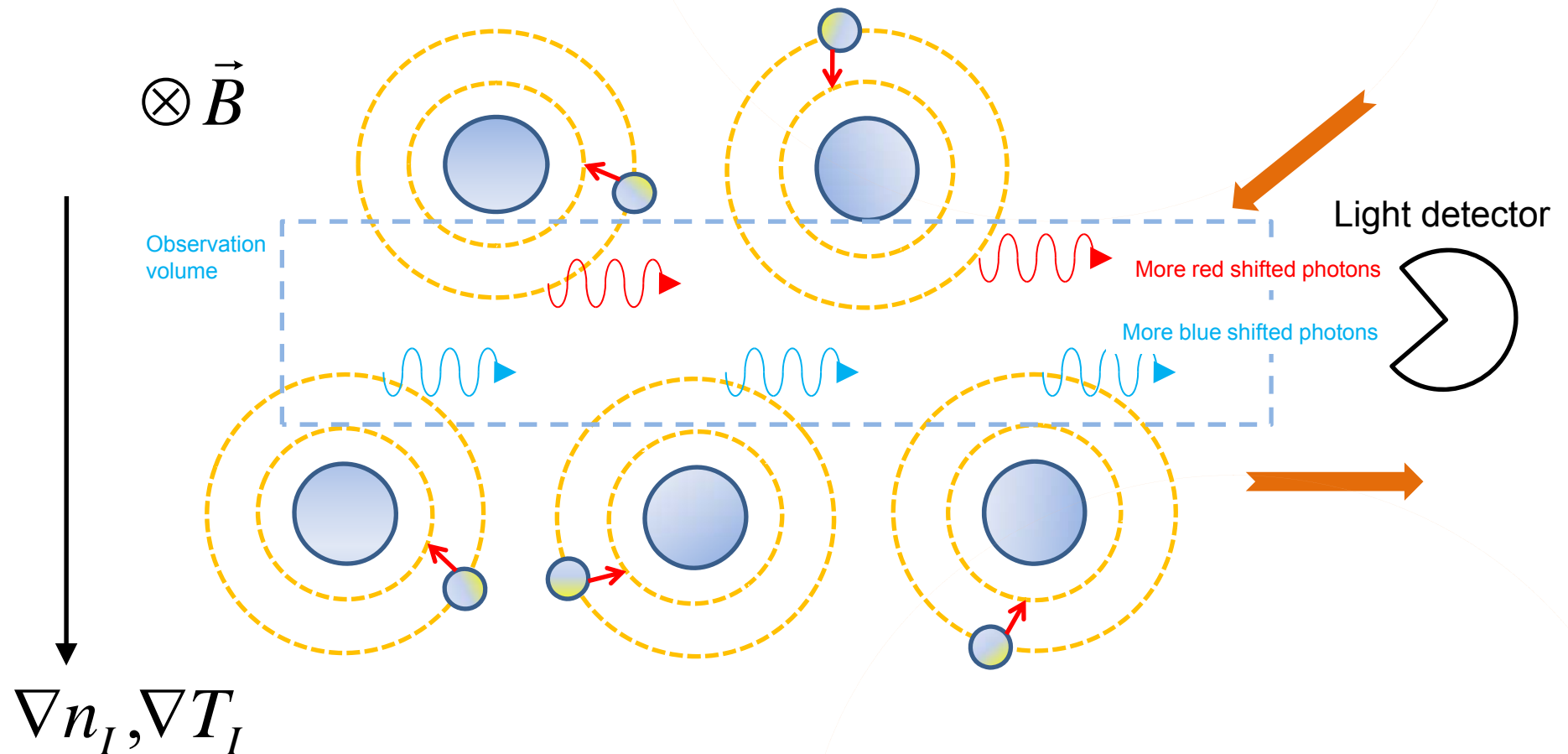
$$\tan \theta = \pm \sqrt{\frac{2I_{\pi}}{I_{\sigma} - I_{\pi}}} ; \quad \tan \varepsilon = \tan \gamma \left(\frac{\cos[\Omega - a]}{\sin \Omega} \right)$$

one can evaluate q by: $\tan \gamma = \frac{r}{Rq}$

$$\theta, \alpha, \Omega, \varepsilon, \phi$$

are angles between the electric field and the viewing line, line of sight and the toroidal direction, between beam and toroidal direction, the measured polarisation angle, the toroidal angle





→ Spectral line shift even with
„fixed“ guiding centres
→ diamagnetic current (drift)





Within the moving reference frame of the ion's Larmor orbit guiding centre holds the equation:

$$\frac{\Delta\lambda}{\lambda_0} = \frac{-T_I}{ceZ_{I+1}B} \cdot \nabla \left\{ \ln(n_{I+1} \cdot T_I \cdot \zeta_I^\gamma) \right\}, \quad \gamma = \frac{(\omega_I \tau_I)^2}{1 + (\omega_I \tau_I)^2}$$



Within the moving reference frame of the ion's Larmor orbit guiding centre holds the equation:

$$\frac{\Delta\lambda}{\lambda_0} = \frac{-T_I}{ceZ_{I+1}B} \cdot \nabla \left\{ \ln(n_{I+1} \cdot T_I \cdot \zeta_I^\gamma) \right\}, \quad \gamma = \frac{(\omega_I \tau_I)^2}{1 + (\omega_I \tau_I)^2}$$

The ion pressure balance equation together with inertial forces reads:

$$m_I n_I \left(\frac{\partial \vec{V}}{\partial t} + (\vec{V} \cdot \nabla) \vec{V} \right) = - \nabla p_I - \langle \nabla \vec{\Pi} \rangle + n_I e Z_I (\vec{V} \times \vec{B} + \vec{E}) + \sum \vec{F}_{\text{external}}$$

$\nabla p_I = \vec{j}_I \times \vec{B} \Rightarrow$



Within the moving reference frame of the ion's Larmor orbit guiding centre holds the equation:

$$\frac{\Delta\lambda}{\lambda_0} = \frac{-T_I}{ceZ_{I+1}B} \cdot \nabla \left\{ \ln(n_{I+1} \cdot T_I \cdot \zeta_I^\gamma) \right\}, \quad \gamma = \frac{(\omega_I \tau_I)^2}{1 + (\omega_I \tau_I)^2}$$

The ion pressure balance equation together with inertial forces reads:

$$\nabla p_I = \vec{j}_I \times \vec{B} \Rightarrow$$

$$m_I n_I \left(\frac{\partial \vec{V}}{\partial t} + (\vec{V} \cdot \nabla) \vec{V} \right) = -\nabla p_I - \langle \nabla \vec{\Pi} \rangle + n_I e Z_I (\vec{V} \times \vec{B} + \vec{E}) + \sum \vec{F}_{\text{external}}$$

this provides for stationary conditions and small friction forces:

$$E_r(r) = \frac{\partial \{n_{I+1}(r) \cdot T_I(r)\} / \partial r}{eZ_{I+1}n_{I+1}(r)} + \frac{T_I(r) \cdot \gamma}{eZ_{I+1}} \cdot \frac{\partial \zeta_I / \partial r}{\zeta_I} + [B_\theta V_\varphi(r) - B_\varphi V_\theta(r)]$$

Within the moving reference frame of the ion's Larmor orbit guiding centres holds the equation:

$$\frac{\Delta\lambda}{\lambda_0} = \frac{-T_I}{ceZ_{I+1}B} \cdot \nabla \left\{ \ln(n_{I+1} \cdot T_I \cdot \zeta_I^\gamma) \right\}, \quad \gamma = \frac{(\omega_I \tau_I)^2}{1 + (\omega_I \tau_I)^2}$$

The ion pressure balance equation together with inertial forces reads:

$$\nabla p_I = \vec{j}_I \times \vec{B} \Rightarrow$$

$$m_I n_I \left(\frac{\partial \vec{V}}{\partial t} + (\vec{V} \cdot \nabla) \vec{V} \right) = -\nabla p_I - \langle \nabla \vec{\Pi} \rangle + n_I e Z_I (\vec{V} \times \vec{B} + \vec{E}) + \sum \vec{F}_{\text{external}}$$

this provides for stationary conditions and small friction forces:

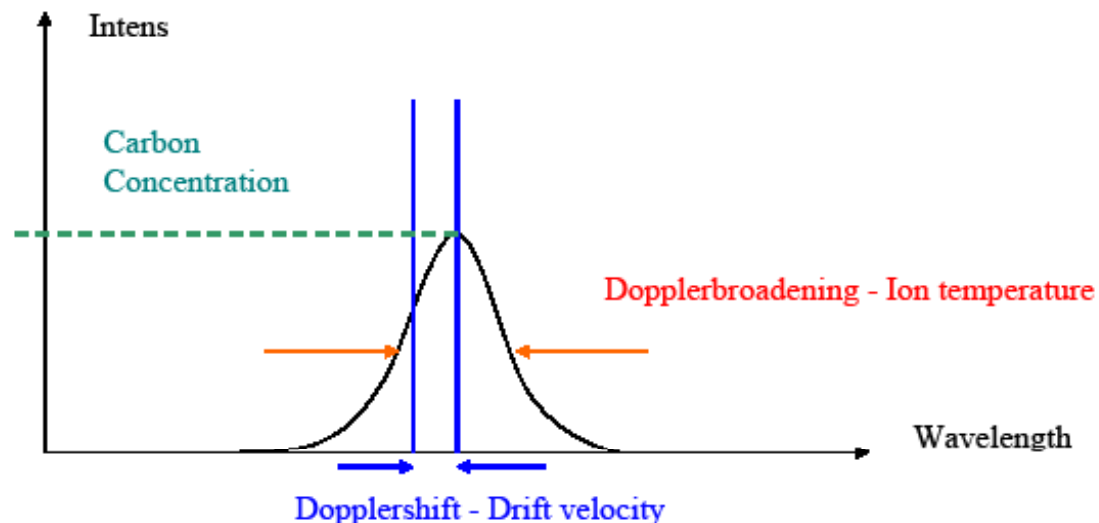
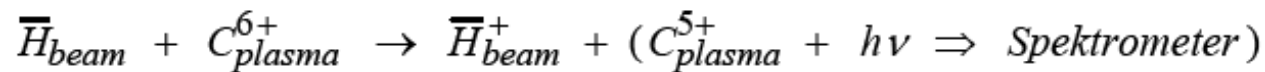
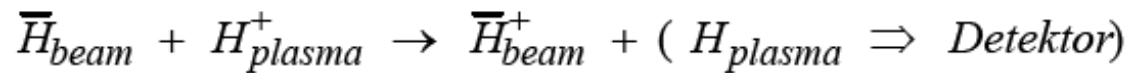
$$E_r(r) = \frac{\partial \{n_{I+1}(r) \cdot T_I(r)\} / \partial r}{eZ_{I+1}n_{I+1}(r)} + \frac{T_I(r) \cdot \gamma}{eZ_{I+1}} \cdot \frac{\partial \zeta_I / \partial r}{\zeta_I} + [B_\theta V_\varphi(r) - B_\varphi V_\theta(r)]$$



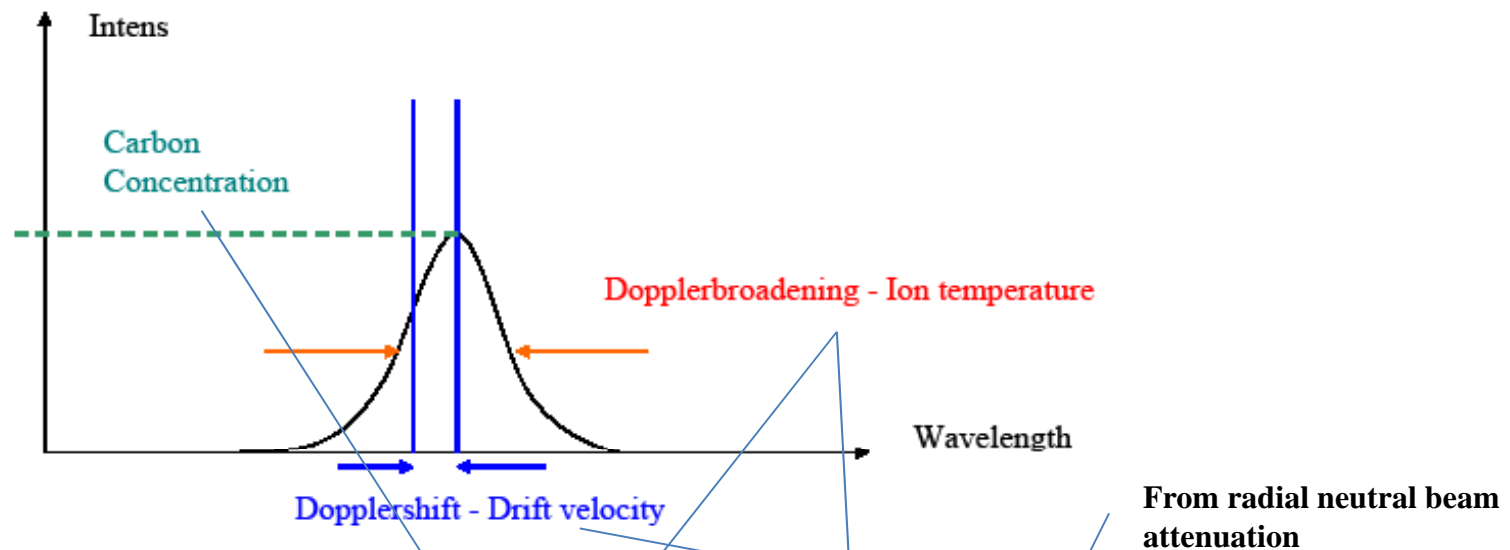
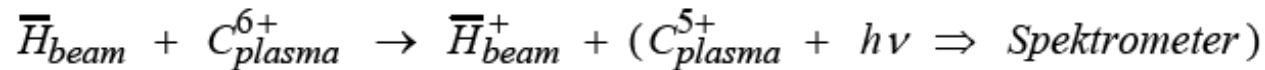
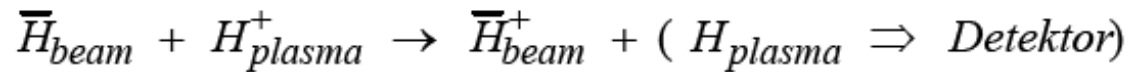
and the normalized radial gradient of the excitation probability

$$\frac{\partial \zeta_I / \partial r}{\zeta_I} = \frac{\sum_{j=1}^3 \langle \sigma_j^{\text{rad}} \cdot V_j^{\text{beam}} \rangle \cdot \partial n_j^{\text{beam}}(r) / \partial r}{\sum_{j=1}^3 \langle \sigma_j^{\text{rad}} \cdot V_j^{\text{beam}} \rangle \cdot n_j^{\text{beam}}(r)}$$

The principle of CXRS (Charge Exchange Recombination Spectroscopy) and the NPA (Neutral Particle spectral Analysis)



The principle of CXRS (Charge Exchange Recombination Spectroscopy) and the NPA (Neutral Particle spectral Analysis)



Using the formula from above:

$$E_r(r) = \frac{\partial \{n_{I+1}(r) \cdot T_I(r)\} / \partial r}{eZ_{I+1}n_{I+1}(r)} + \frac{T_I(r) \cdot \gamma}{eZ_{I+1}} \cdot \frac{\partial \zeta_I / \partial r}{\zeta_I} + [B_\theta V_\phi(r) - B_\phi V_\theta(r)]$$



Outline of this talk:

- 1) Basics, measured quantities, principles and some physics
(here we stick to the magnetic field, electrons and protons)
- 2) Techniques, practical considerations and some results
(and now we see that (fusion) life has even more aspects....)

Technical problem: how to get access to the plasma ?

Restricted space situation, narrow and long ports, restrictions by strong power densities, laser beams, high voltage, neutron radiation, magnetic field,

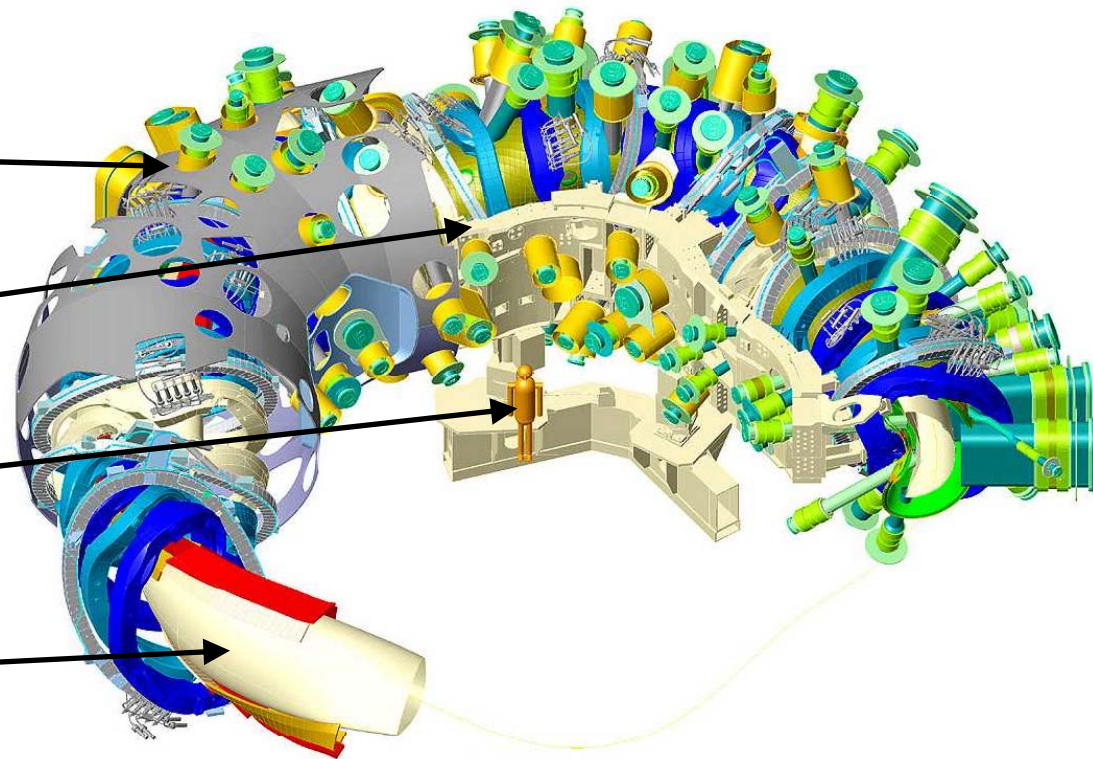
Example: W7-X

Cryostat

Mechanical supports

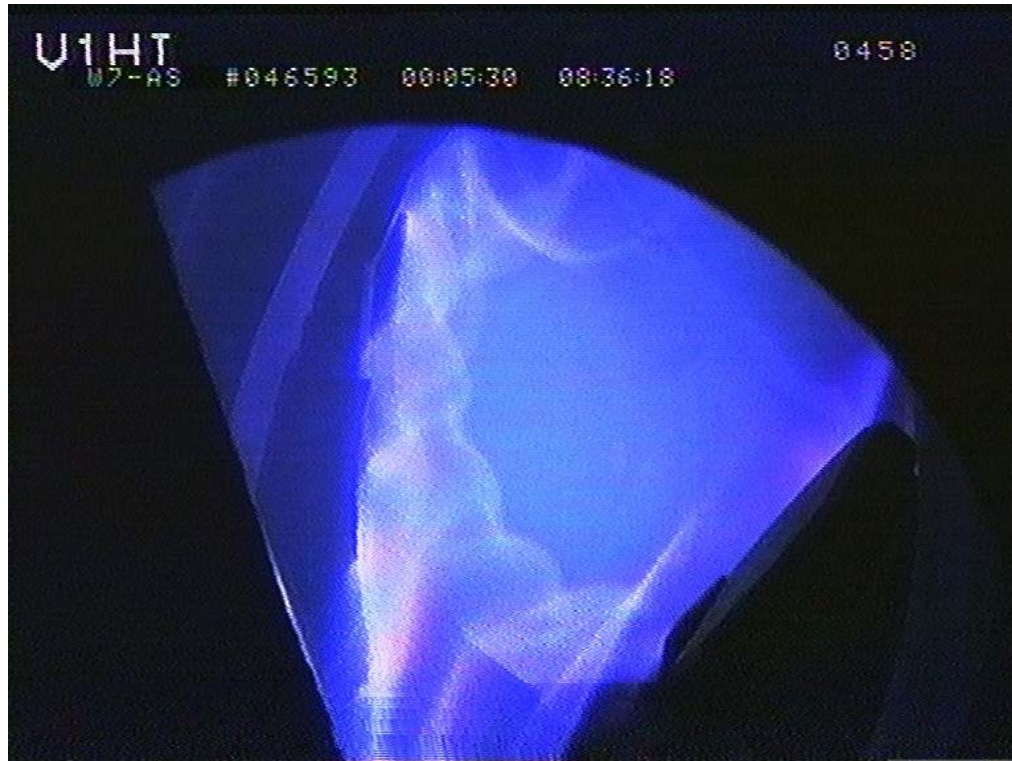
1 human being

And, finally, the plasma.....

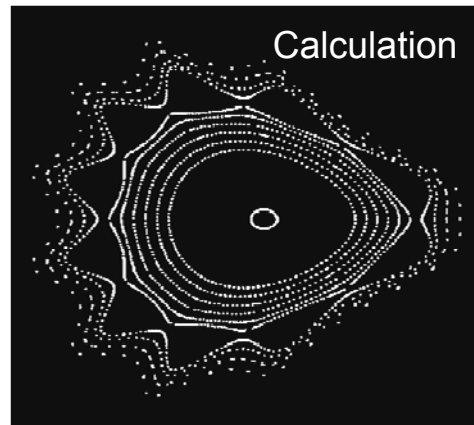




.....and again, the magnetic field.....



Video screenshot of a
W7-AS plasma with
magnetic islands
at the plasma edge



T. S. Pedersen_Stell. News 2004

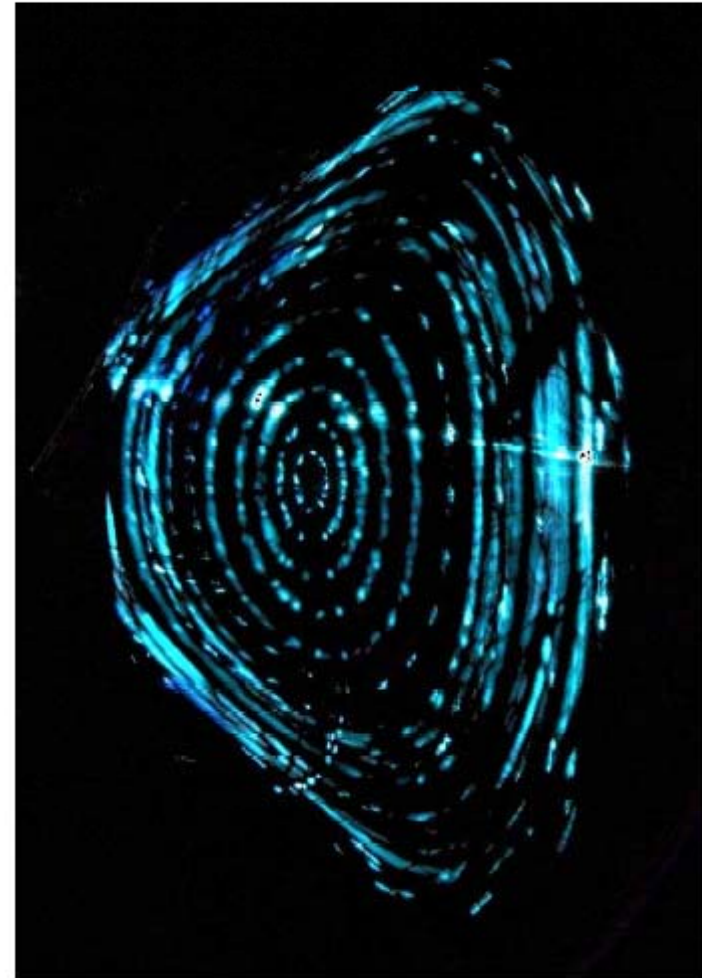
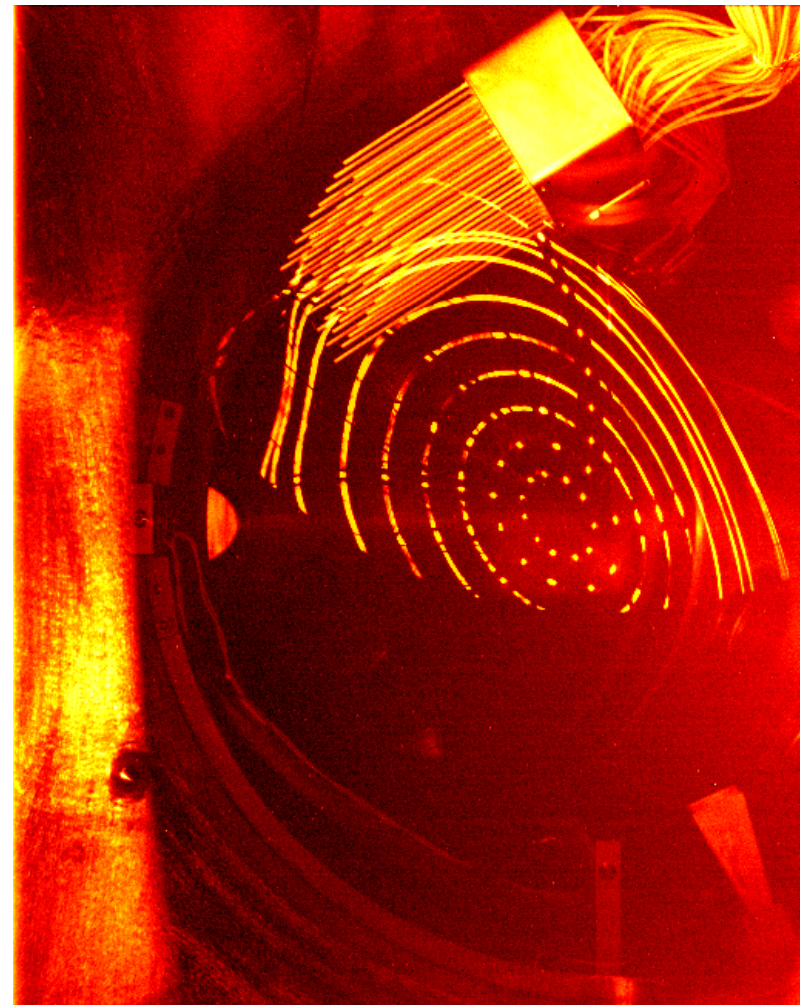
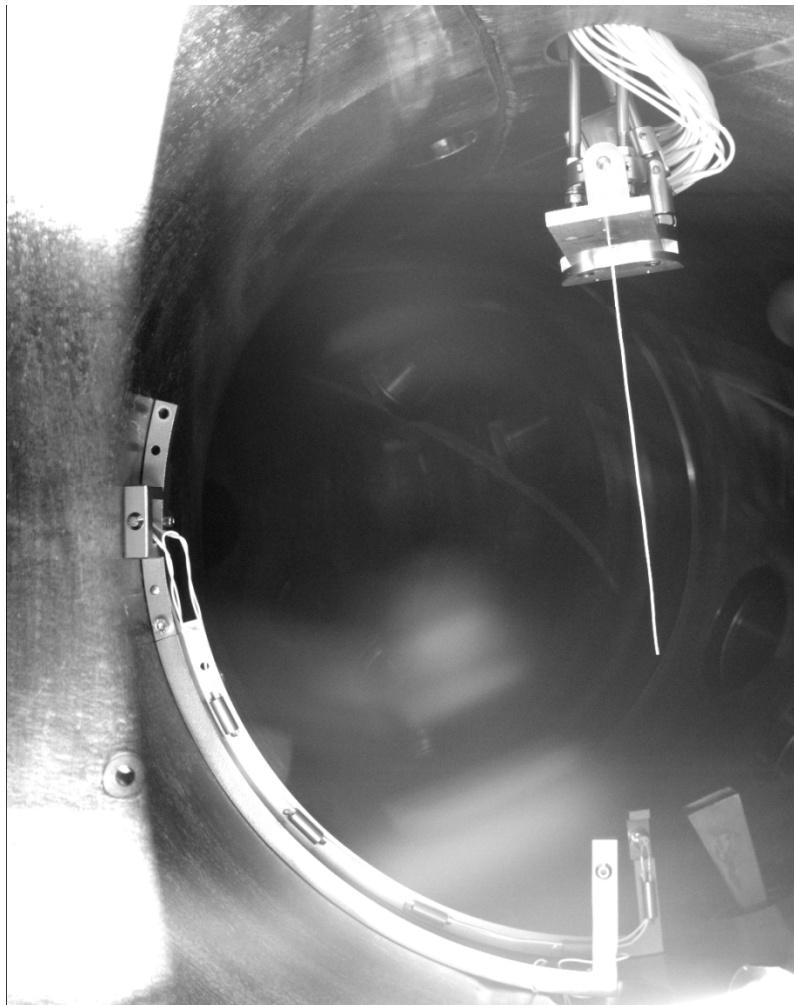


Fig. 3. Nested magnetic surfaces in CNT, mapped out
using an electron beam and two rotatable ZnO-coated
rods.

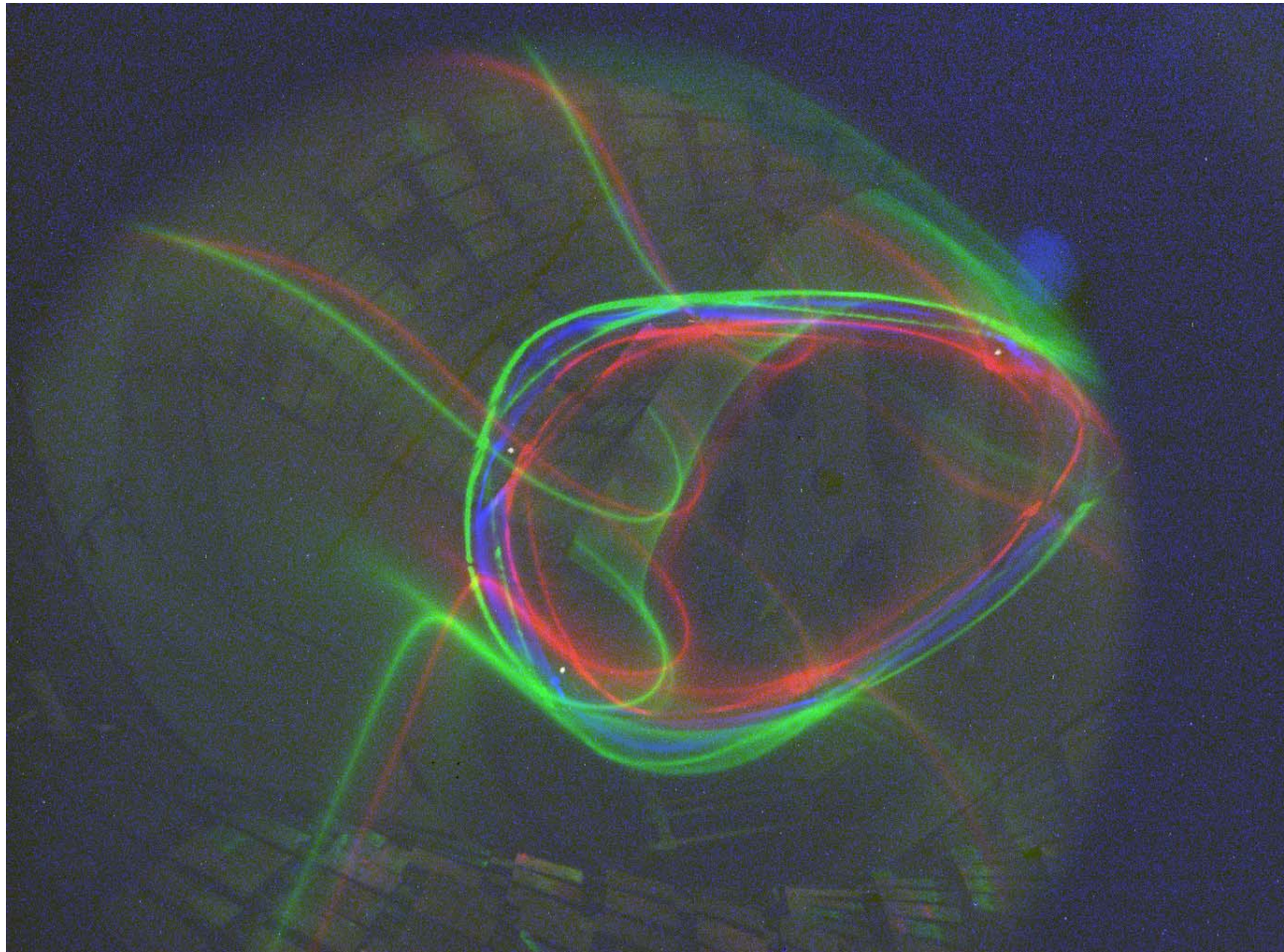
Demonstration examples from WEGA: the fluorescence rod (ZnS) and the electron beam together with the Langmuir probe array

M. Otte, W7-X Team



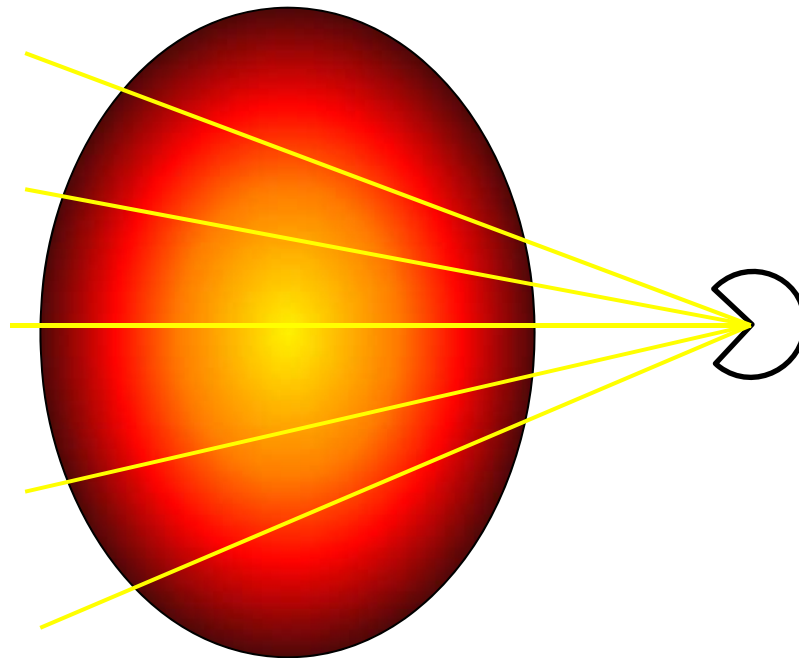


Example from W7-X: the 5/6 edge island. Green = 12kA, blue = 10kA, red = 2 kA nominal coil current.

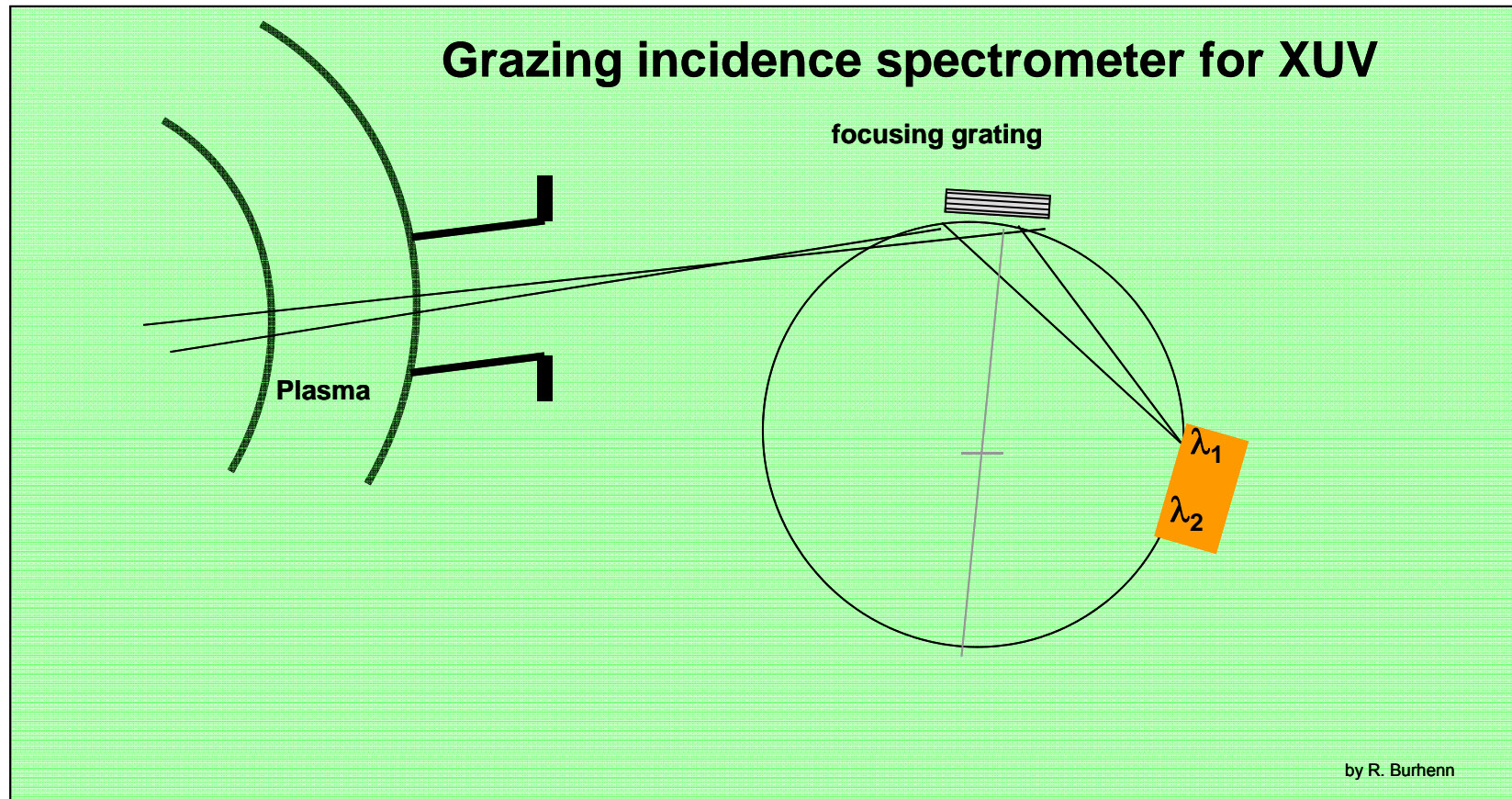




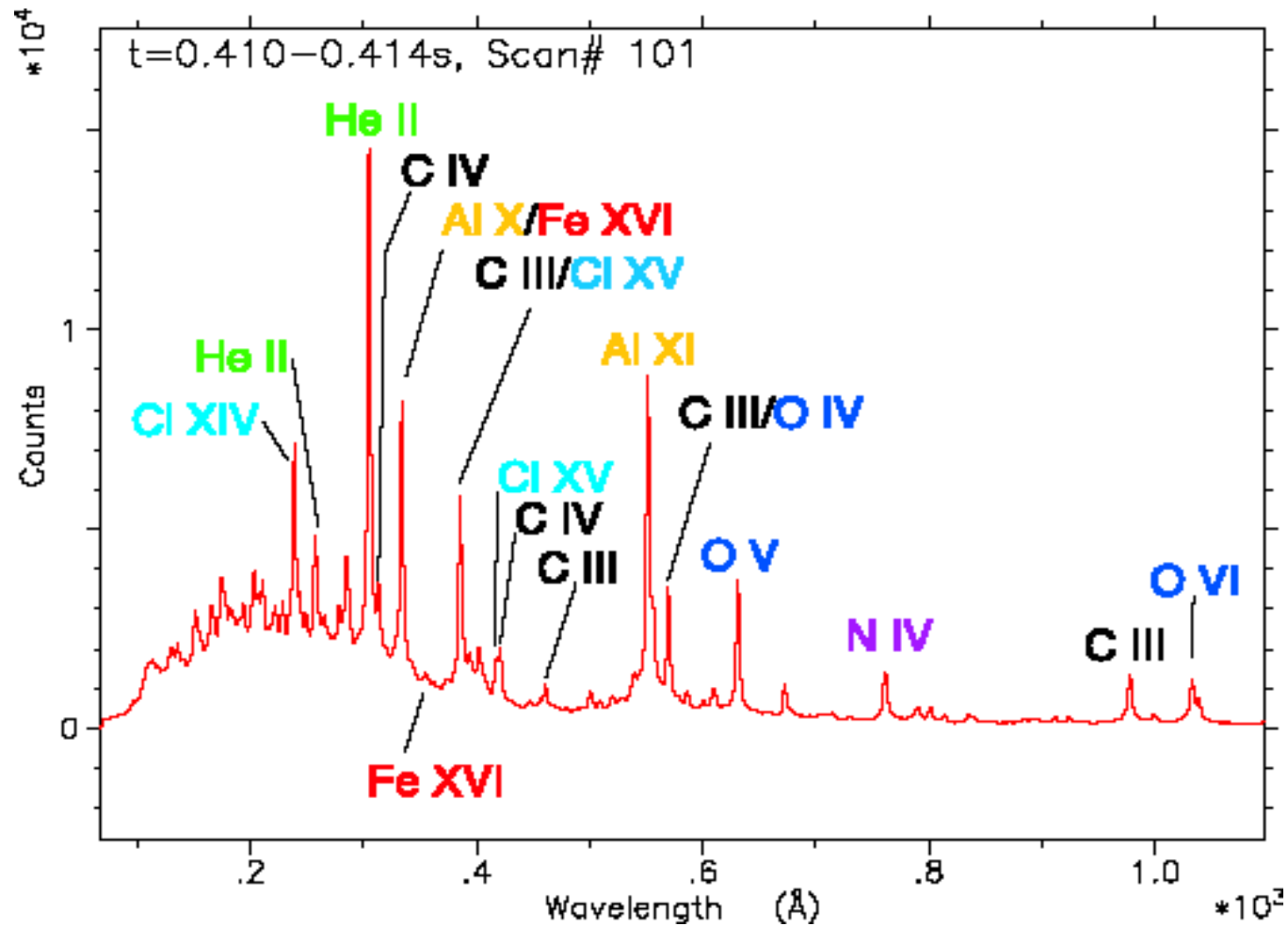
Fan of chords



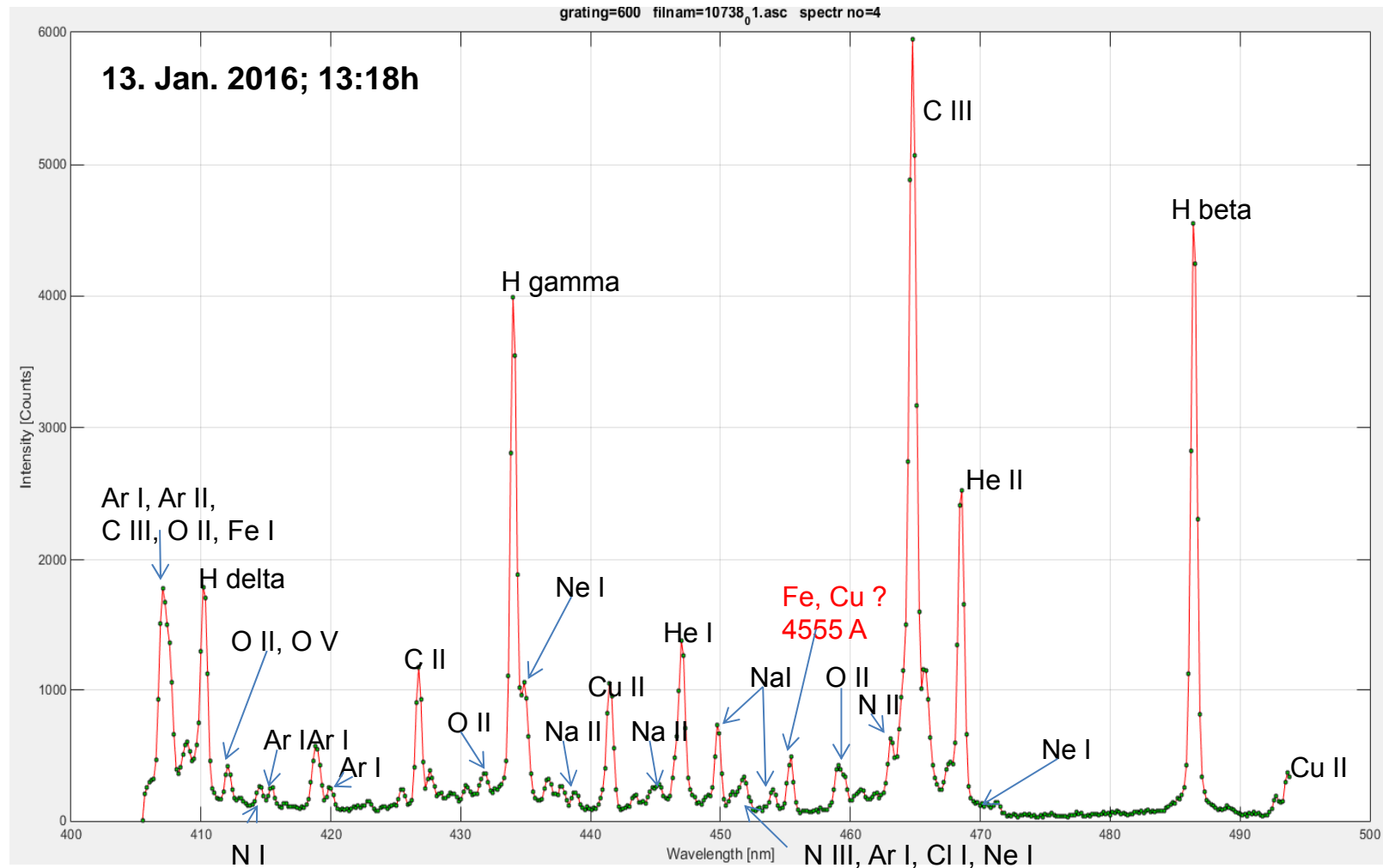
Detector



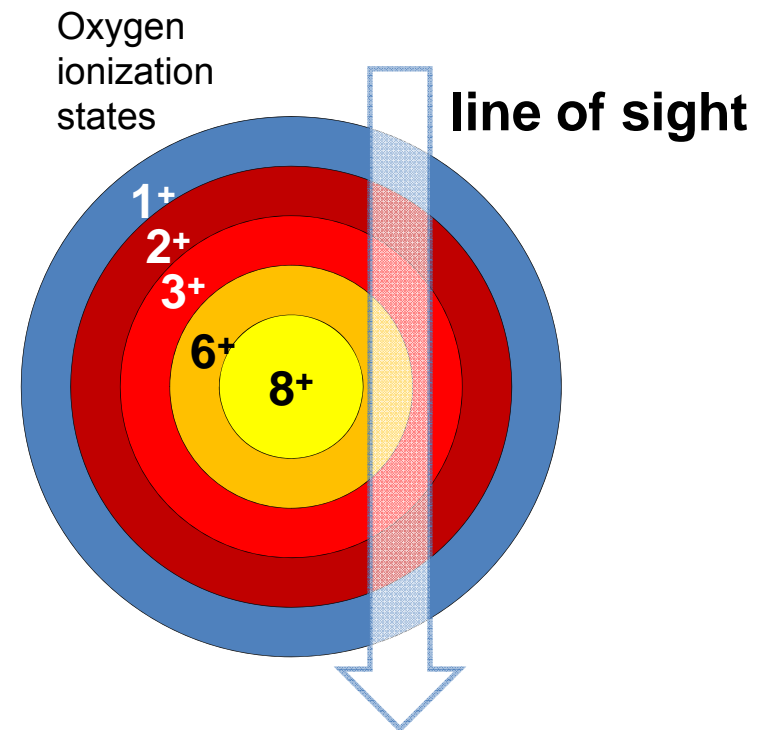
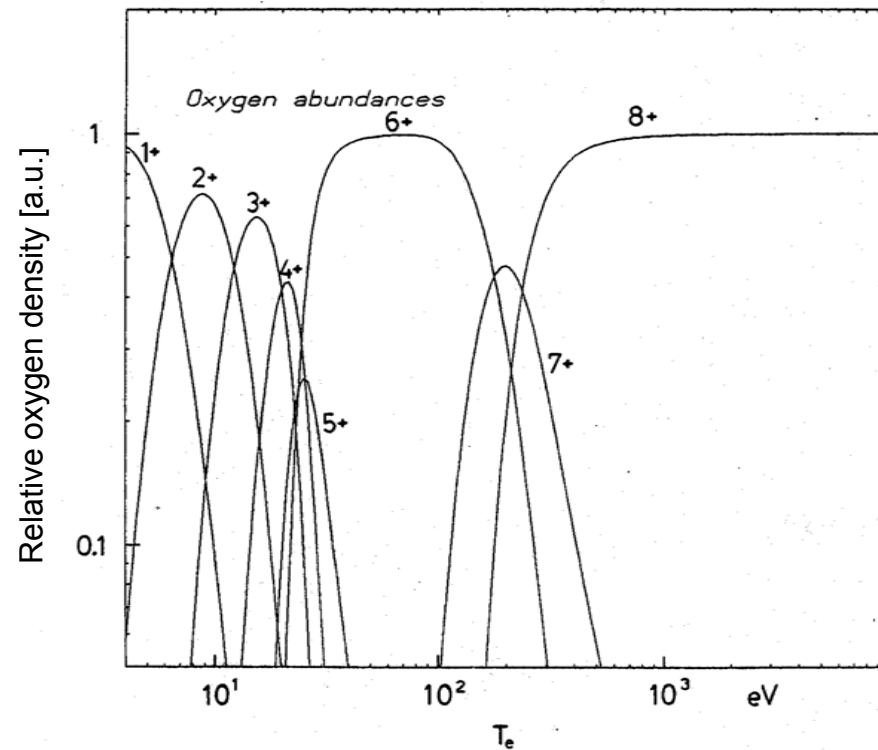
In the VUV-range: observation of highly ionized, heavy impurities



Dominating lines of Fe, C, N, Al,



Dominating lines of Ar, C, Ne, Na,



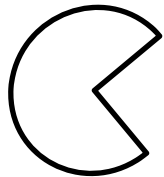
Principle of the line-of-sight integration

For transitions $p \rightarrow q$

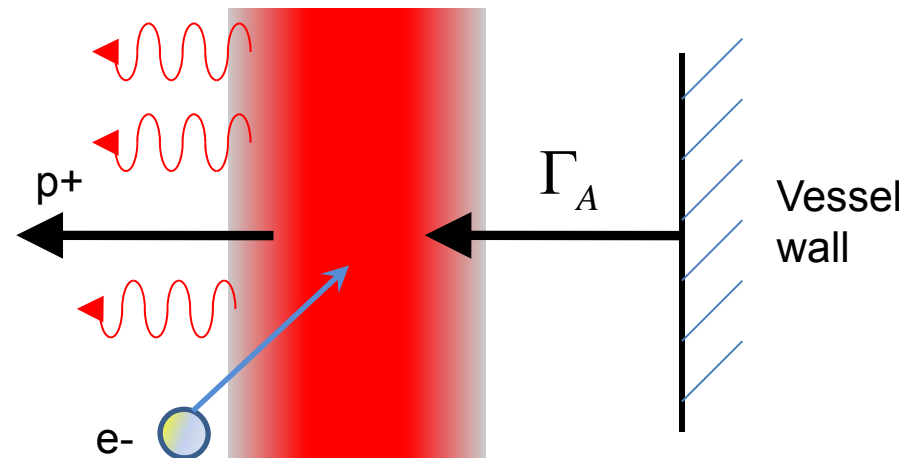
$$I_A^{H\alpha} = \Gamma_A \cdot \frac{h\nu \cdot \left(A_{pq} / \sum_{q < p-1} A_{pq} \right)}{4\pi} \cdot \frac{\int_{r1}^{r2} n_e(r) n_A(r) \langle \sigma_{\text{impact}} V_e \rangle dr}{\int_{r1}^{r2} n_e(r) n_A(r) \langle \sigma_{\text{ionizat}} V_e \rangle dr} = \Gamma_A \cdot \frac{h\nu \cdot \{\text{Branch.}\}}{4\pi} \cdot \frac{\{\text{Excit.}\}}{\{\text{Ioniz.}\}}$$

For fusion plasma edges: $n_e = 10^{19} \text{ m}^{-3}$ and $T_e = 10 \text{ eV}$ holds as a „good value“: $\frac{\text{Branch} * \text{Excit}}{\text{Ioniz}} \approx \frac{1}{15}$

H α detector



$\nabla n_e, \nabla T_e \leftarrow$





The net radial particle transport driven by fluctuation:

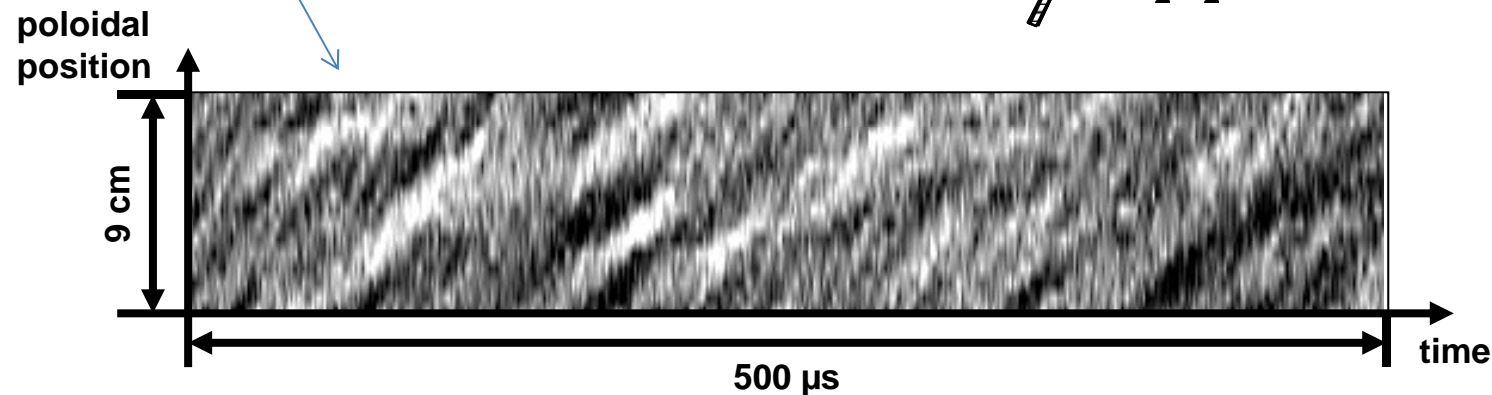
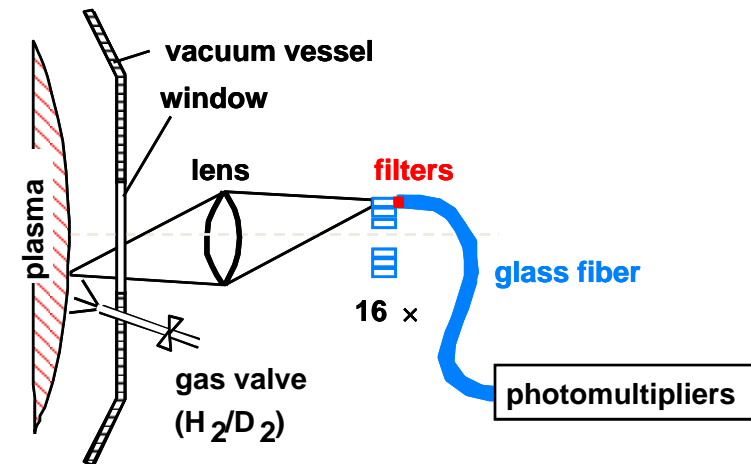
$$\Gamma_r = \left\langle \bar{n} \bar{V}_r + \bar{n} \tilde{V}_r + \tilde{n} \bar{V}_r + \tilde{n} \tilde{V}_r \right\rangle_{time}$$

Steady state
values

cancels out
out

contributes
for $\phi \neq 90^\circ$

Measured by probes or optically:





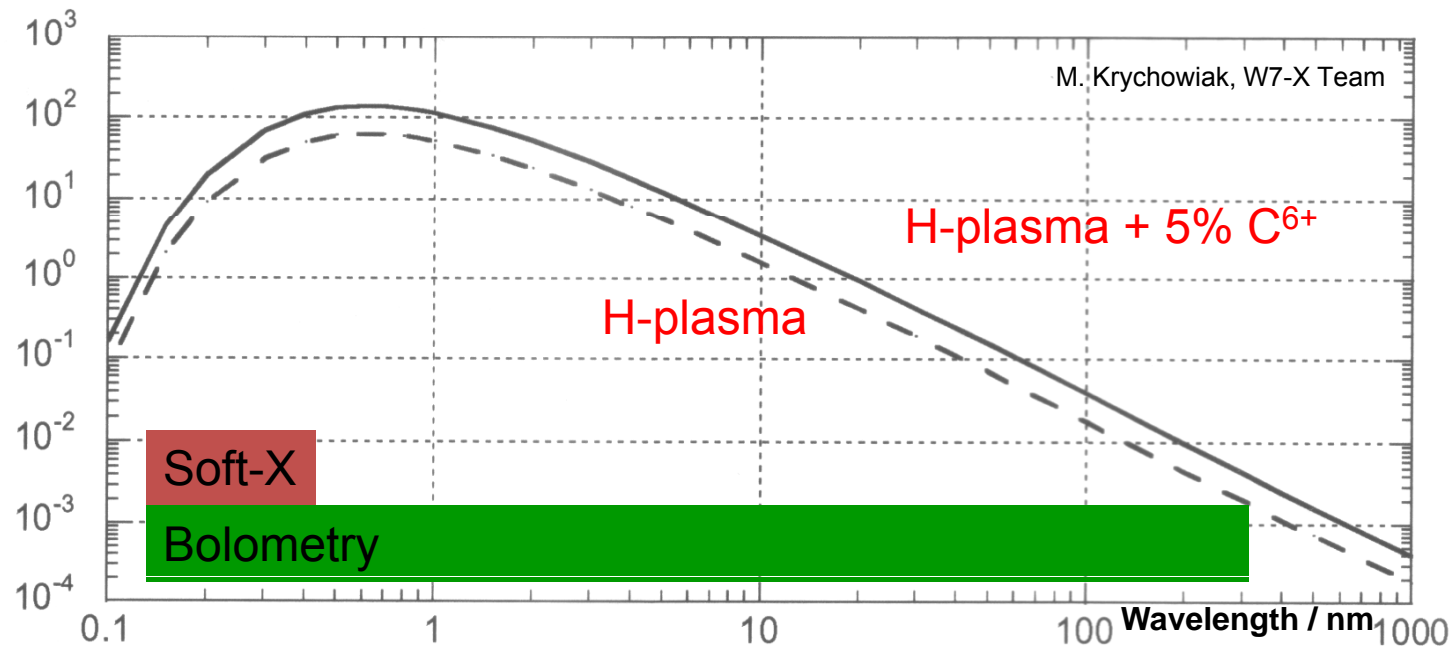
$$Z_{\text{eff}} = \frac{\sum n_e n_i Z_i^2}{n_e^2} \Rightarrow Z_{\text{eff}} \geq 1$$

$$\frac{dP}{d\omega} = 1,02 \cdot 10^{-33} \cdot n_e^2 \cdot \bar{g}_{\text{ff}} \cdot Z_{\text{eff}} \cdot \frac{\exp\{-\hbar\omega / kT_e\}}{\sqrt{kT_e}}$$

T-averaged free-free Gaunt factor
summarized for all impurities

$\epsilon_{\lambda}^{\text{ff}}$ [W/m³ster Å]

Bremsstrahlung





Important for bolometry and soft-X diagnostics: the high energy emission. The sources are:

- Bremsstrahlung (scattered electrons in the ion Coulomb field)
- line radiation (radiating excited electron states in impurity ions)
- thermal plasma emission (blackbody radiation, minor contribution)

-The number of photons per time, per volume and per energy interval into 4π reads:

$$\frac{dN}{dE_x} = \alpha \cdot n_e \cdot \frac{\exp\{-E_x/T_e\}}{E_x \sqrt{T_e}} \cdot [n_{prot} g_{ff} + Z_{eff}^2 n_Z g_{ff}^Z + n_Z g_{fb} F(n_e, T_e)], \quad \alpha = 9,6 \cdot 10^{-20} \text{ eV}^{1/2} \text{ m}^3 \text{ s}^{-1}$$

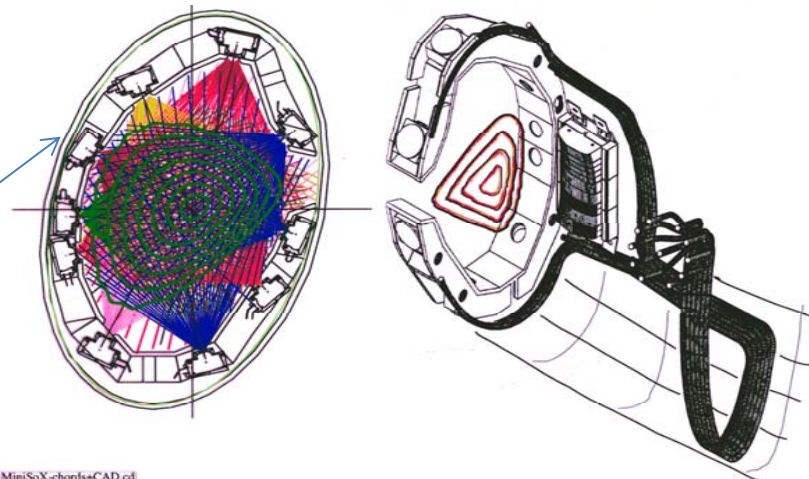
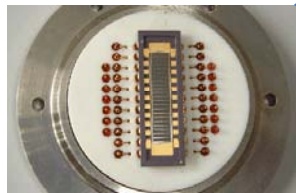
Bremsstrahlung - electrons-protons

electrons-impurities

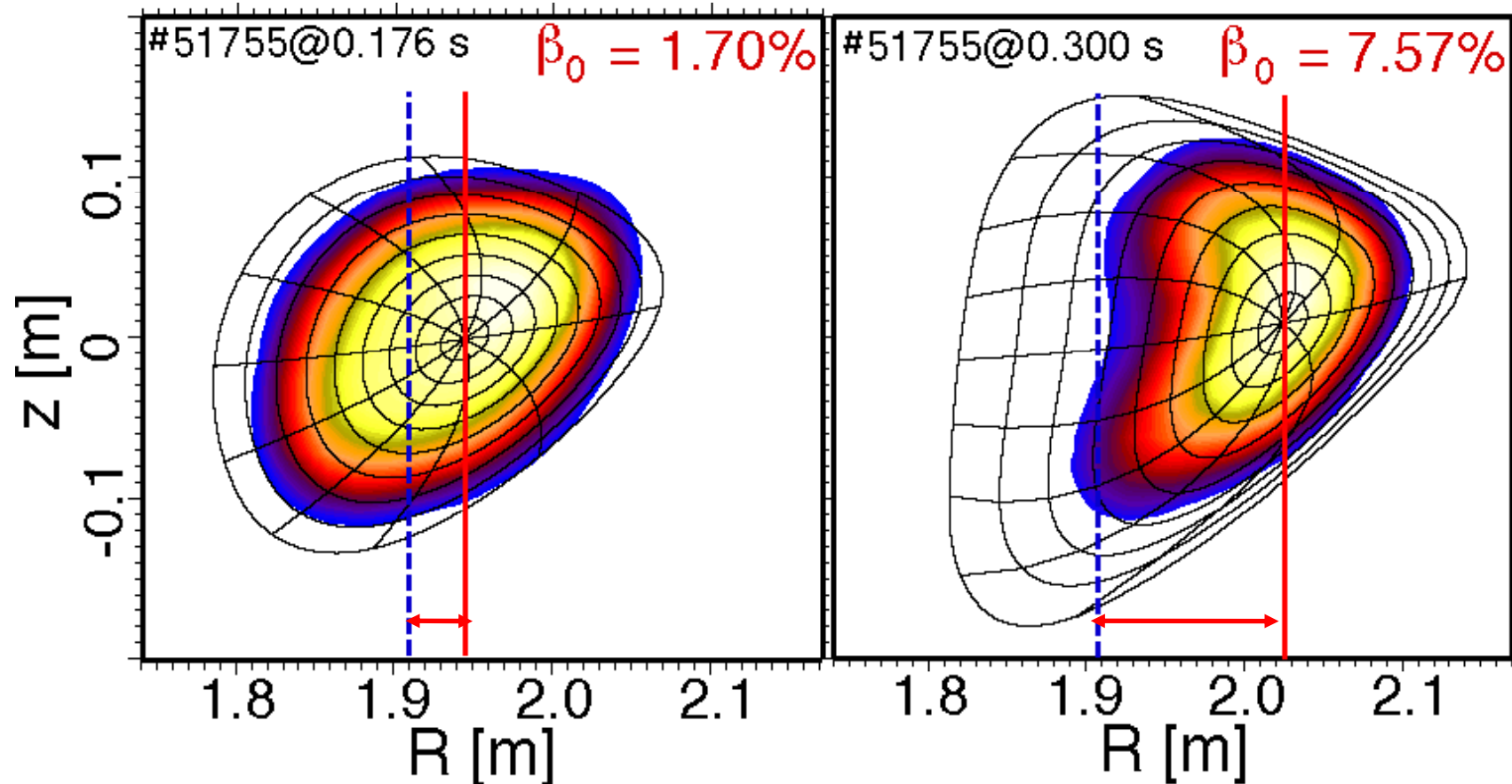
line radiation impurities/recombination

The W7-AS soft-X tomography system

Si- Photodiode arrays

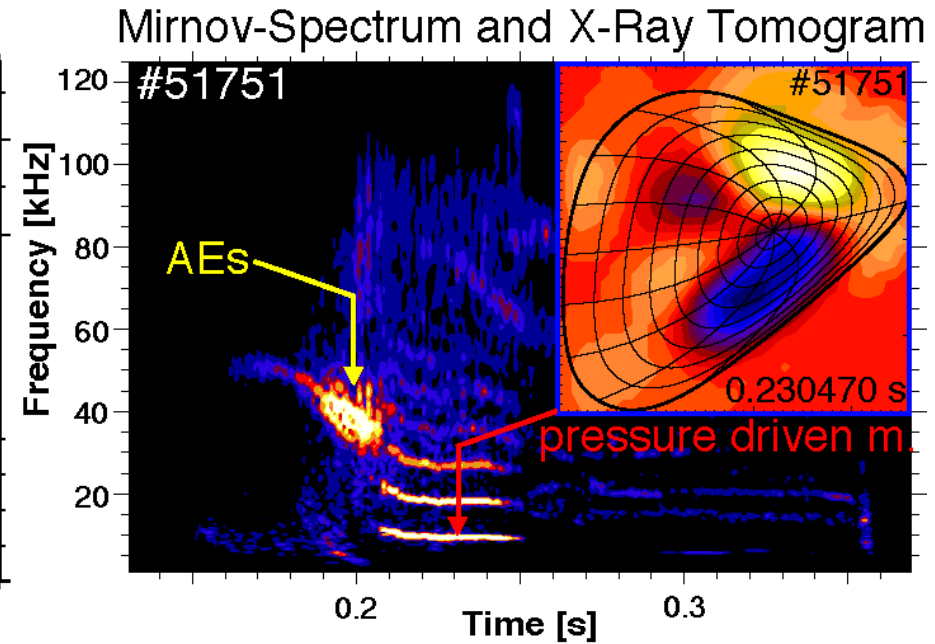
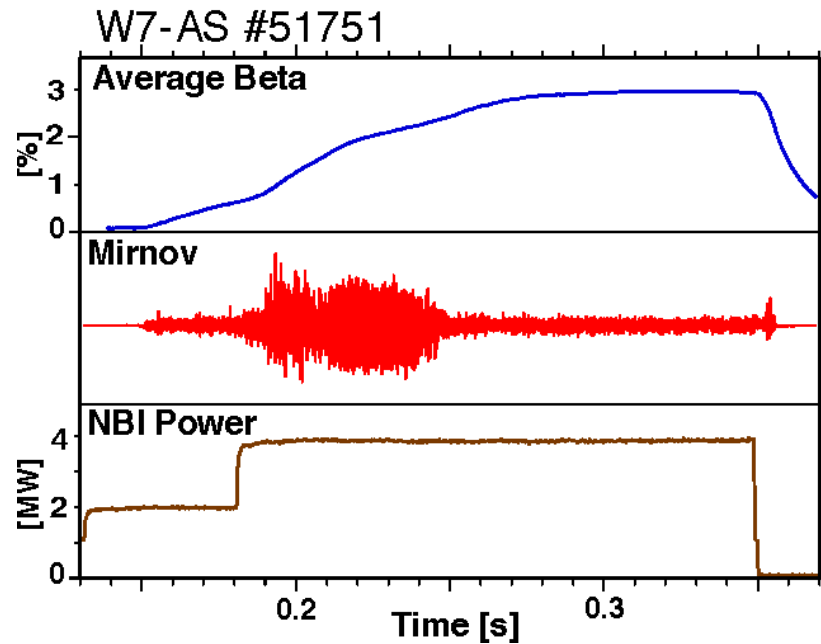


Soft-X diagnostics is sensitive to line radiation, Z_{eff} , n_e and T_e , the emissivity is a function of the magnetic flux



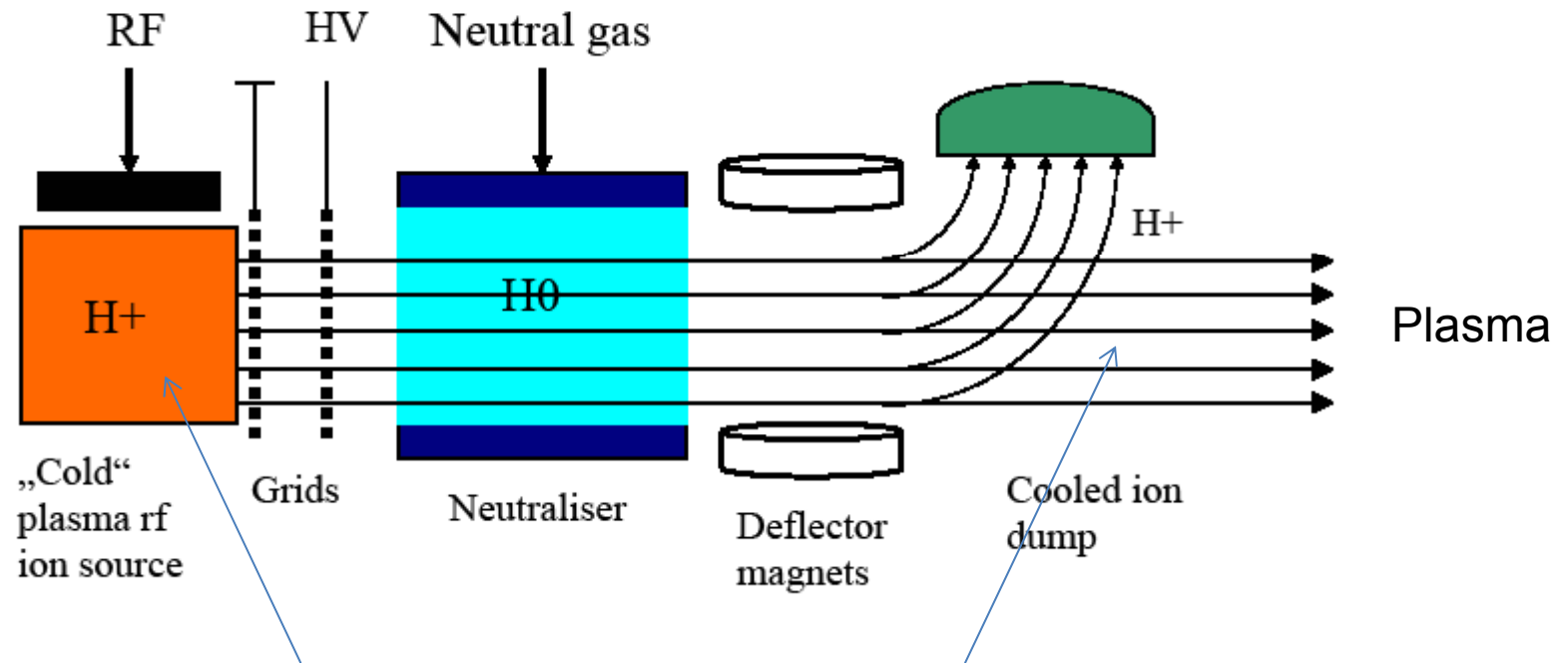
W7-AS: demonstration of the Shafranov shift due to the plasma pressure

Arthur Weller, ASDEX-U Team



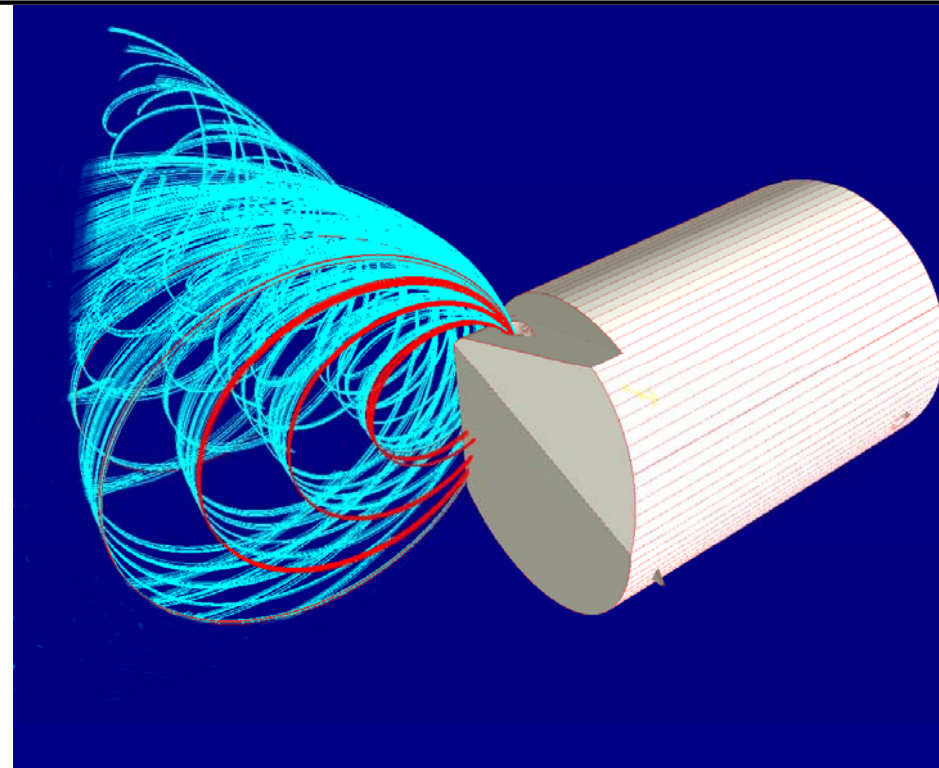
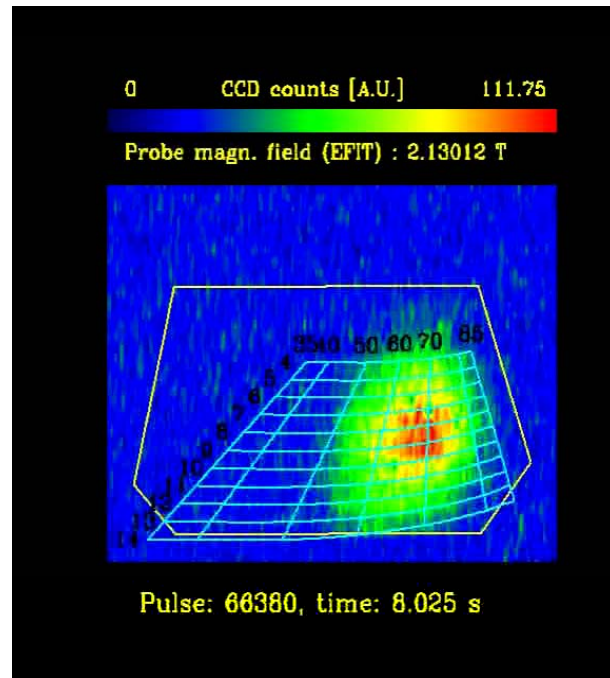
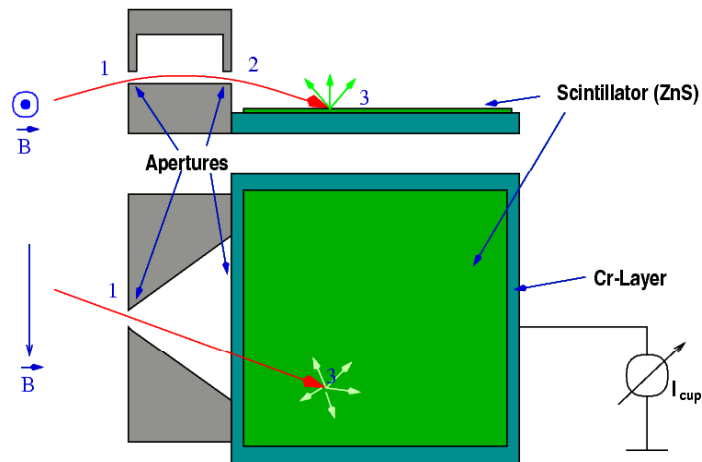
Within a certain pressure-window Alfvén eigenmodes can survive,
for higher plasma pressure they vanish

Neutral Beam Injection NBI: Sketch of the arrangement



p^+ protons
 H_2^+ , H_3^+ molecules
 H_2O^+ molecules

→ Energy-mix in the beam:
 U_{acc} , $1/2 U_{acc}$, $1/3 U_{acc}$, $1/18 U_{acc}$



Scintillator light yields ion fluxes

Important for confinement studies

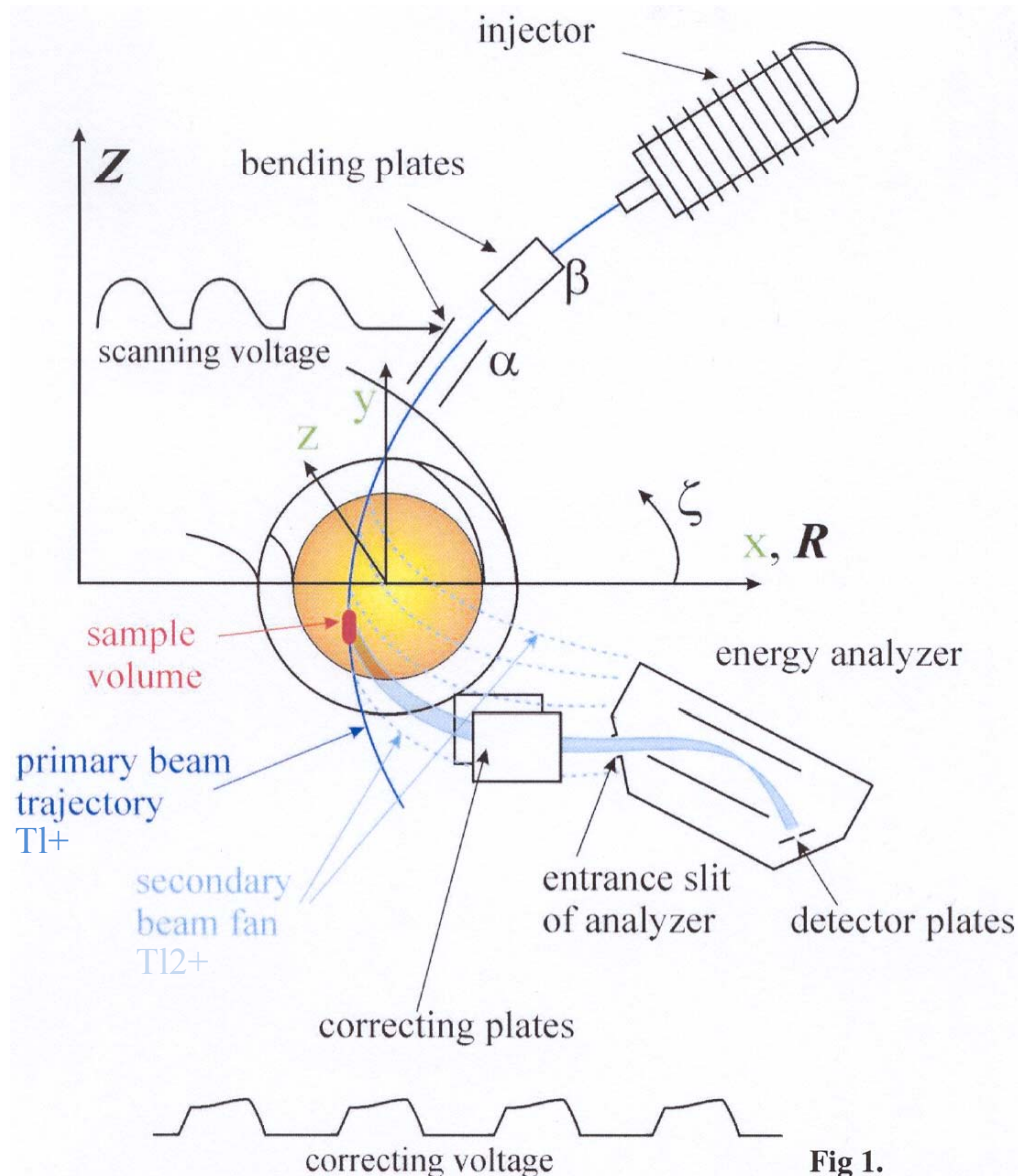
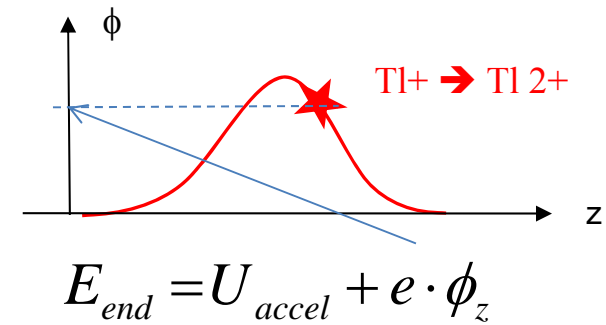


Fig 1.



The measurement of $E_r(r, \theta, \phi)$
becomes accessible

High time resolution
 $\rightarrow \tilde{E}_r$ becomes accessible

U_{accel} typically 1-2 MeV (W7-X)

I_{prim} typically 100 μA

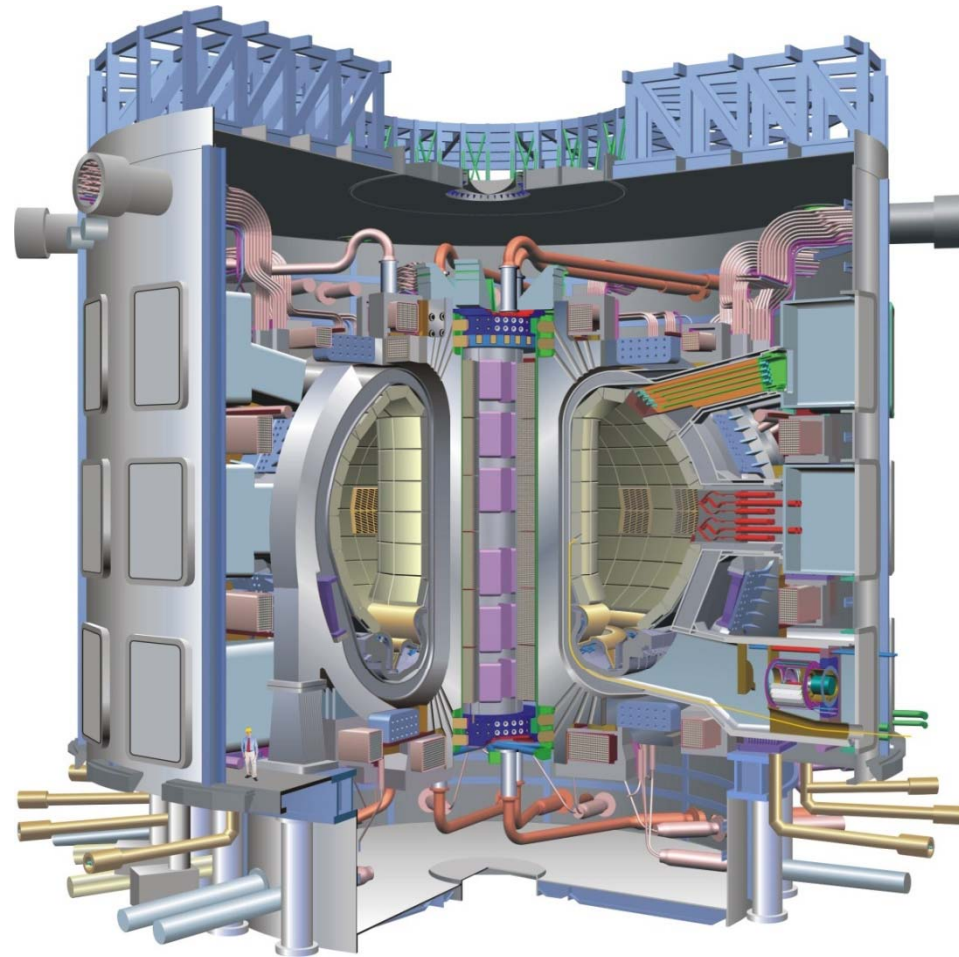
I_{second} typically 300 nA

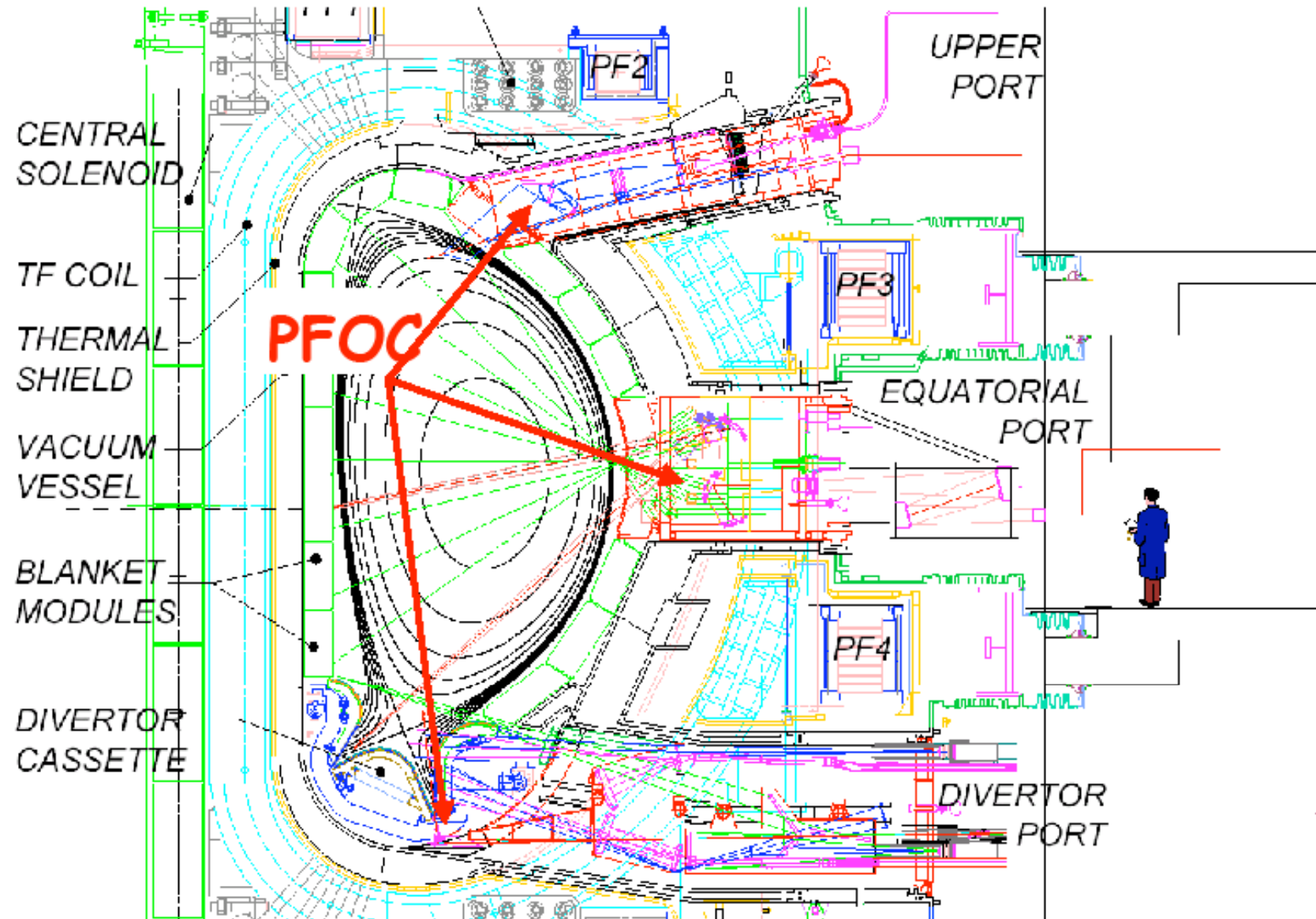
Time resolution typ. MHz



The way to ITER:

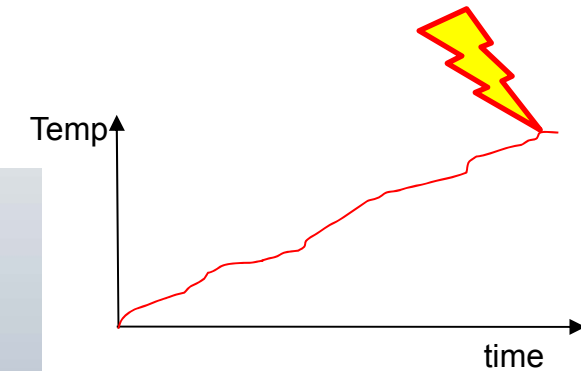
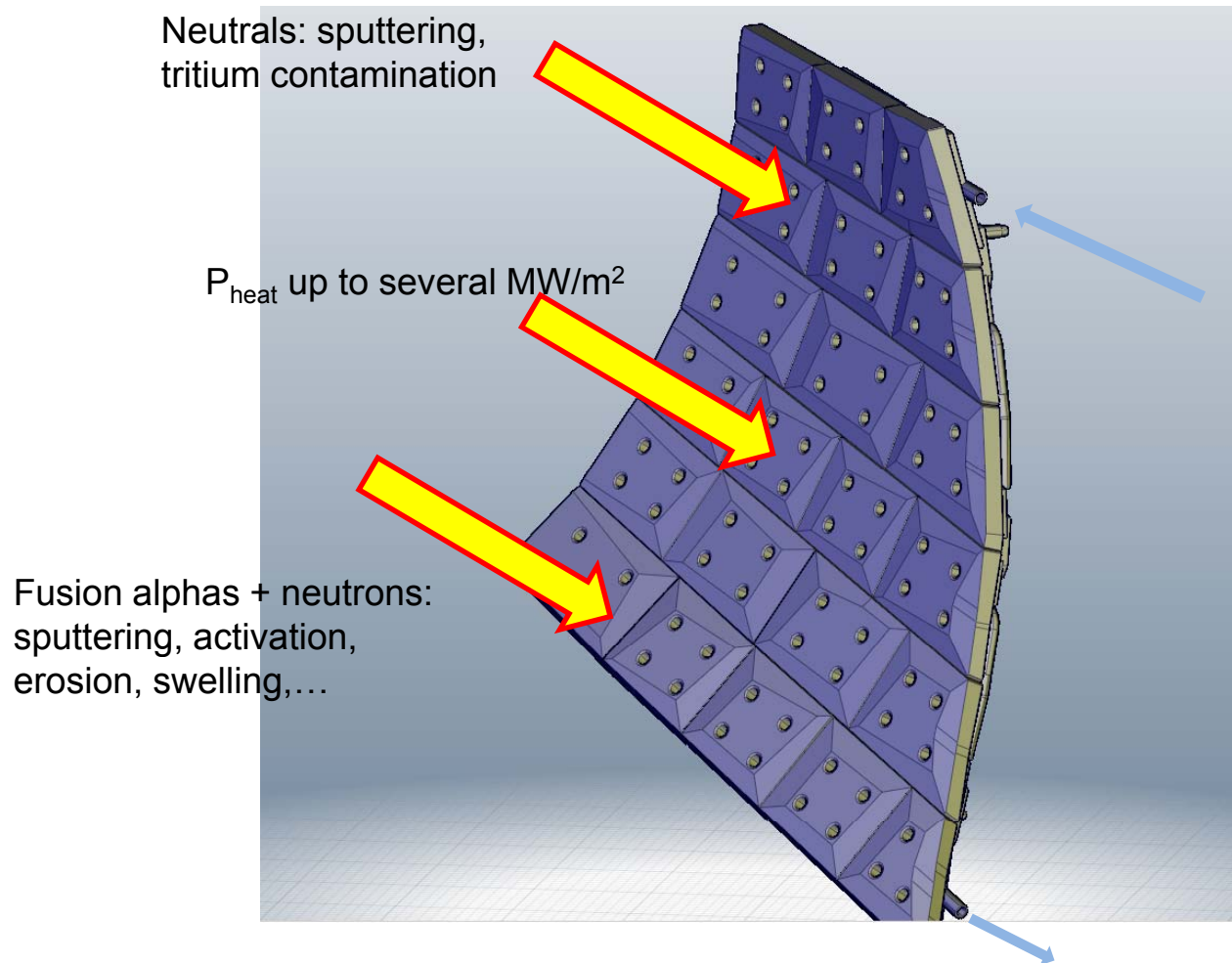
- Huge and long ports
- Very difficult diagnostic access to the plasma
- High neutron/gamma radiation level
- No human access to the operating machine
- Long pulse operation
- Huge amount of measurement data
- High thermal radiation load
- Long operation lifetimes for components required
- Large, very specialized + expensive components
→ first design must fit





Temperature control of all plasma facing components (graphite, tungsten, steel)

- safety interlock becomes mandatory
- active cooling is required for all plasma facing components



Cooling water:

- requirement of water flow + temperature control
- control of possible tritium contamination
- activation of Na after neutron capture

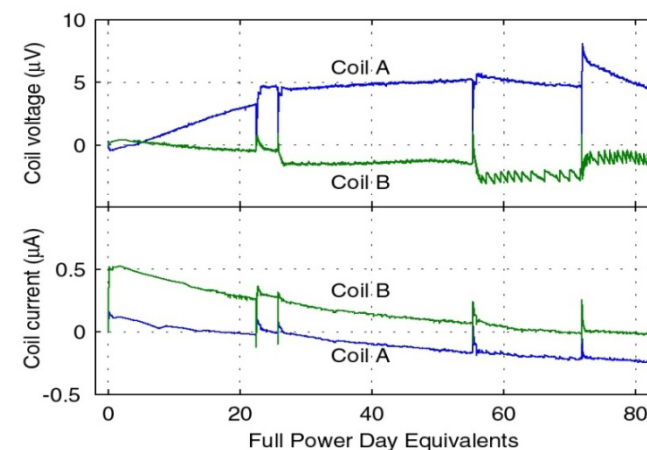
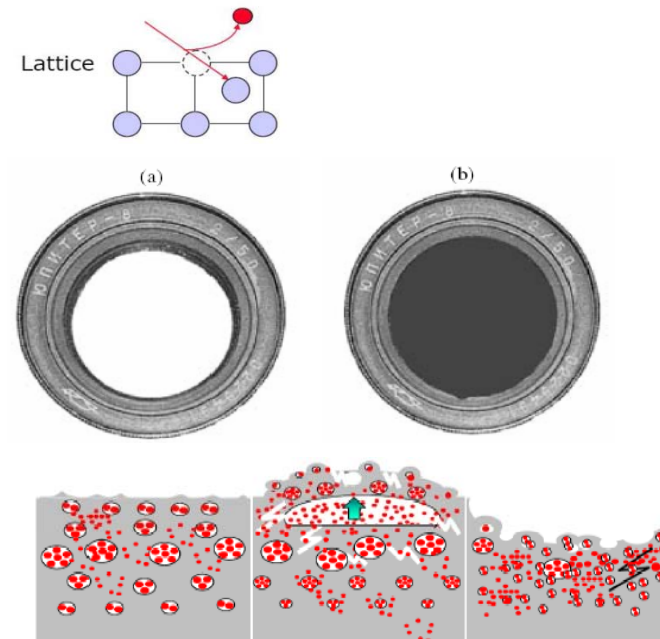


High neutron fluxes
in ITER $8 \times 10^{17} \text{m}^{-2} \text{s}^{-1}$

Optical systems are getting dark
+ radio-luminescence occurs

Mirrors are better suited,
but swelling by neutrons and
CX atoms happens
+ plasma erosion + particle deposition

Cables (impact on magnetics), capacitors:
- RIC – radiation induced conductivity
- RIEMF – RI electromotive forces
- radiation induced change of the dielectric
constant ϵ_r





- John Wesson: *Tokamaks*, Oxford Science Publications, Clarendon Press
- Richard Dendy: *Plasma Physics*, Cambridge University Press
- R.D. Hazeltine, J.D. Meiss: *Plasma Confinement*, Addison-Wesley Pub. Comp.
- I.H. Hutchinson: *Principles of Plasma Diagnostics*, Cambridge University Press
- W. Lochte-Holtgreven, *Plasma Diagnostics*, AIP, New York
- H.J. Hartfuss, R. König, A. Werner: *Steady-state diagnostics for fusion plasmas*,
Plasma Phys. Contr. Fusion **48** (2006) , p. R83

.....thank you very much for your attention
(and sorry for the rather inhomogeneous, incomplete collection of bits and pieces)



Types of diagnostics:

- „Passive“ line-of-sight integrated, and „active“ supported by beams
- „Local“ and „global“ diagnostics

Looking at:

- Electromagnetic emission (light, microwaves, radio-waves, X-ray, B-fields,
- Particle + power fluxes (neutrals, impurities, neutrons, heating power,
-



Some of the plasma parameters we want to observe

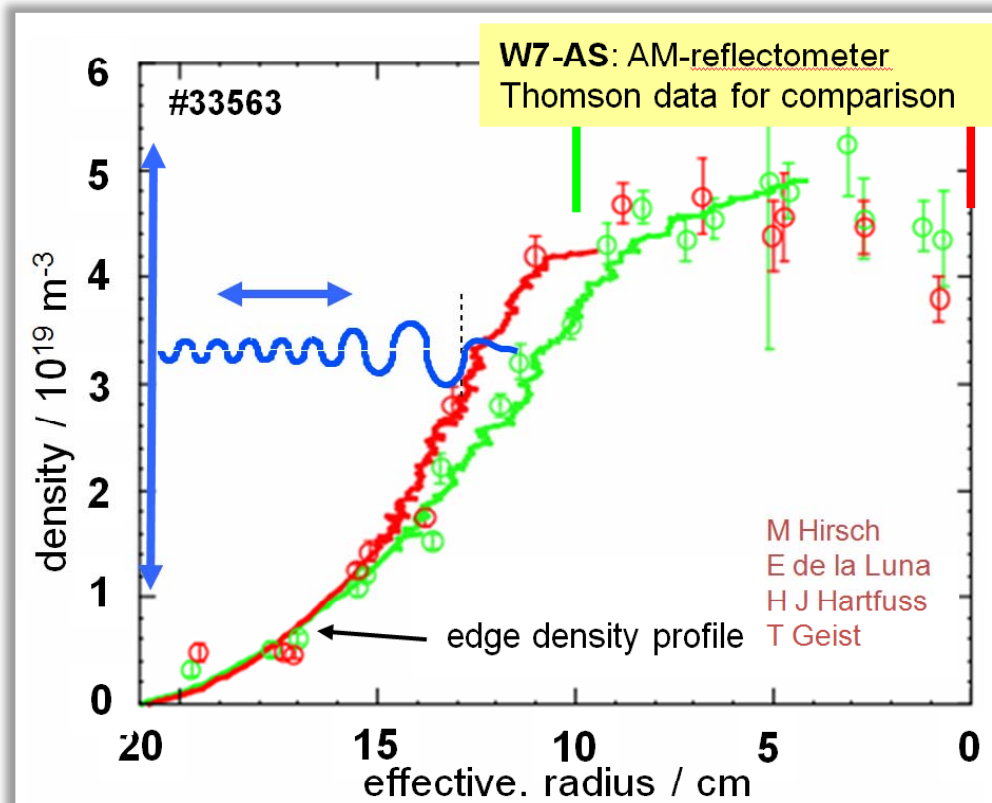


Energy content	W_{dia}
Temperatures	T_i, T_e
Densities	$n_i, n_e, n_Z, n_{neutrals}$
Currents	$J_{toroidal}, j(r)$
Power fluxes	$P_{heating}, P_{radiation}, P_{wall}$
Fields	$E_r, B_{toroidal}, B_{poloidal},$
Fluctuations, oscillations	$\tilde{B}, \tilde{E}, \tilde{n}_e$
Particle fluxes	$\Gamma_{neutrals}, \Gamma_{impurities}, \Gamma_{fast\ ions}$
Others	$V_{toroidal}, V_{poloidal}, f(r), \dots$

$$N^2 \approx 1 - \frac{\omega_p^2}{\omega^2}; \quad \omega_p = \sqrt{\frac{n_e e^2}{\epsilon_0 m_e}}$$

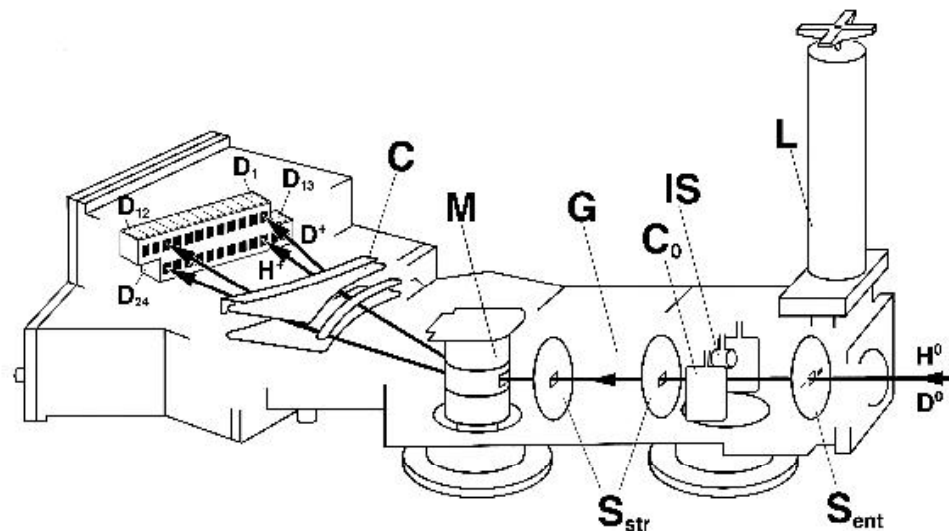
Reminder: EM-waves are reflected when $N \rightarrow 0$

This provides a tool for the measurements of n_e (RADAR principle)



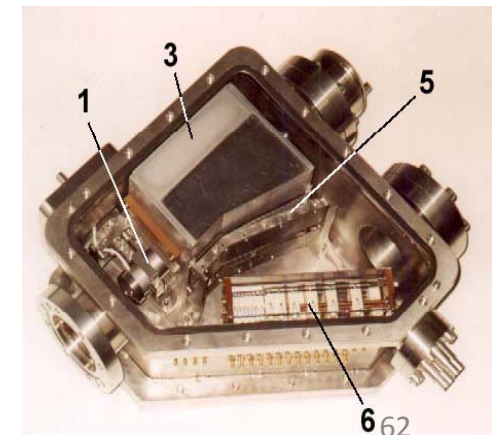
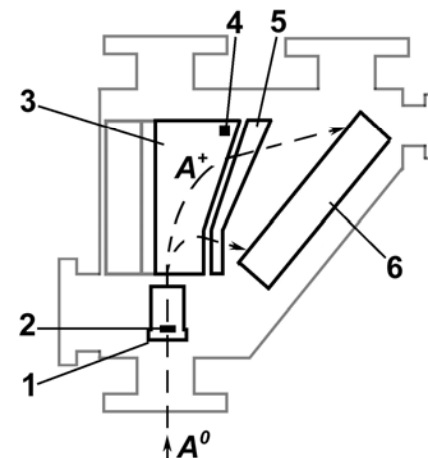
Prerequisite: n_e must be monotonically increasing

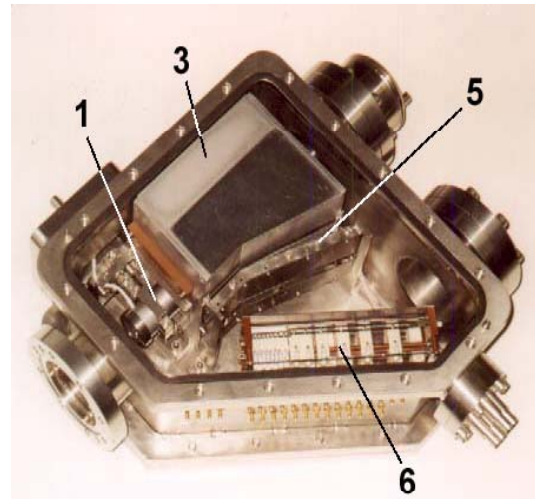
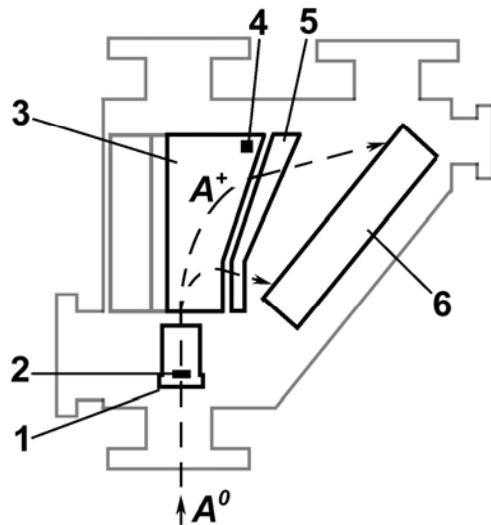
Broadband data evaluation provides information about electron density fluctuations \tilde{n}_e



(L) vacuum shutter; (S_{ent}) “step like” entrance slit; = 1
 (C_0) “cleaning” electrostatic condenser, removing charged particles from the flux; = 2
 (G) stripping cell chamber; = 2
 (S_{str}) stripping chamber slits;
 (M) electromagnet; = 3
 (C) analysing electrostatic condenser; = 5
 ($D_1 - D_{24}$) two rows of detectors;
 (IS) auxiliary ion source for NPA testing; (H^0, D^0) atoms emitted by the plasma; (H^+, D^+) secondary ions.
 Hall probe = 4
 Detector = 6

Absolutely calibrated single chord Neutral Particle Analyzer (NPA)
 H/D discrimination
 Energy range up to 100 keV
 24 channeltron detectors (dual mass)

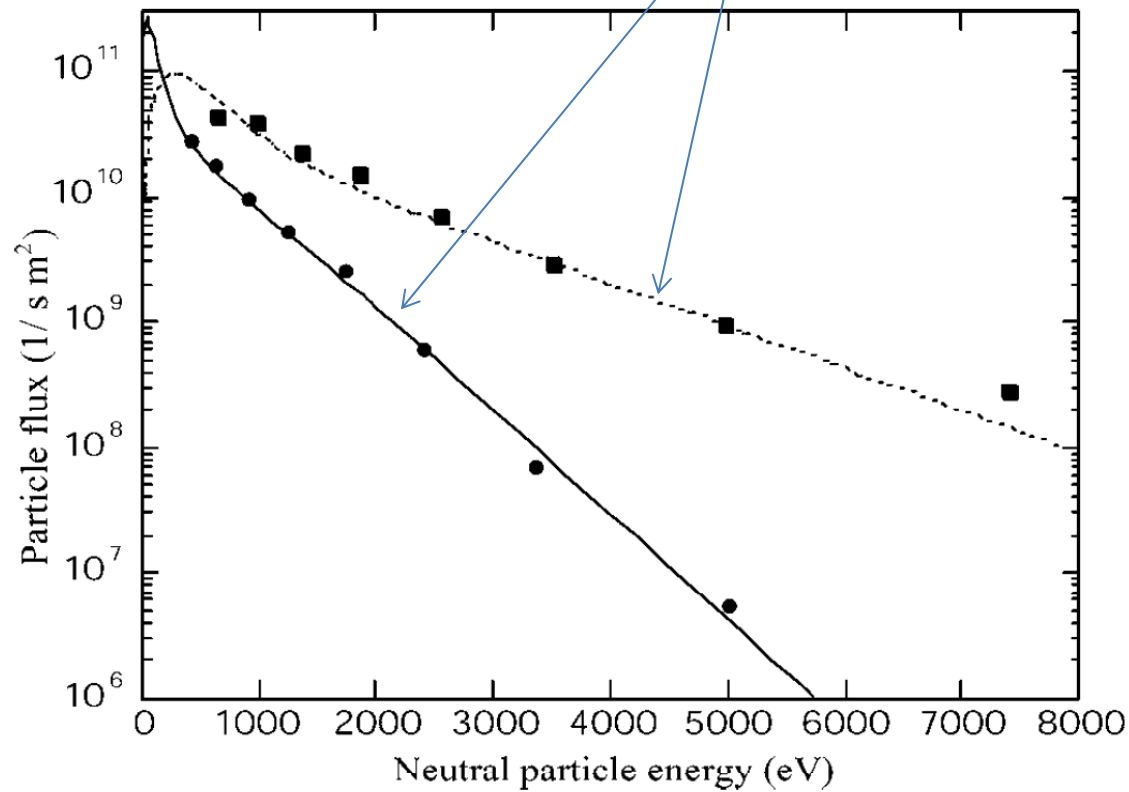




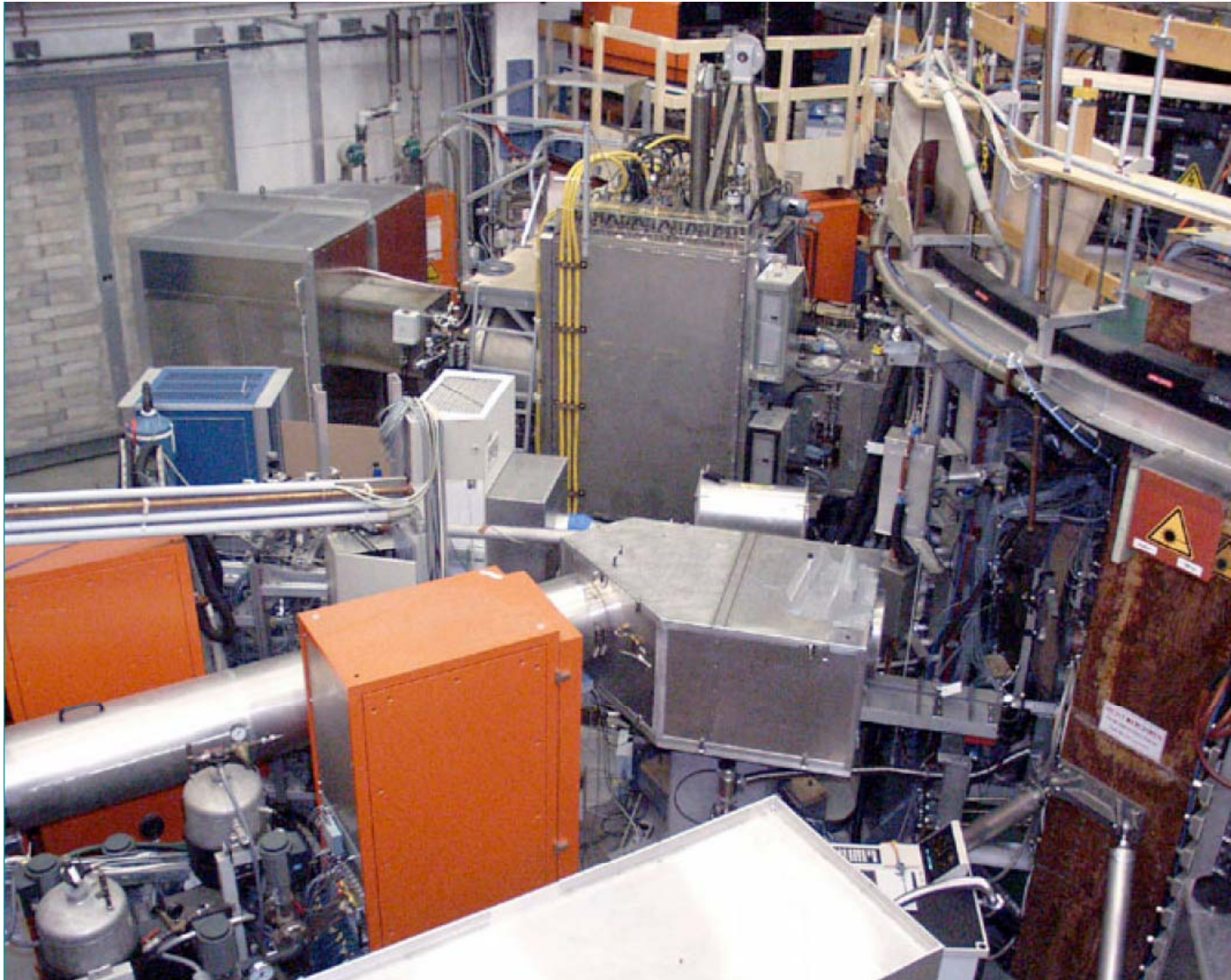
- (1) acceleration/stripping unit
- (2) stripping foil
- (3) analysing magnet
- (4) Hall probe
- (5) analysing electrostatic condenser
- (6) detector array

Energy range	0.8-80 keV (H), 0.8-40 keV (D)
Size	169 × 302 × 326 mm
Weight	42.5 kg
Stripping	Carbon foil (100 Angstrom)
Acceleration of secondary ions	+ 5 kV
Permanent magnets	NdFeB, $B_r \sim 1$ T
Number of energy channels	14 × 2 rows
Purpose	Measurements of thermal and suprathermal CX-fluxes (H and D – simultaneously)

$$d n_0 = N_0 \cdot n_i(r) \cdot \sqrt{\frac{m_i}{2\pi k T_i}} \cdot \exp\left\{-\frac{E_i^{kin}}{k T_i}\right\} dV_z$$



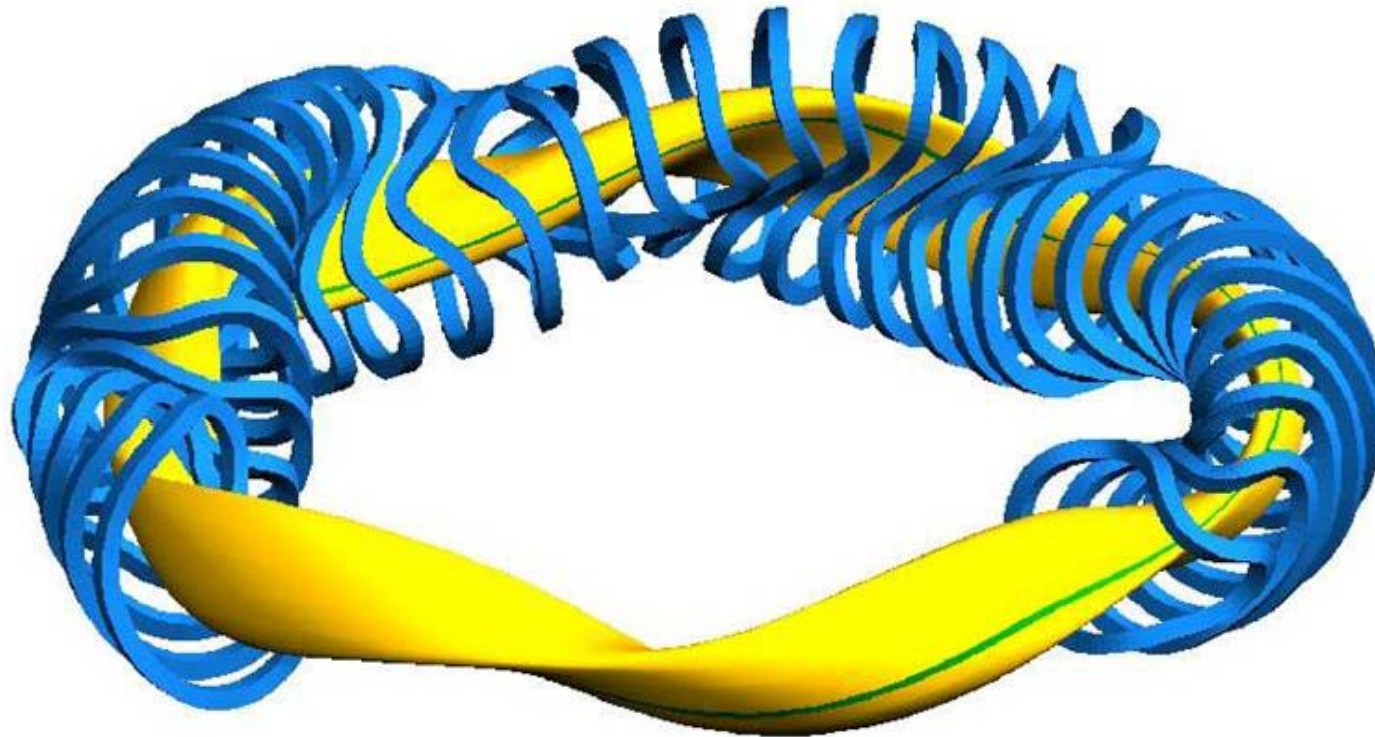
Example: two discharges with
different energy confinement
(different T_i)

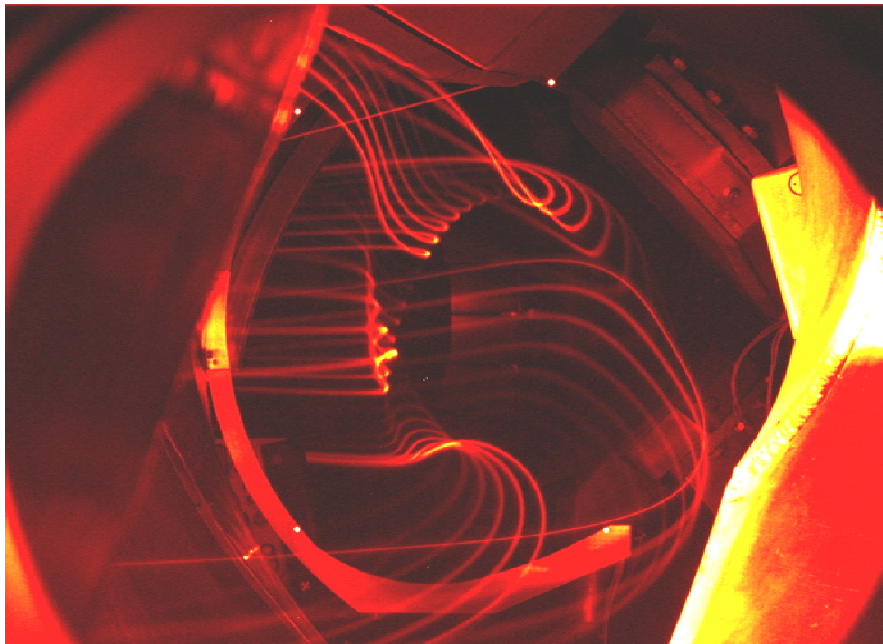






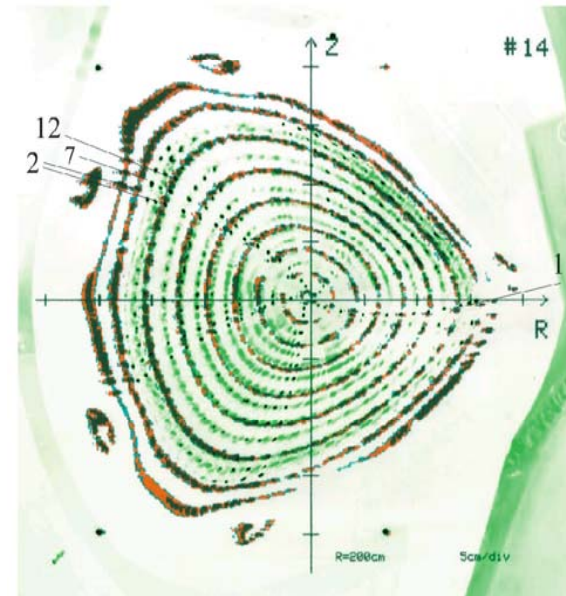
Sketch of the toroidal facility W7-X: only the plasma and some nonplanar coils





W7-AS:

Field-line tracing with an electron beam using
fluorescence in hydrogen gas (false colour).



W7-AS:

flux surface measurements
before operation (dark) and
after 56000 discharges (green)

Simplifying assumption:

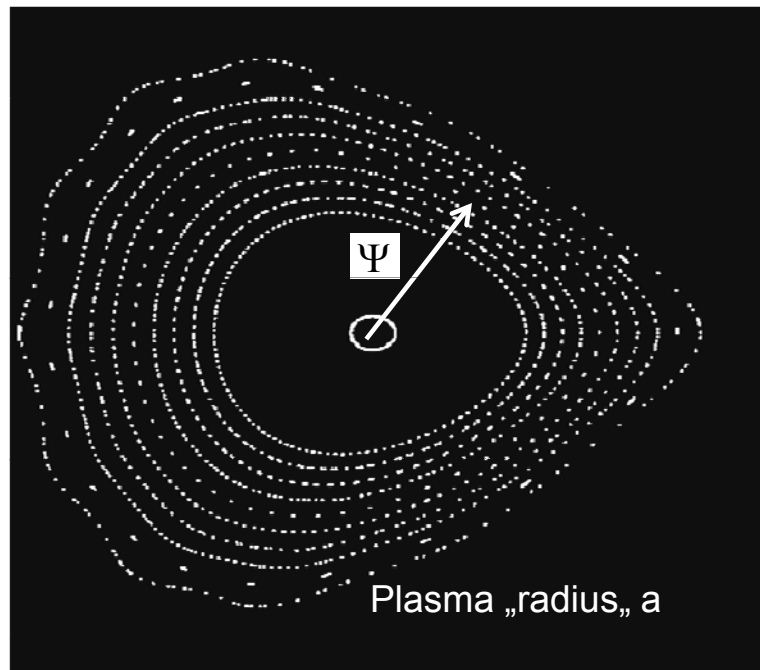
Plasma parameters are (more or less) constant on magnetic flux surfaces (label Ψ)

Distribution function $f(\vec{r}, \vec{V}, t) = f(\Psi, \vec{V}, t)$
with the (toroidal magnetic flux) function Ψ

Plasma parameters $g(r) = g(\Psi) = g(\rho)$; $\rho = r/a$

Due to the fast transport parallel to the magnetic lines, this holds mainly for the quantities:

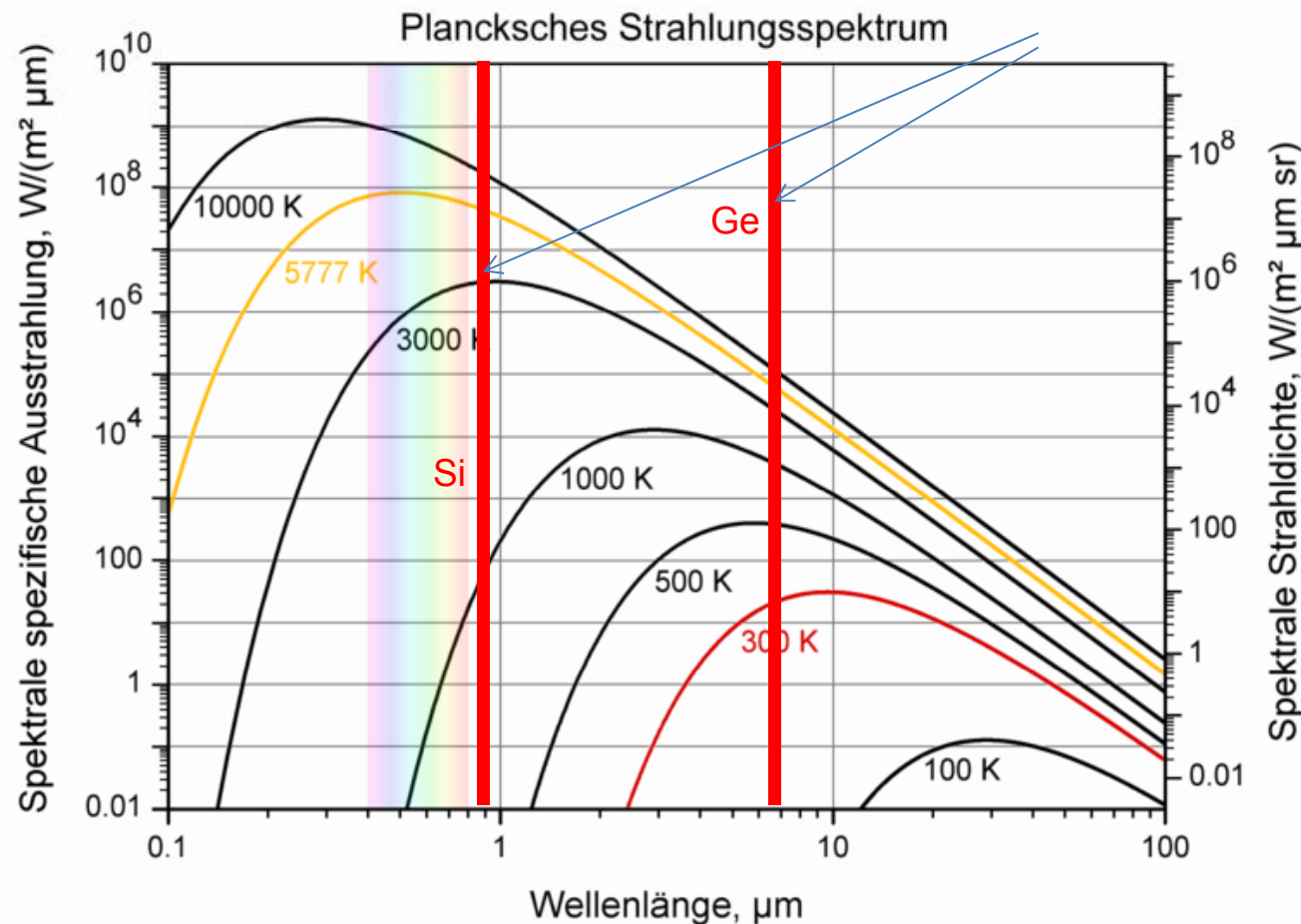
$$\phi(\rho) , T_e(\rho) , T_i(\rho)$$



Poincaré - plot

.....can reveal, by passive observation, the surface temperature of wall components

$$I(T) = S(\text{Ge}) / S(\text{Si})$$



With Planck's law:

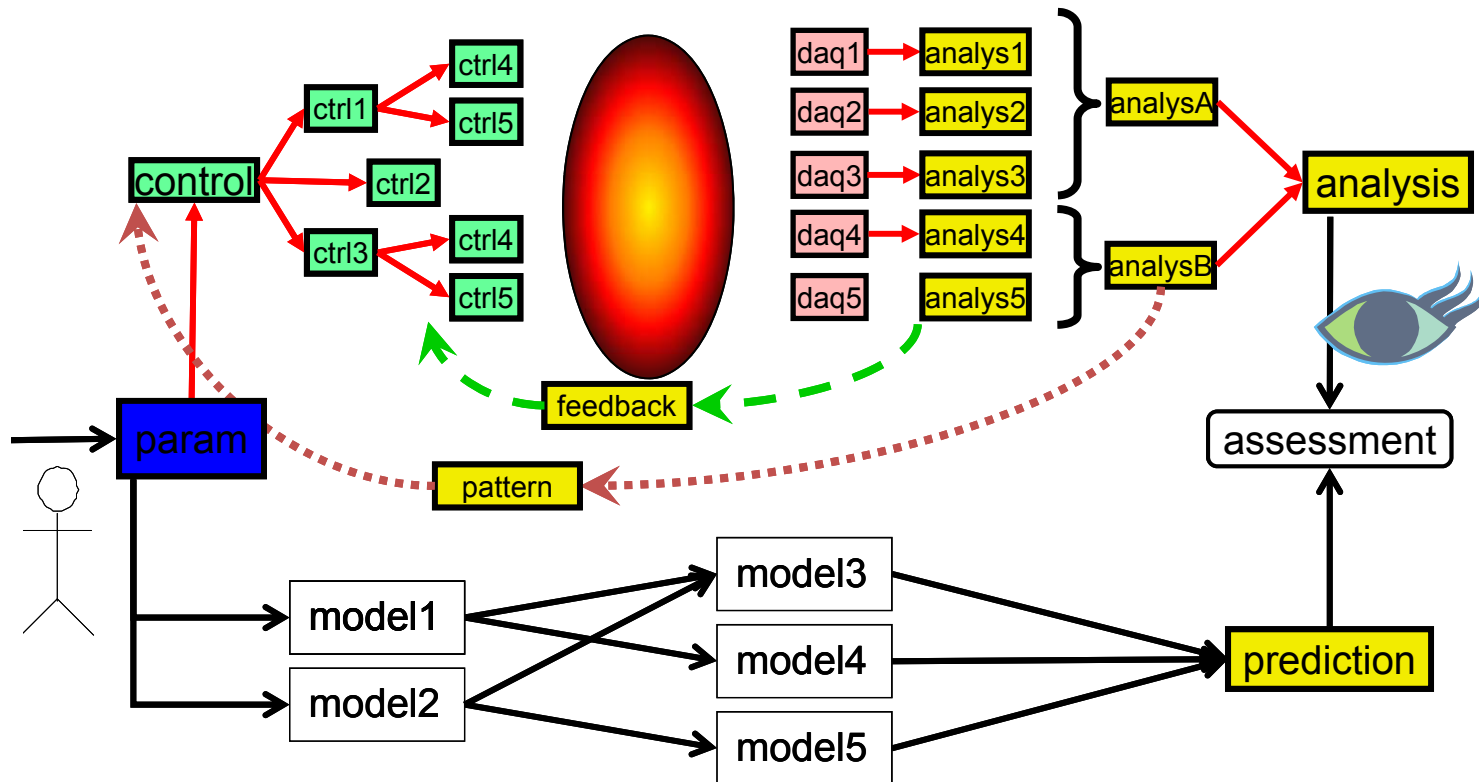
$$\frac{dP}{d\lambda} = \frac{2\pi hc^2}{\lambda^5} \left(\exp\left\{ \frac{hc}{\lambda kT} \right\} - 1 \right)^{-1}$$

and Stefan-Boltzmann:

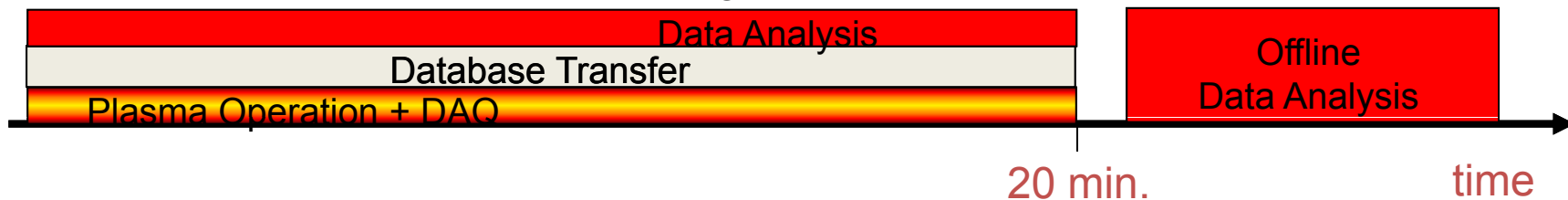
$$P_{total} = \epsilon \sigma_{SB} T^4 A$$



.....and finally a brief outlook to the future.....



2 GB/s 5 TB/discharge





Inference

How likely do we find results H GIVEN data D
with background information I ?

Bayes Theorem

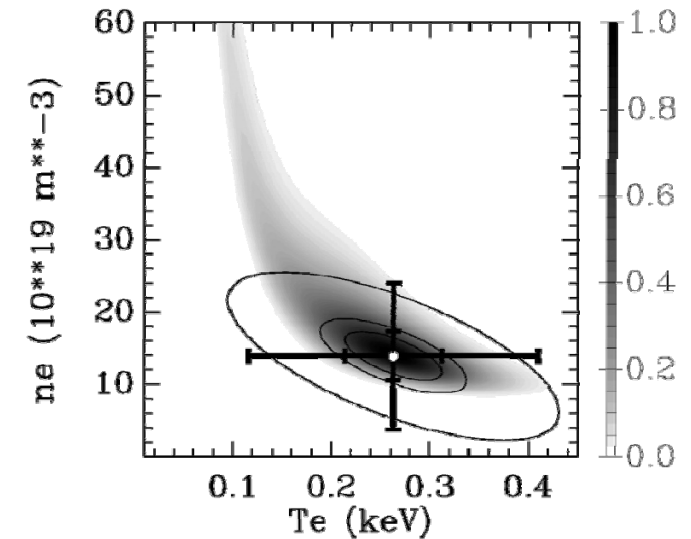
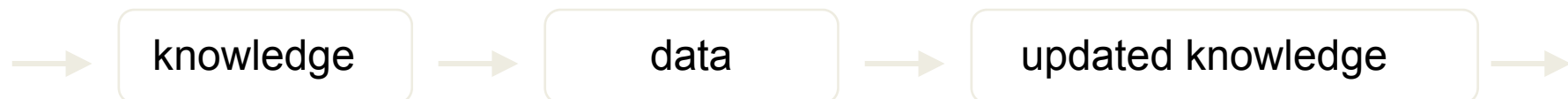
learning

$$\Rightarrow p(H|D, I) \sim p(H|I) \times p(D|H, I)$$

posterior pdf
prior pdf
likelihood

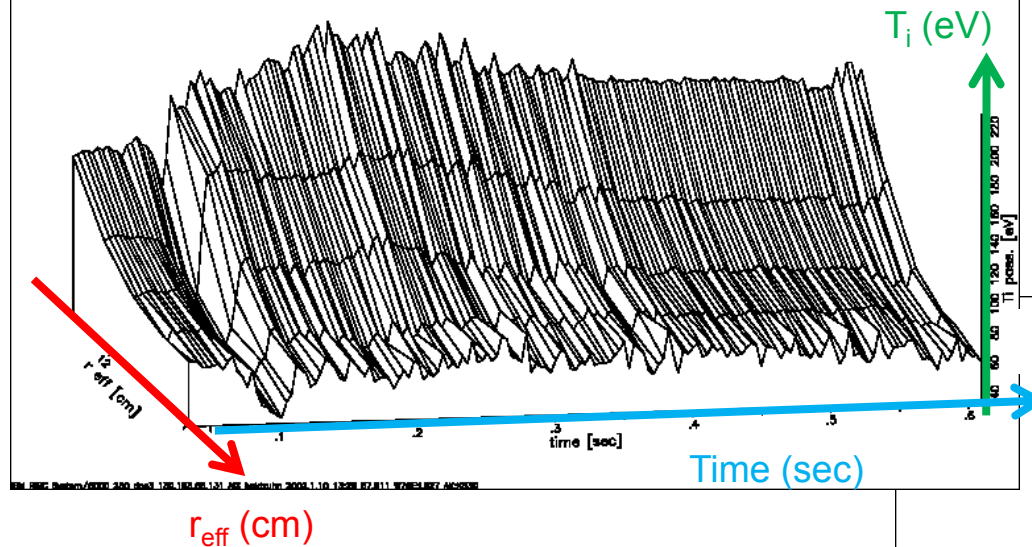
measurement

inference



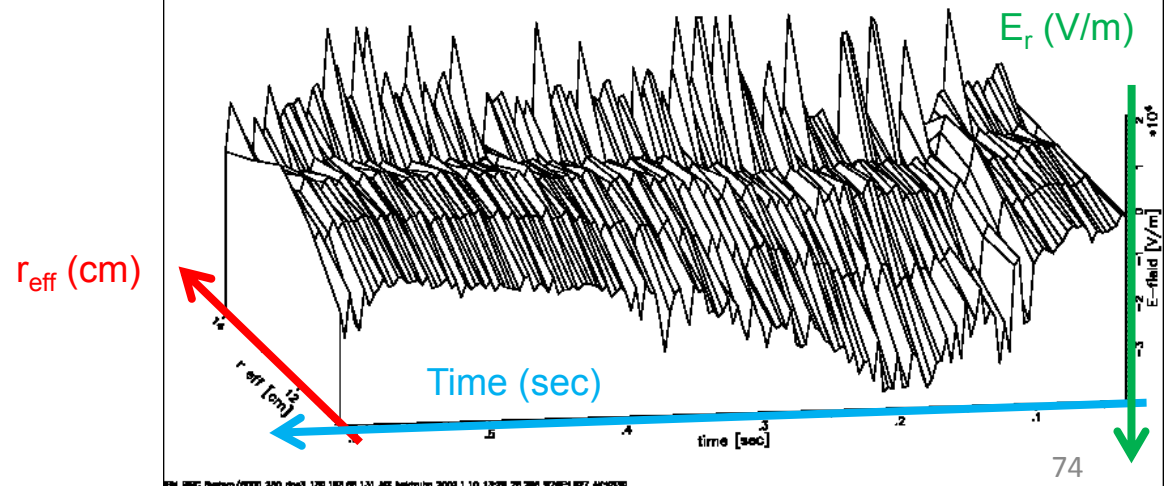
Posterior of
Thomson scattering
new: full error propagation
 $n_e \uparrow \leftrightarrow T_e \downarrow$
'... measures P_e '

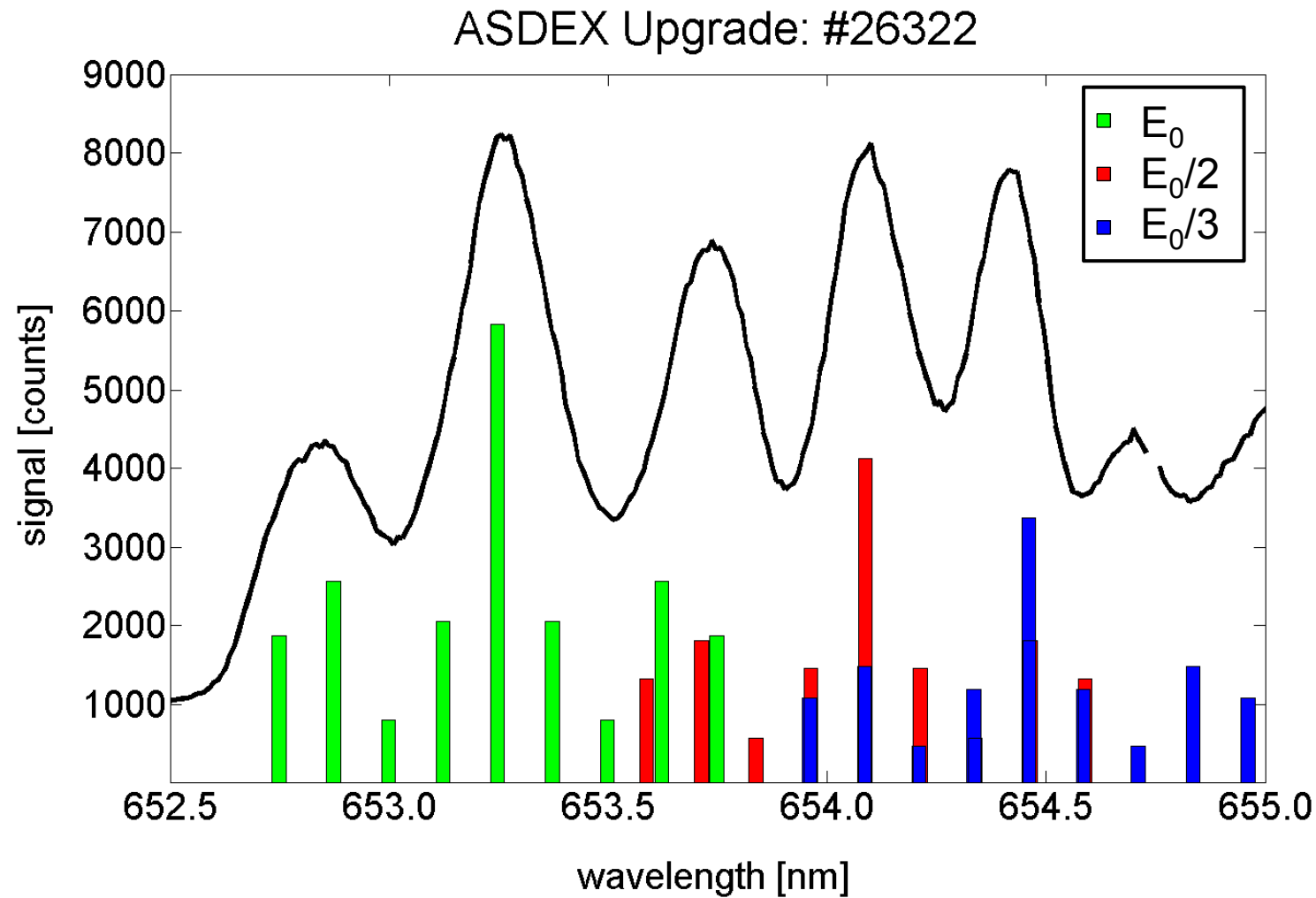
Edge ion temperature profile

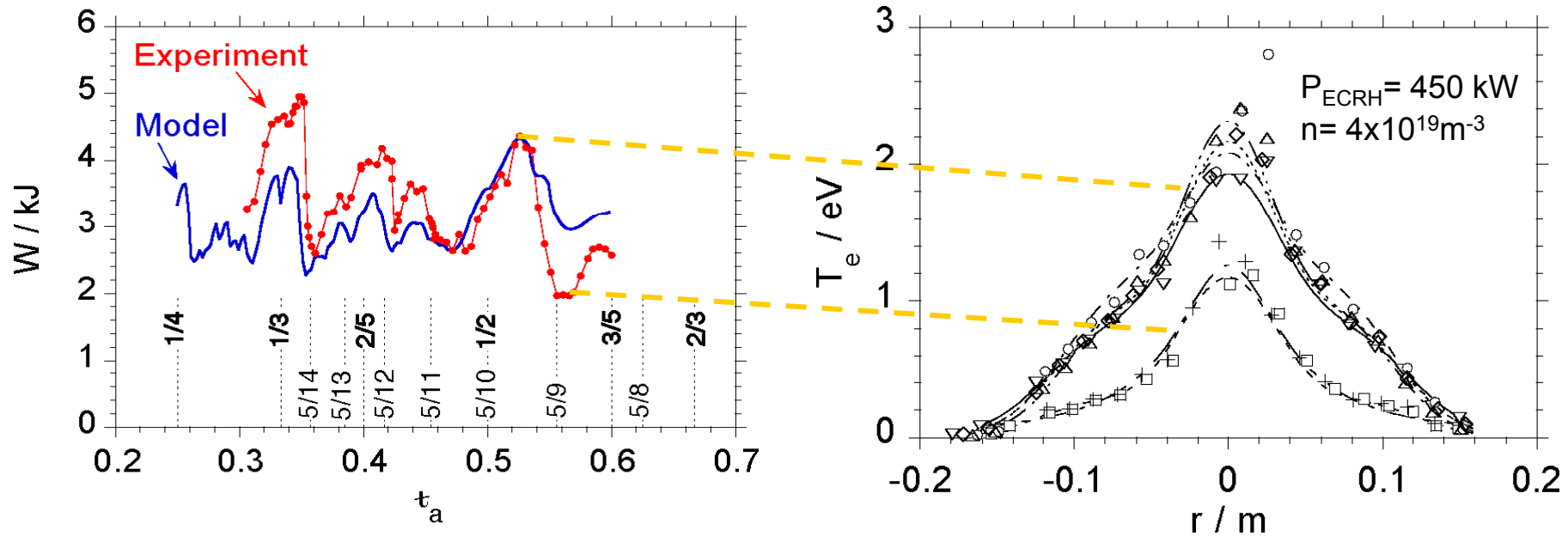


Examples of time traces for passively
measured T_i , E_r

Edge radial electric field profile







The plasma confinement in a low-shear stellarator depends strongly on the edge Rotational transform ι (via the anomalous, turbulence driven) transport

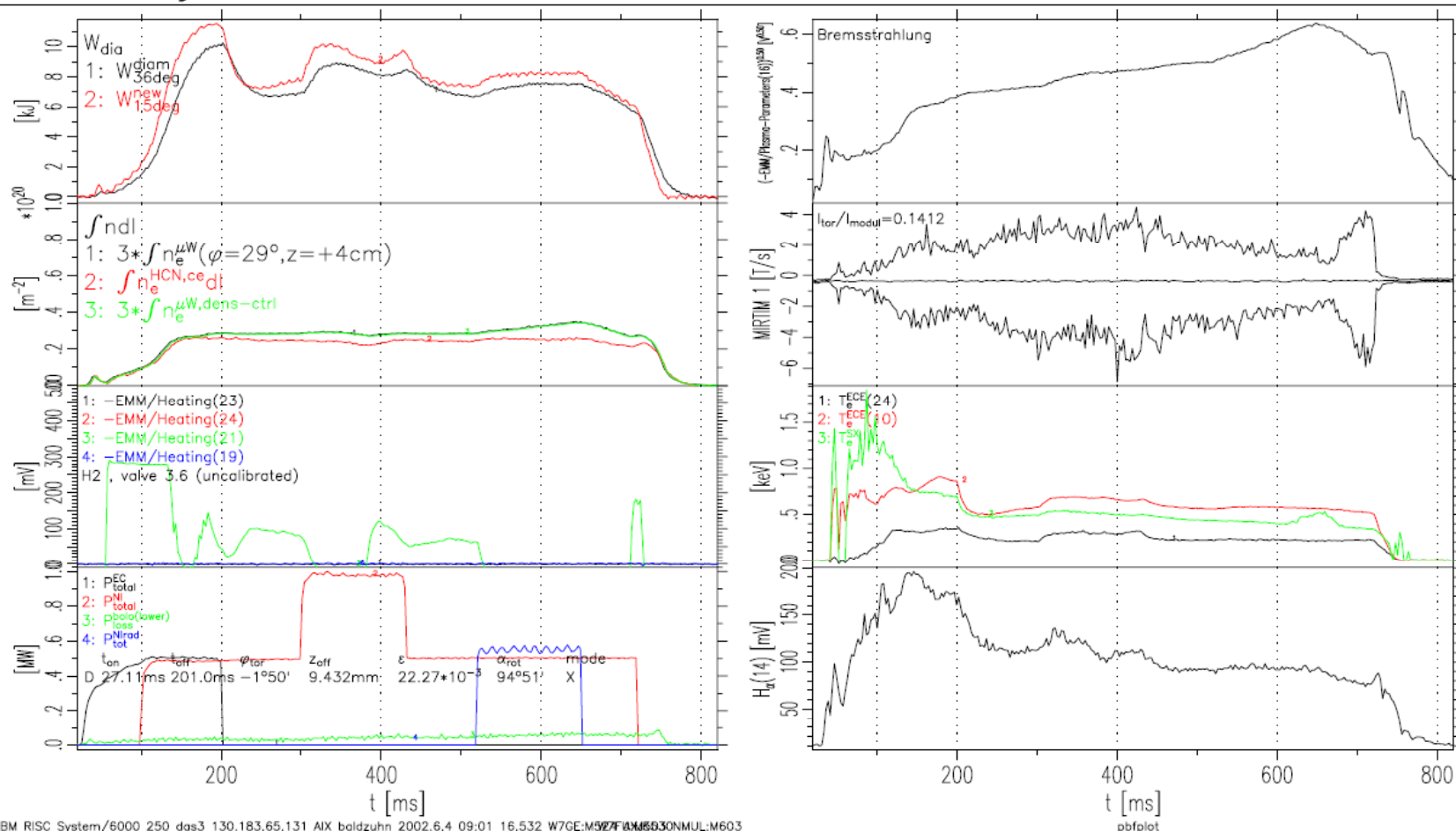
➔ At rational ι -values it drops

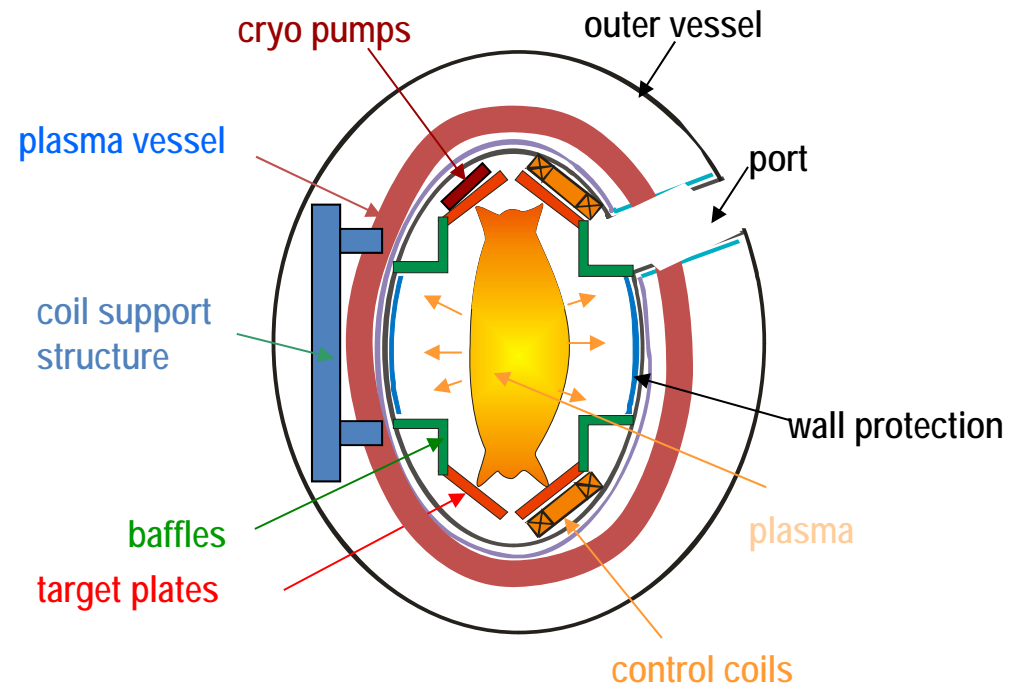
➔ In close vicinity to low-order rationals it increases

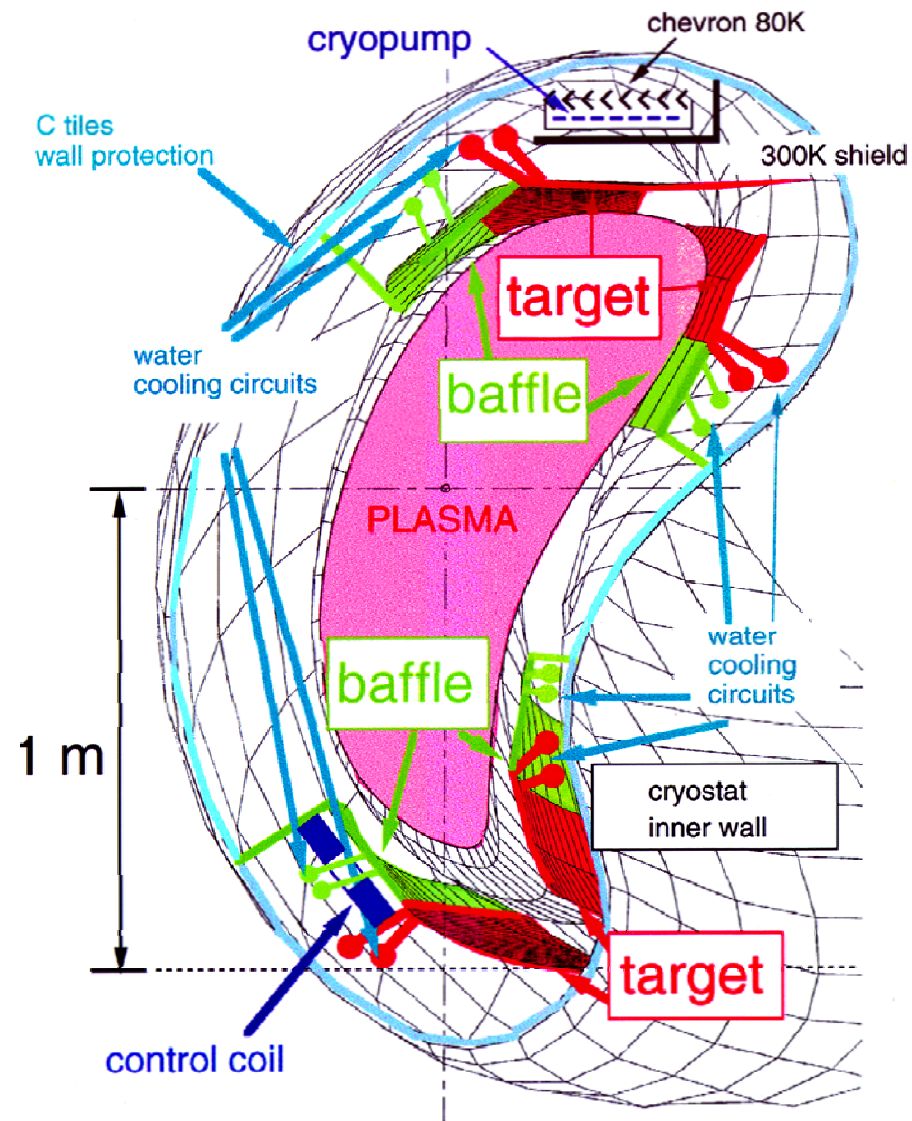
$$\tau_E = \frac{W_{\text{dia}}}{P_{\text{heat}}}$$

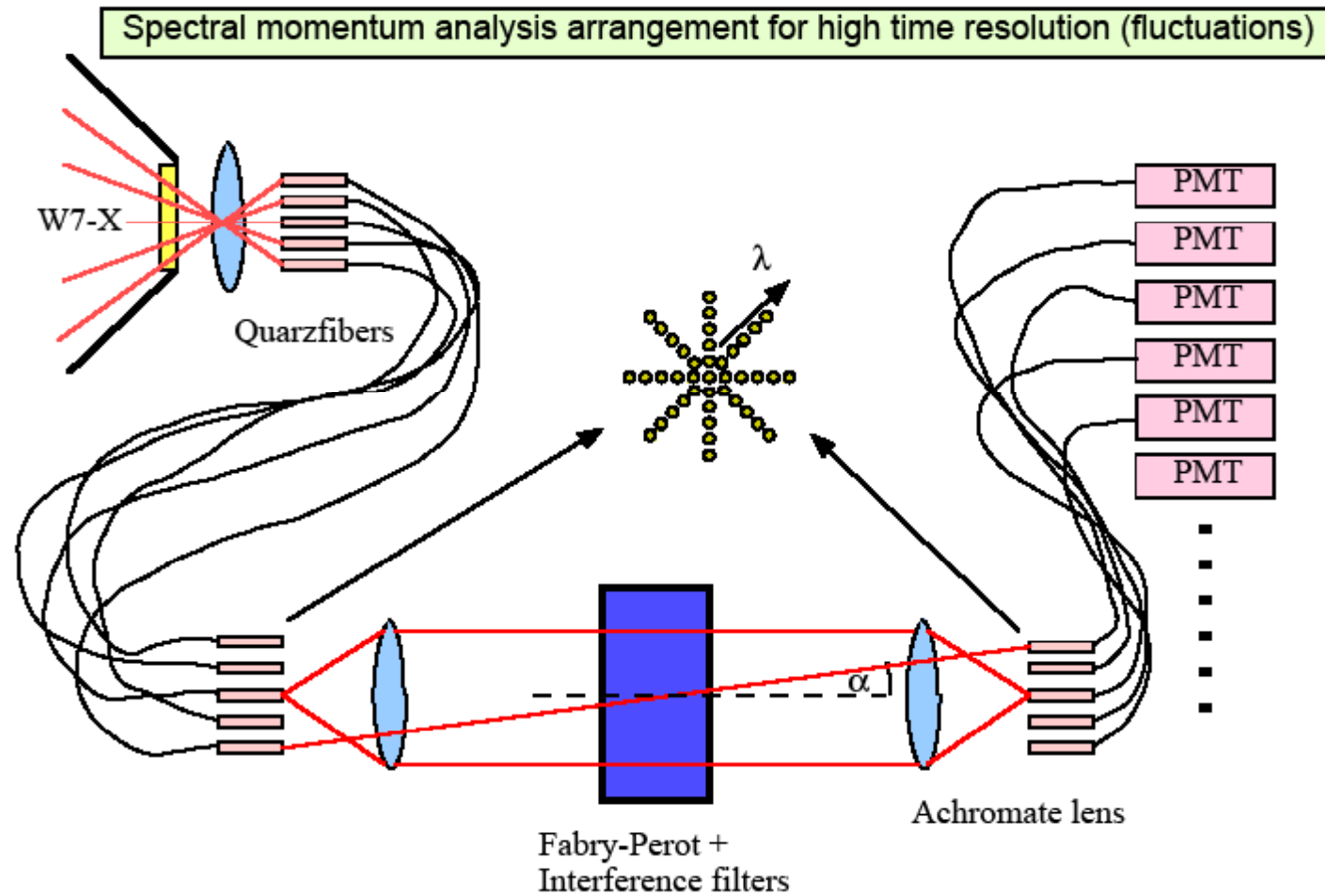
$$\iota = \frac{2\pi}{q} = R \oint \frac{B_\theta}{B\phi} ds \approx \frac{R}{r} \frac{B_\theta}{B_\phi}$$

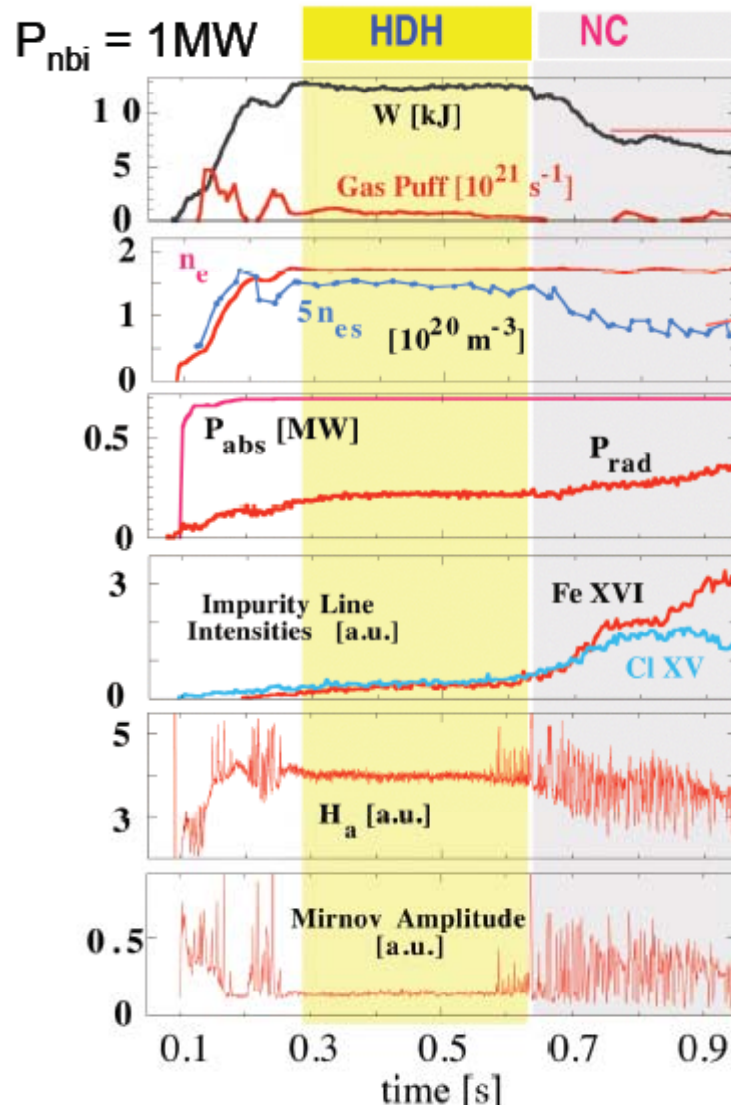
W7-AS Shot 55774 (2002.5.29 10:57) $B_0^{\text{bddeg,new}} = -2.520\text{T}$
 $a_p = 15.70\text{cm}$ $B_z = -19.87\text{mT}$ $\iota_a = 0.3416$ $\iota_a^{\text{old}} = 0.3424$ $t_{\text{TH}} = 599.9\text{ms}$
 ECRH: 140 GHz, NBI $I_{\text{cc1}}/I_{\text{modul}} = 0.0$
 Radialinjektion mit Deuterium











Results Stellarator W7-AS

Stored Energy is lower in NC

Separatrix density n_{es} is lower in NC
- for the same line-averaged density

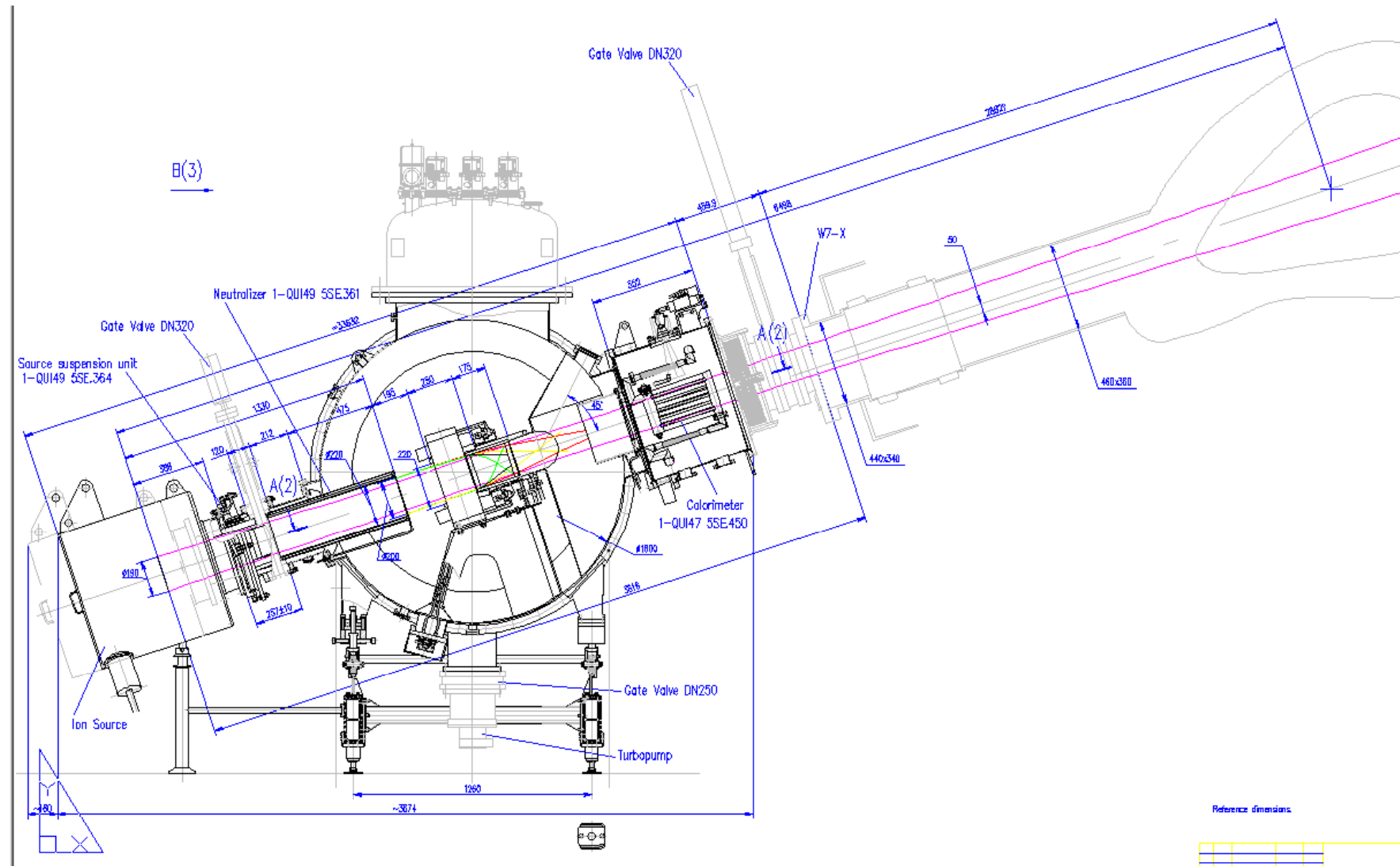
P_{rad} increases in NC

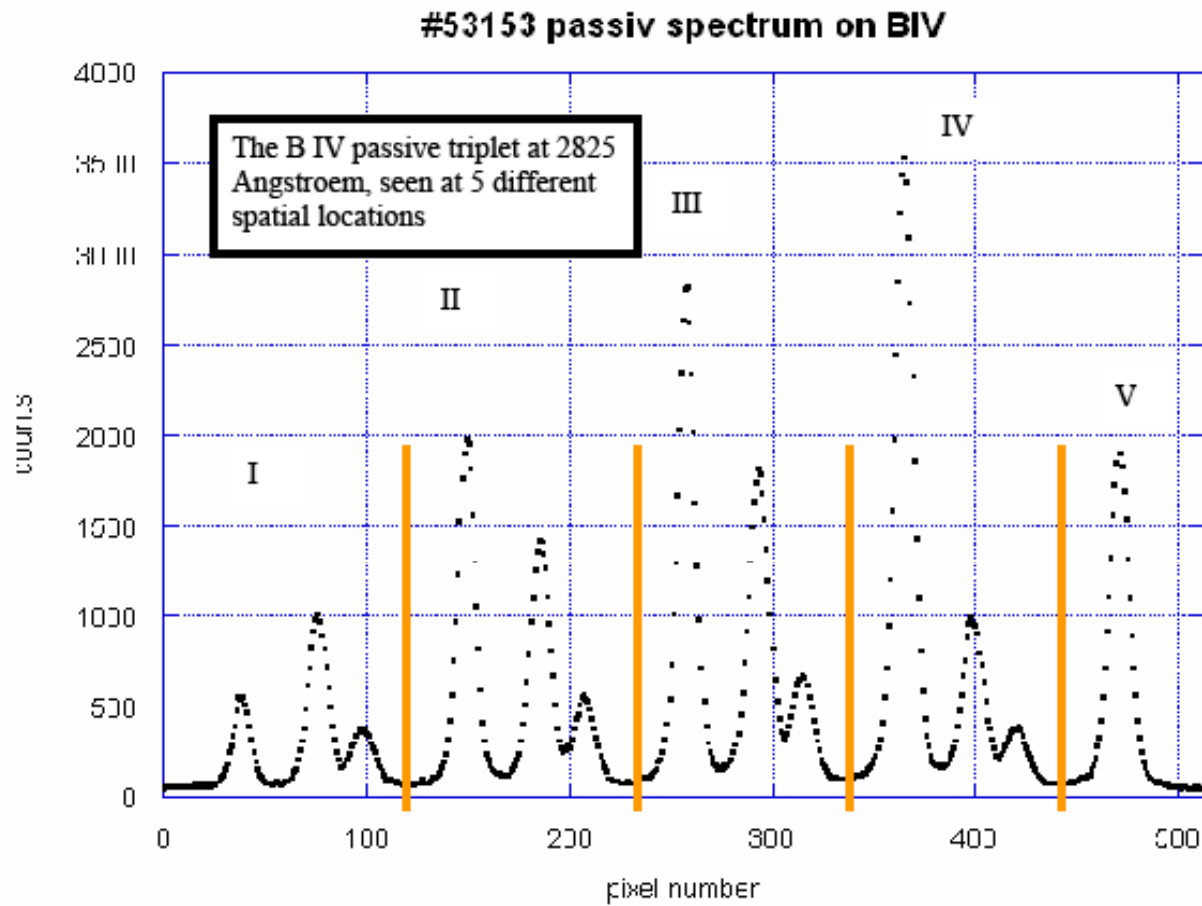
Impurity line intensity increases in NC

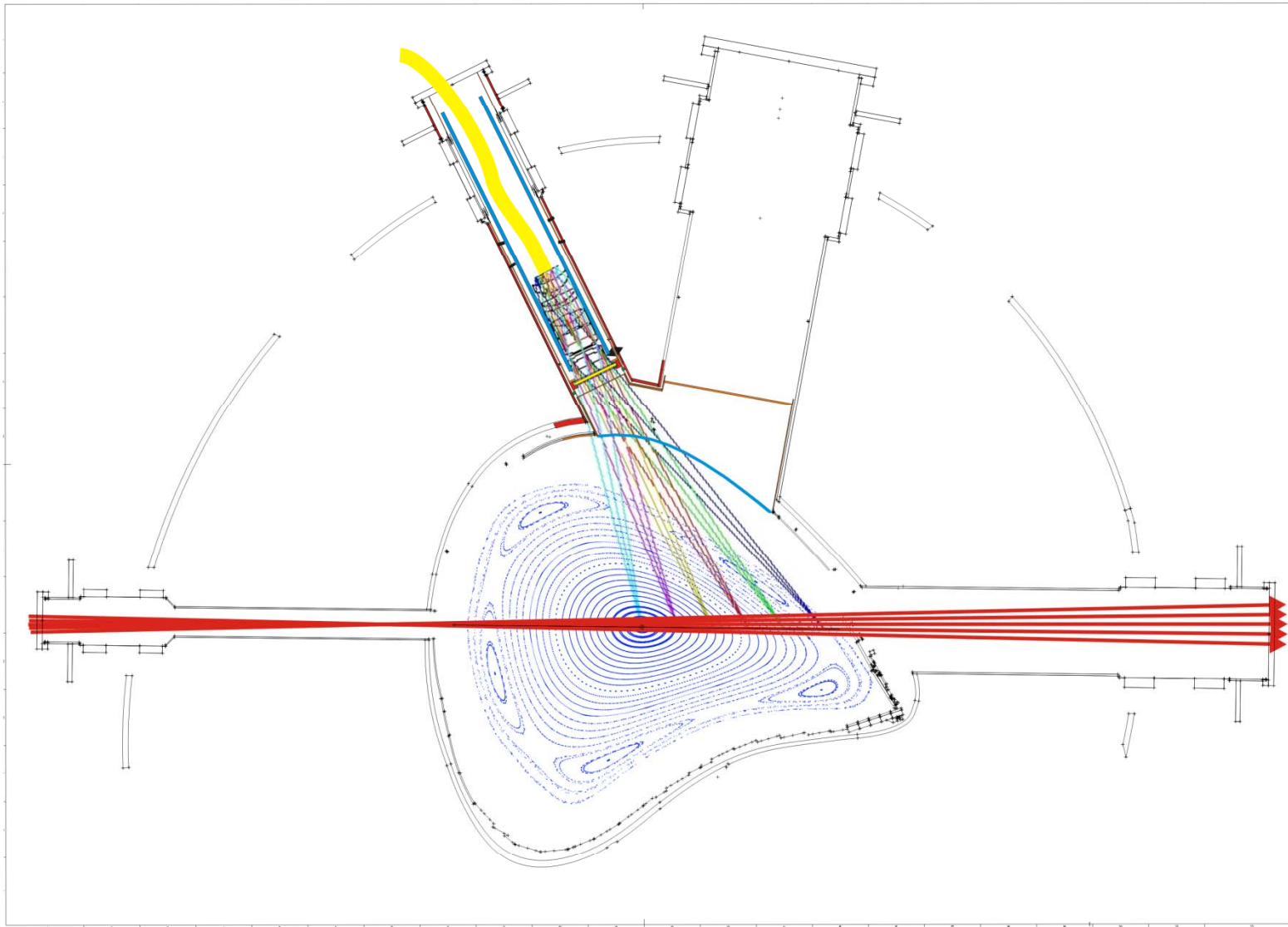
HDH shows no evident ELM activity

HDH shows reduced MHD activity

McCormick et al. 2004









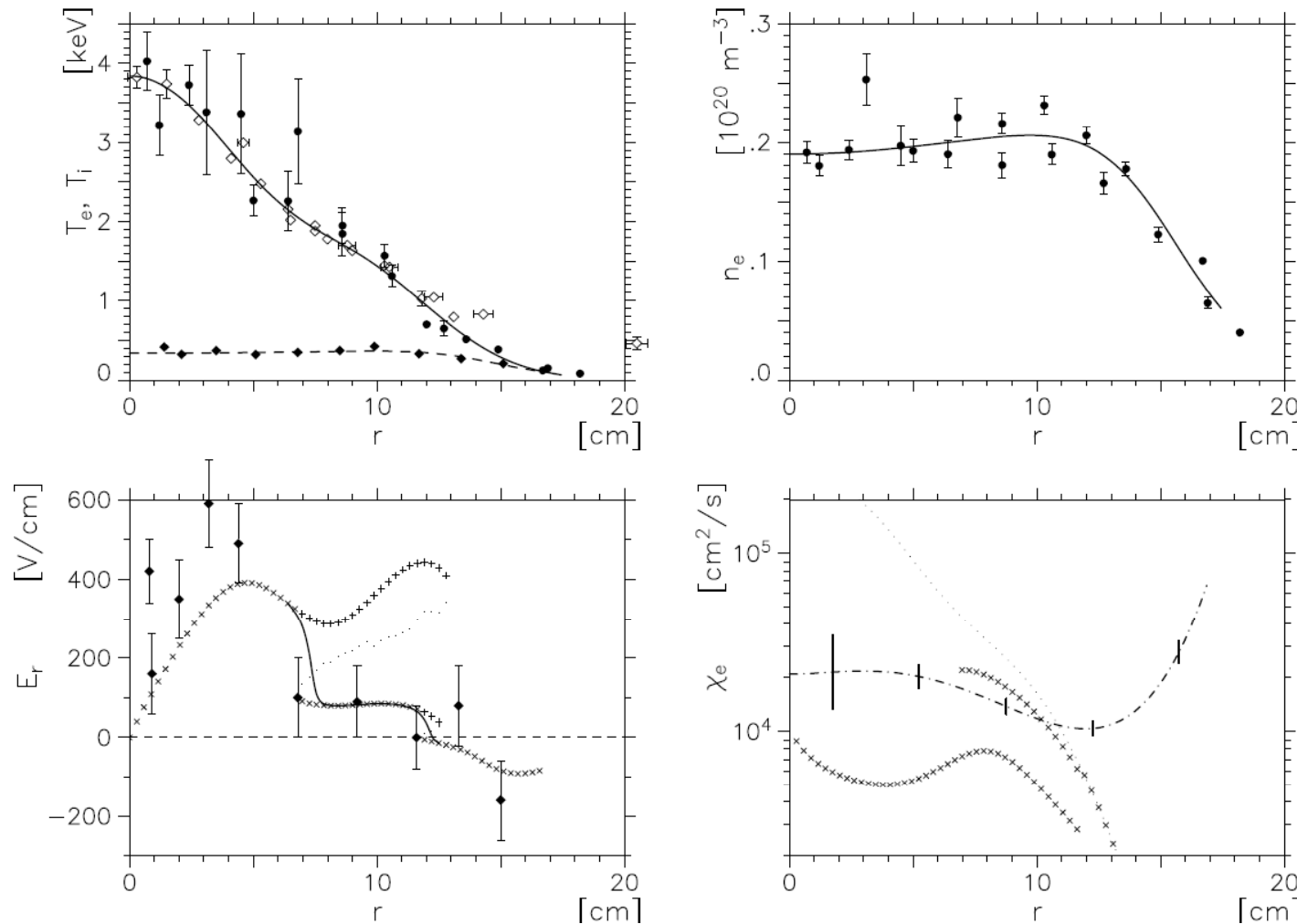
→ Important plasma parameters can be simply plotted versus an (effective) minor radius

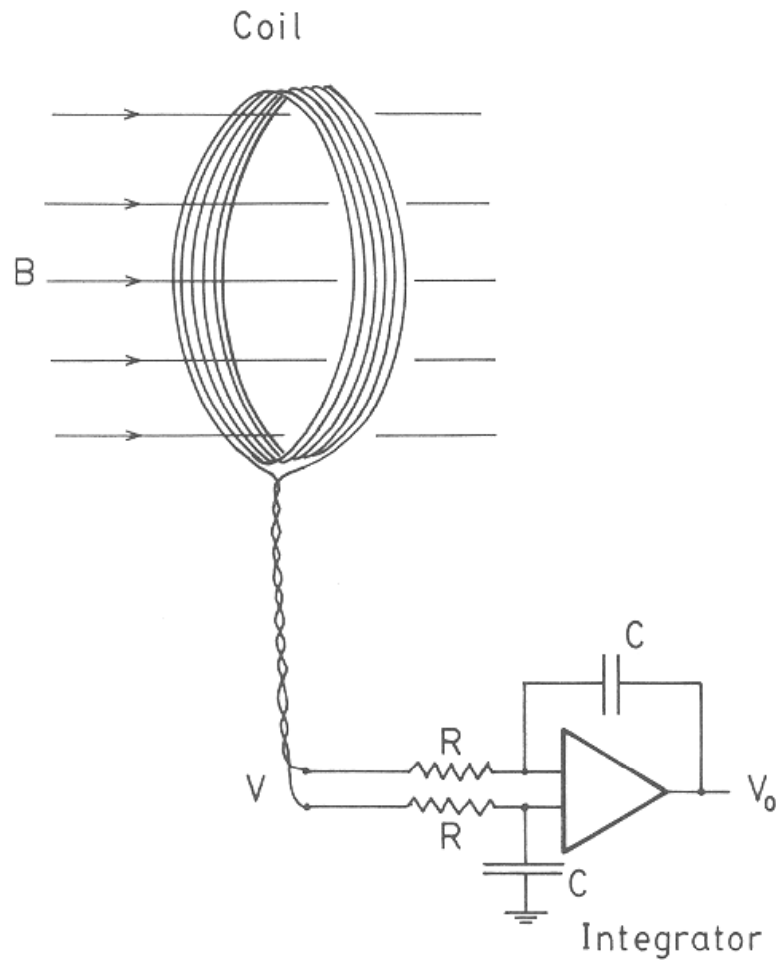
W7-AS

36908 – 36908

$t = 0.400$ s

28-OCT-96





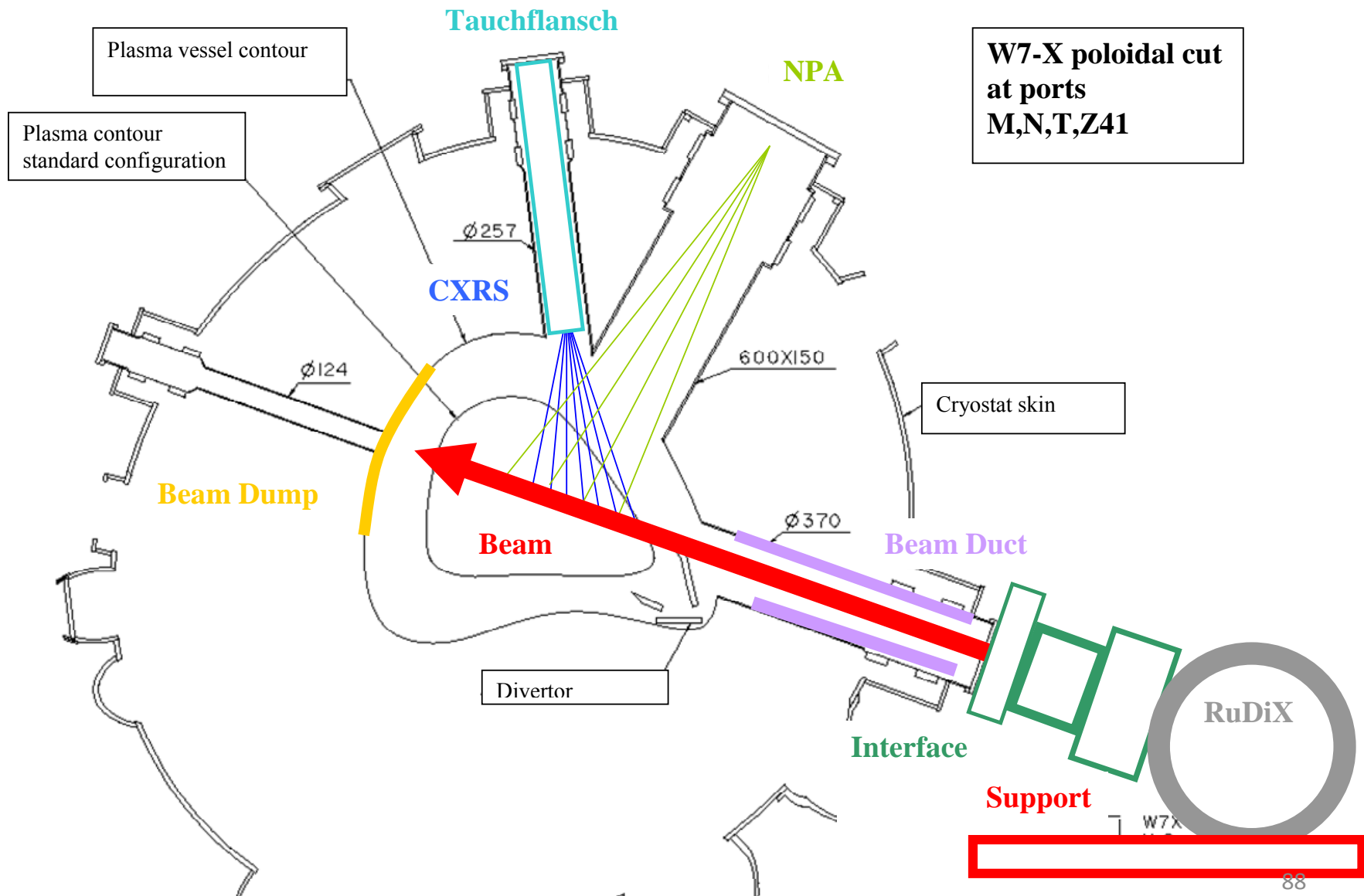
$$U_{ind} = -N \frac{d}{dt} (\vec{B} \cdot \vec{A})$$

$$B_{meas} \propto V_{out} = -\frac{1}{RC} \int_{t_0}^{t_1} U_{ind}(t') dt'$$



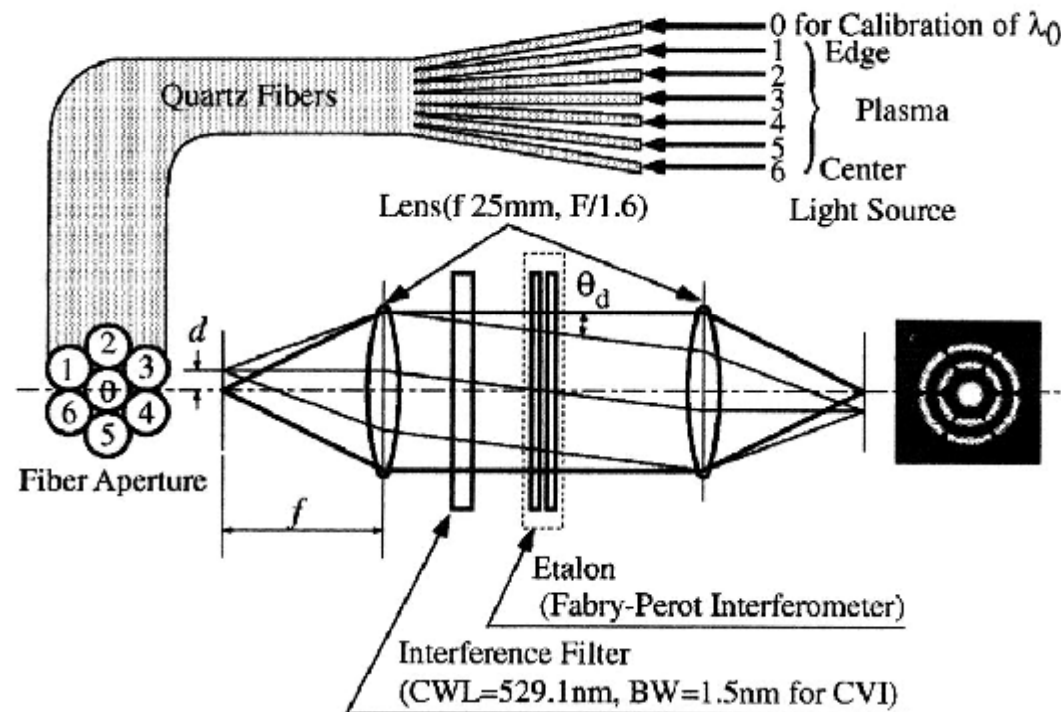
CXRS active lines of interest in order of wavelength

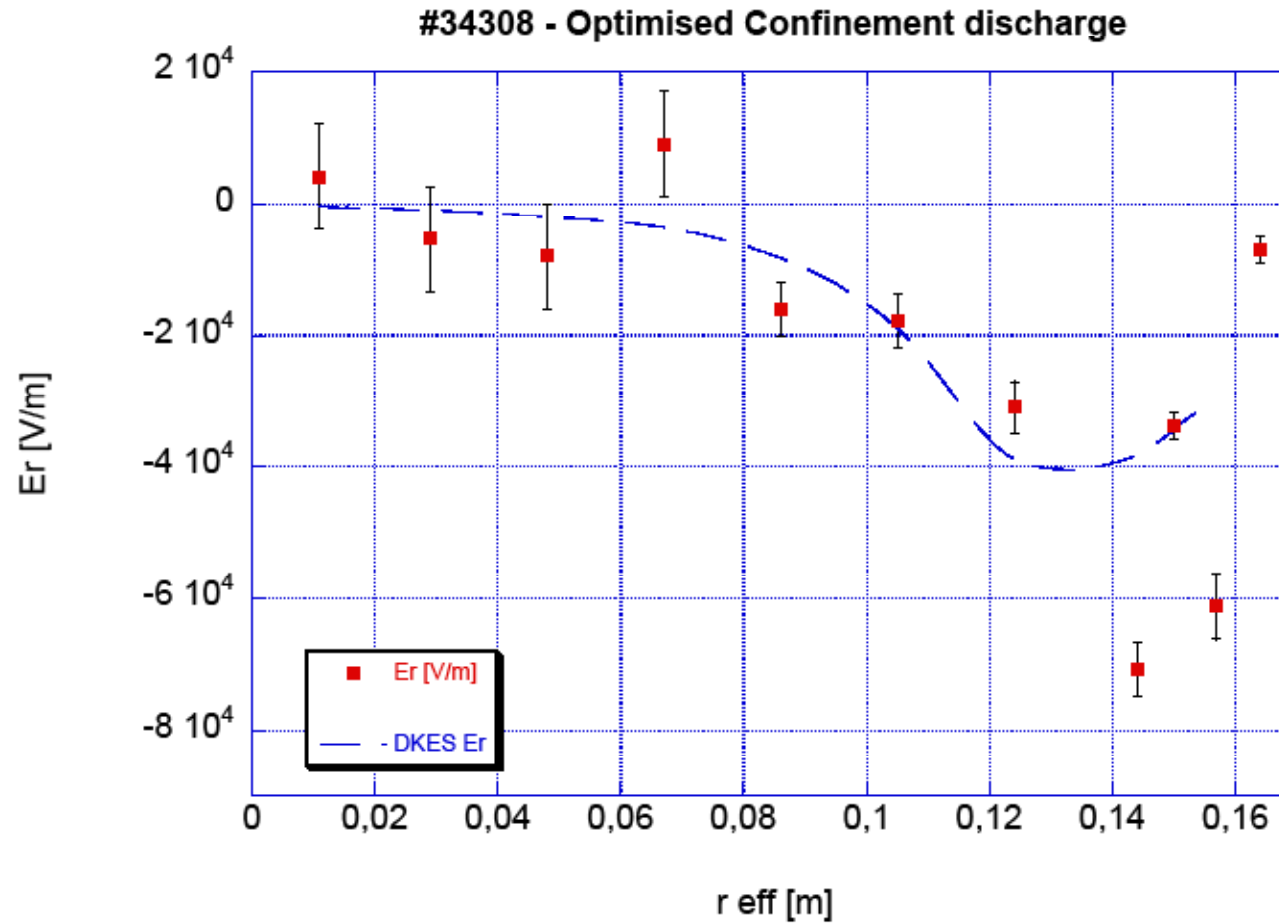
Wavelength nm	transition	Ion species
252.4	7 → 6	N VII
297.5	9 → 8	O VIII
298.1	6 → 5	B V
343.4	7 → 6	C VI
388.8	8 → 7	N VII
436.6	14 → 13	Ar XVI
468.6	4 → 3	He II
494.5	7 → 6	B V
522.4	16 → 15	Ar XVIII
524.9	11 → 10	Ne X
529.1	8 → 7	C VI
566.9	9 → 8	N VII
606.9	10 → 9	O VIII
656.3	3 → 2	H α



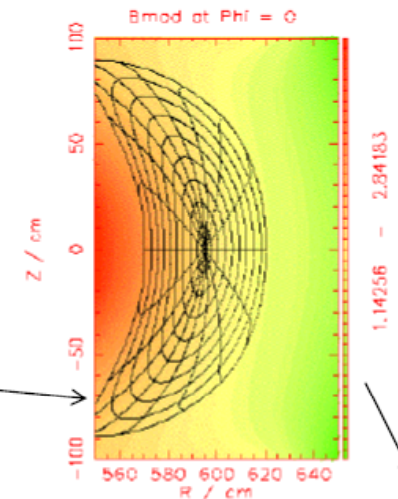
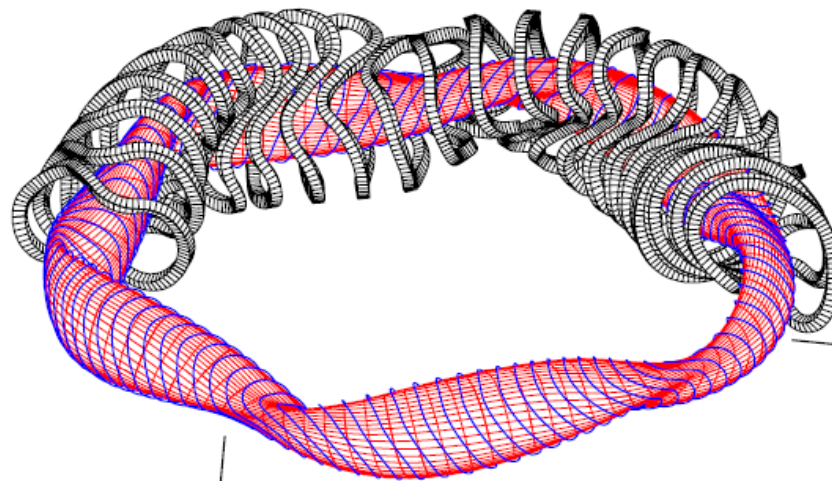
Arrangement of the W7-AS Fabry-Perot spectrometer

(see M. Yoshinuma NIFS, Japan: M. Yoshinuma, J. Baldzuhn, K. Ida, Rev. Sci. Instr. Vol. 75, (2004), p. 4136)



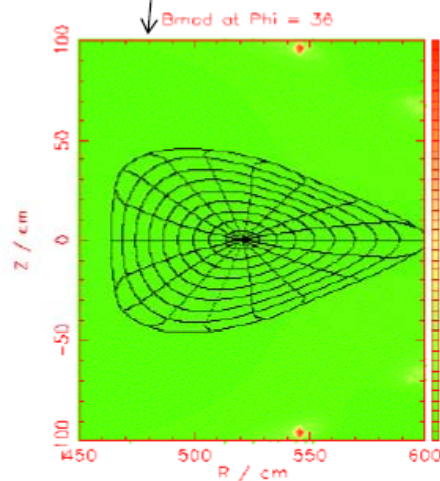


W7-X Stellarator Optimisation concept: drift optimisation + reduced parallel currents



diamagnetic + PS
current paths:
reduced PS currents !

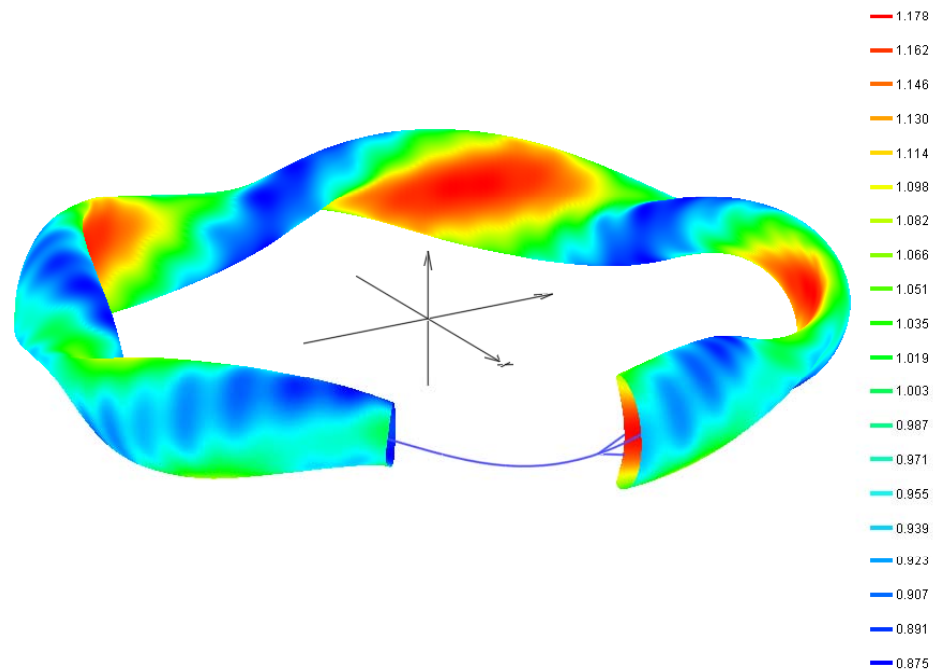
grad(B) high \Rightarrow high grad(B) drift. BUT:
B-field high: trapped particle population reduced
 \Rightarrow net reduced drift losses. AND:
High "tokamak" elongation \Rightarrow reduced mean ripple



grad(B) low \Rightarrow low grad(B) drift. AND:
B-field low: trapped particle population enhanced
 \Rightarrow drift losses play only a minor role.



Distribution of $b=B/B_{00}$ on the Last Closed Magnetic Surface



Unternehmung
Wendelstein 7-X



Max-Planck-Institut
für Plasmaphysik
EURATOM Assoc.



